Interactions with Iron:

Ferrous Iron Transport and Resistance in *Shewanella oneidensis* strain MR-1

A DISSERTATION
SUBMITTED TO THE FACULTY OF
THE UNIVERSITY OF MINNESOTA
BY

Brittany Dawn Bennett

IN PARTIAL FULFILLMENT OF THE REQUIREMENTS
FOR THE DEGREE OF
DOCTOR OF PHILOSOPHY

Advisor: Jeffrey A. Gralnick

January 2017

Acknowledgements

First and foremost, I must thank my advisor, Jeffrey Gralnick, for being an amazing mentor. Your high expectations and confidence in my abilities have helped me achieve greater things than I would have thought possible otherwise. Thank you for fostering an environment of scientific rigor that just happens to also be really fun. The Gralnick lab was a wonderful place to complete my PhD, and I consider myself lucky to have spent the formative years of my scientific career there.

The Gralnick lab would not have been such a fantastic environment without the contributions of all the fabulous people I have had the privilege to work with there. Benjamin Bonis, thank you for being a great friend and a good listener. I will miss our talks and your keen insight into everything scientific and otherwise. Aunica Kane, thank you for being so supportive and for giving me feedback on nearly everything I wrote in grad school. Your help and friendship have been invaluable. Audrey Harris, you are such a good friend, with uncanny intuition. My stomach still aches from talking and laughing with you late into the night. Nicholas Kotloski, thank you for patiently helping me during prelims, but more importantly thank you for shenanigans, the Greenskeepers, darts, ice ball, and all the other ways you made our lab so much fun. Eric and Aubree Kees, thank you for movie nights, New Year's Eve cover bands, and the honor of being in your wedding. I hope we remain friends for a very, very long time. Evan Brutinel, thank you for making Tn-Seq in *Shewanella* a thing and for being one of the first people to welcome me to the lab.

Kaitlyn Redford: thank you for being the best undergrad ever. Working with you has been such a pleasure, and I owe a big part of one of these chapters to your hard work. I look forward to watching you grow into the marvelous scientist you are already well on the path to becoming.

Thanks must also go to folks in the Bond Lab. Daniel Bond, of course, for expounding more deeply upon electrons and ruminants than anyone I will ever know. Jonathan Badalamenti, Chi Ho Chan, and Caleb Levar, thank you for the unending Tn-Seq help and all your support during prelims.

To my thesis committee (Jeff Gralnick, Sandra Armstrong, Daniel Bond, Gary Dunny, and Brandy Toner), thank you for providing me with different points of view from which to evaluate my work. Thanks especially to my chair, Sandy, for writing countless letters of recommendation on my behalf. Sandy and Brandy, thank you for being great female scientist role models.

My experience in the Microbiology, Immunology, and Cancer Biology PhD program could not have been better. I've met too many wonderful people in MICaB to name here, but thanks to all of you for making it such a fun and supportive community. Thanks to the amazing Louise Shand for keeping the program running like a well-oiled machine and for being one of the nicest people on Earth. Thanks to Sarah Elliot and Nicholas Dillon for your help during prelims. Thanks to Joanne Dehnbostel for braving a year of student representation with me.

Thanks to Wei-Shou Hu and Claudia Schmidt-Dannert for running the Biotechnology Training Program, which funded my research and some of my travel for two years.

Thanks to LeeAnn Higgins and Todd Marowski in the Center for Mass Spectrometry and Proteomics for many patient hours of proteomics training and advice.

I could not have made it this far, of course, without the love and support of the people closest to me. To my parents, Brett and Joleen Bennett: thank you for always telling me I could accomplish anything I set my mind to. I wouldn't have dreamed I could do this if you hadn't built a foundation of hard work, high expectations, and unending encouragement from the very beginning. My brother Brendon, thanks for being excited about my work (sometimes more so than me) and keeping the family lore alive. To Uncle Jack and my cousin Kerry, thank you for your constant love and optimism and for making me feel like I make you proud. And to my late Aunt Joanne, thanks for putting me on the scientific path in the first place.

Finally, thank you to my best friend and partner Brandon LaPlante. There were times when, of the two of us, you were the only one who believed in me. I don't know if I would have made it through this without you. At the very least, my posters wouldn't have looked nearly as pretty. I can't wait to take on the next adventure with you.

Abstract

All living cells have requirements for metals, largely for the catalytic functions of metalloenzymes and other metal-containing proteins. However, metals become toxic to cells at higher concentrations. Therefore, it is imperative that organisms maintain intracellular metal concentrations within a viable range. As such, cells have many means through which to import, export, store, and detoxify metals, in order to fine-tune the intracellular concentration and reduce the toxicity of each.

Iron is one of the most-used metals in metalloproteins, due to both its abundance in the Earth's crust and its redox flexibility. Easily reduced to the ferrous state (Fe^{2+}) or oxidized to ferric state (Fe^{3+}), iron is widely used in enzymes involved in electron transfer, such as cytochromes, or redox sensing, such as transcription factors. The importance of iron is underscored by the large number of cellular processes that have been discovered in all domains of life that regulate the concentration and usage of iron. Multiple transport systems, for example, mediate the influx and efflux of both Fe^{2+} and Fe^{3+}. Additionally, the redox flexibility of iron and its midrange redox potentials make iron a potential substrate for anaerobic respiration.

Shewanella oneidensis strain MR-1 is a dissimilatory metal-reducing bacterium that lives in the redox transition zones of aquatic sediments. *S. oneidensis* produces numerous cytochromes that allow it to respire a wide variety of substrates, including extracellular, insoluble Fe^{3+} compounds, which are reduced to Fe^{2+}. Fe^{2+} is much more soluble than Fe^{3+} in physiologically relevant conditions; therefore, *S. oneidensis* must contend with increasing local concentrations of soluble Fe^{2+} as it continues to respire Fe^{3+}. How *S. oneidensis* interacts with Fe^{2+} and resists Fe^{2+} toxicity is the subject of this thesis.

The second and third chapters of this thesis describe two newly discovered Fe^{2+} transport proteins in *S. oneidensis*. The first, which has been named FeoE (*f*erro*u*s iron *e*xport), is an Fe^{2+} exporter that reduces the intracellular Fe^{2+} concentration during Fe^{3+} respiration by *S. oneidensis*. FeoE belongs to the Cation Diffusion Facilitator superfamily of divalent metal efflux proteins, which includes transporters of Cd^{2+}, Co^{2+}, Cu^{2+}, Fe^{2+}, Ni^{2+}, and Zn^{2+}. Studies presented in this dissertation demonstrate that FeoE is

exclusively an Fe^{2+} exporter. The transporter described in Chapter 3, which was named FicI (*f*errous *i*ron and *c*obalt *i*mporter), is an Fe^{2+} and Co^{2+} importer. FicI belongs to the Magnesium Transporter-E (MgtE) family of Mg^{2+} and Co^{2+} importers; this is the first discovery of an MgtE protein that imports Fe^{2+} and not Mg^{2+}. FicI appears to represent a secondary Fe^{2+} importer active at higher Fe^{2+} concentrations. FicI doesn't require nucleotide hydrolysis for Fe^{2+} import, unlike the primary Fe^{2+} importer FeoB, therefore allowing the cell to conserve energy under high Fe^{2+} conditions.

The fourth chapter in this thesis concerns the ATP-dependent protease ClpXP. ClpXP has previously been found to be involved in various cellular functions in several bacterial species, including releasing stalled proteins from ribosomes and the regulation of sigma factors, which influence the transcription of large groups of genes. The work presented in Chapter 4 shows that ClpXP is needed for the resistance of *S. oneidensis* to higher concentrations of Fe^{2+}, which does not appear to involve previously described functions of ClpXP. Data presented in Chapter 4 indicate that ClpXP may target metalloproteins during Fe^{2+} stress, a finding that implicates high Fe^{2+} concentrations in protein mismetallation and misfolding. Supplementary Tables S1 and S2 contain transposon screen and protein-trapping results, respectively, relevant to this chapter.

The work in this thesis expands the knowledge of the ways in which *S. oneidensis* interacts with Fe^{2+}, including its uptake and efflux, and presents a potential mode of Fe^{2+} toxicity under anoxic conditions. As iron is an essential metal to most living organisms, and as there are many microorganisms living in metal-rich environments, the work presented here is relevant both to the study of *S. oneidensis* and to microbiology in general. The protein families discussed here are highly conserved among many microorganisms, and their newly discovered functions in *S. oneidensis* are likely to apply in others as well. More broadly, this work presents several widely-conserved proteins that have been repurposed or given added functions to meet the needs of an organism in order for it to thrive in a particular environmental niche, which reflects the adaptive nature of evolution.

Table of Contents

List of Tables

List of Figures

Chapter 1: Introduction on Bacterial Interactions with Metals.

1.1 The respiratory versatility of *Shewanella*

Cellular respiration is the process by which organisms transfer electrons, generated by the oxidation of reduced molecules, across a membrane to compounds called terminal electron acceptors (reviewed in White 2012). Respiration is the major means by which cells create energy: electron transfer is coupled with the generation of an electrochemical ion gradient across a membrane (Mitchell 1961), which the cell can then utilize to make ATP (Maloney 1974). Electrons are transferred along a redox potential gradient from more reducing compounds with lower potential to more oxidizing compounds with higher potential. Respiration pathways in cells are arranged in such a way as to pass electrons from an electron donor through carriers with increasing potentials and finally to a terminal electron acceptor. Along a respiration pathway, the free energy of electron transfer between membrane-bound electron carriers is used to move protons across the membrane.

One of the highest potential electron acceptors is O_2. However, cellular life preceded atmospheric oxygen by hundreds of millions of years, and early life forms first developed anaerobic respiration, or the respiration of electron acceptors other than O_2 (Castresana 1995). Anaerobic respiration pathways continue to be utilized by numerous bacterial, eukaryotic, and archaeal species living in anoxic environments, such as the Earth's subsurface, hot springs, the deep ocean, and animal intestinal tracts.

In recent decades, a handful of bacterial species have been discovered that are capable of anaerobically respiring insoluble, extracellular metals (Myers 1988, Lovley 1988, Roden 1993, Rosselló-Mora 1995, He 2003, Wrighton 2011). The genus *Shewanella*, of the class Gammaproteobacteria, is comprised of the most diverse organisms discovered to date in terms of their respiratory capabilities (Nealson 2006). *Shewanella oneidensis* MR-1, originally isolated from Lake Oneida in New York State (Myers 1988), lives in metal-rich redox transition zones, such as lakebed sediments, where the oxygen concentration is continually in flux (see discussion of *S. oneidensis* environments in "Reactive sediment minerals" below). *S. oneidensis* has multiple electron carrier pathways, some of which end in the periplasm while others lead to the outside of the cell, which allows the organism to respire both soluble and insoluble, extracellular electron acceptors. Unlike obligate anaerobes, *S. oneidensis* appears to be

a “respiratory opportunist” that upregulates many anaerobic respiratory pathways at once in the absence of oxygen (Barchinger 2016), in what appears to be an evolutionary strategy of respiring any accessible electron acceptor to survive until conditions again turn oxic. Compounds that can be used as terminal electron acceptors by these facultatively anaerobic bacteria include oxygen, fumarate, sulfite, thiosulfate, nitrite, nitrate, and trimethylamine *N*-oxide (Myers 1988), as well as metals such as manganese (Myers 1988), iron (Kostka 1995), cobalt (Liu 2002), chromium (Myers 2000), and uranium (Lovley 1991).

Only a few of the metal respiratory pathways harbored by some of the Gram-negative metal-respiring species have been determined; the general structure is an electron conduit composed of cytochromes leading from the inner membrane, crossing the periplasm and outer membrane, and terminating at the cell surface (see example of the *S. oneidensis* metal-reduction cytochrome pathway in Fig 1.1). These extracellular respiration pathways can also transfer electrons to electrodes, thus generating an electrical current. The respiratory diversity of *S. oneidensis* and other metal-respiring microbes gives them great potential for biotechnological applications, including in microbial fuel cells (Hamamoto 2016), biosensors for detection of toxic contamination (Webster 2014), and bioremediation of heavy metal-contaminated environments (Lovley 2003). Understanding the means by which *S. oneidensis* naturally interacts with metals and resists metal toxicity will allow for optimal microbial engineering for biotechnology purposes.

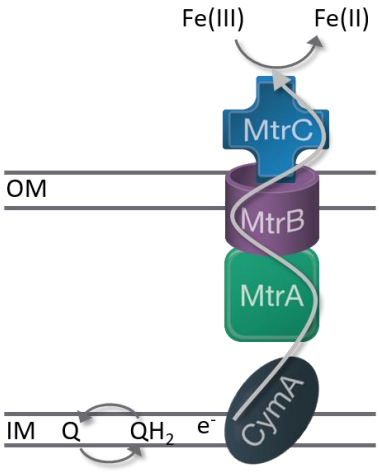

Figure 1.1 *S. oneidensis* extracellular respiration pathway. OM, outer membrane; IM, inner membrane; Q, oxidized quinone; QH_2, reduced quinone; CymA and MtrCAB, cytochromes.

1.2 Reactive sediment minerals

Soils and sediments are composed of minerals that originate from the weathering of rocks, producing phyllosilicates and hydrous metal oxides with highly reactive surfaces (Nesbitt 1997, Essington 2015). In sediments, these minerals are often poorly crystalline and react easily with other compounds (Canfield 1989). Iron and manganese transform easily between redox states (Nealson 1994), allowing minerals containing these metals, such as ferrihydrite, birnessite, and siderite, to serve as sources of electron acceptor or donor to the numerous microorganisms living in sediments (Ottow 1971, Jones 1983, Nealson 1994, Chaudhuri 2001). Mineral respiration and oxidation are particularly relevant in the oxic-anoxic transition zones that begin a few centimeters below the sediment interface with oxic water (Matisoff 2005), where oxygen concentrations ebb and flow due to environmental conditions and the activities of resident microbes (Jonasson 2012). It is in these redox transition zones that the vast majority of microbial respiratory interaction with metals occurs (Thamdrup 1994).

The oxidation and reduction of metals in minerals greatly impact biogeochemical cycling in aquatic sediments. As the valence state of a metal changes, so do its physical

properties, including solubility (Marshall 1979, Nealson 1994). Iron and manganese in their oxidized forms (Fe^{3+}, or ferric iron, and Mn^{4+}) are solid at circumneutral pH, but in their reduced states (Fe^{2+}, or ferrous iron, and Mn^{2+}), they may be either soluble or part of insoluble compounds, depending on the pH and chemical composition of the medium (Nealson 1994, Thamdrup 1994). Mn^{3+} is generally unstable and only occurs naturally in minerals with mixed Mn oxidation states (Davison 1993). The composition, reactivity, and redox potential of iron and manganese minerals changes with the oxidation state of the metals therein (Fischer 1987, Nealson 1994). As minerals break down or reform due to microbial respiration and oxidation, the surrounding soluble chemical composition changes. Manganese and iron hydroxides act as major adsorbents, and upon reduction those minerals can release previously sequestered cations, phosphates, and other molecules (Wang 2015), in addition to soluble Mn^{2+} or Fe^{2+}. Conversely, metal oxidation can cause the formation of solid minerals and the sequestration of free molecules. Shifting soluble concentrations of metals and other molecules affects the microbial communities living in sediments, as they must adapt to continual fluctuations in bioavailable toxins, nutrients, and metals.

1.3 Iron and other metals in living cells

Metals are required for numerous cellular functions, largely as cofactors in enzymes. It has been estimated that, on average, one-fourth to one-third of all cellular proteins and around 40% of enzymes require metals (Waldron 2009, Andreini 2008). The metal most frequently associated with enzymes is magnesium, followed by zinc, iron, and manganese; calcium, cobalt, molybdenum, tungsten, copper, and nickel associate with enzymes least frequently (Andreini 2008). This series roughly correlates with both the relative abundance in the cytoplasm (Foster 2014) and the ionic radius of each metal (Hughes 1991), save for magnesium, which has the smallest ionic radius but the largest hydration shell of the biologically relevant cations (Moncrief 1999). As the ionic radius of a metal decreases, the strength of its interaction with ligands increases, making metals like copper and nickel most likely to bind to a protein (Irving 1953, Hughes 1991, Foster 2014). Metalloproteins with different enzymatic reactions require different properties of their bound metal ion(s); therefore, cells have evolved means of ensuring insertion of the proper metal into each protein. Metals with higher ligand

affinities are tightly controlled within a cell, both in concentration and in delivery to proteins, in order to prevent their misincorporation into a metalloprotein requiring a metal with lower affinity. Various metal delivery systems exist to ensure proper protein metallation, including for copper (Argüello 2013), nickel (Brayman 1996, Song 2011, Xia 2009), cobalt (Raux 1997, Raux 1998), molybdenum (Leimkühler 2011), and iron (Ferreira 1995). Conversely, metals with lower ligand affinity, such as magnesium and manganese, often get inserted into proteins simply based on their higher abundance in the cytoplasm (Tottey 2008, Hung 2011).

Metalloproteins are involved in myriad cellular processes as disparate as respiration (Méjean 1994), RNA processing (Keppetipola 2008), DNA repair (Rudolf 2006), and substrate transport across membranes (Coudray 2013). Iron, being the fourth-most abundant element in the Earth's crust (McDonough 2000), is one of the most common metals found in metalloproteins. Iron is readily reduced to Fe^{2+} or oxidized to Fe^{3+}; due to this oxidative flexibility, iron is often involved in electron transfer between substrates. Iron-sulfur clusters frequently serve as the active centers in oxidoreductases (Teintze 1982), dehydratases (Flint 1996), photosystems (Vassiliev 2001), redox-sensing transcription factors (Hidalgo 1994), and enzymes involved in enzyme radical formation (Broderick 1997) and RNA modification (Kimura 2015), among others. Iron-containing hemes are ubiquitously utilized as electron carriers in cytochromes (reviewed in Liu 2014). Multiple other iron-containing proteins exist that do not utilize heme or iron-sulfur clusters, including transcriptional regulators (Tucker 2007), phosphodiesterases (Diethmaier 2014), and oxidases (Rui 2014). Altogether, iron enzymes comprise 18% of metal-containing enzymes with known structures (Andreini 2008).

1.4 Metal concentration control: transport

Cells utilize many transport proteins to control the intracellular concentrations of biologically relevant metals. There are many protein families involved in the transport of numerous metals; the following is but a brief introduction to some of them. For further information on transport protein families, the Transporter Classification Database is a comprehensive source for membrane transport system literature (Saier 2006).

Many metal uptake systems have been discovered in all domains of life. One of the more widespread groups of metal ion importers is the Nramp ("natural resistance-associated" macrophage protein) family (Gunshin 1997). Nramp2 proteins are found only in eukaryotes and are highly promiscuous, with a preference for Fe^{2+} followed by Zn^{2+}, Mn^{2+}, Co^{2+}, Ca^{2+}, Cu^{2+}, Ni^{2+}, and finally Pb^{2+} (Gunshin 1997). Nramp1 members (MntH in bacteria), on the other hand, are more substrate-specific, with a strong preference for Mn^{2+} (Kehres 2000).

Bacterial cells have various ways to take up iron, with different systems specific for either ferric or ferrous iron. Many bacteria, particularly those growing aerobically, largely depend upon chelation of Fe^{3+} by secreted siderophores to bind, solubilize, and import iron (Rosenberg 1974). The periplasm-spanning TonB system was originally discovered as essential for Fe^{3+} uptake in *Escherichia coli* (Wang 1969a), and has since been implicated in the uptake of numerous substrates including vitamin B_{12}, Ni^{2+}, and carbohydrates, in addition to chelated Fe^{3+}, in Gram-negative bacteria (reviewed in Schauer 2008). In other bacterial species, or under anaerobic conditions, Fe^{2+} is frequently the dominant iron species targeted for import. The GTPase FeoB is an inner-membrane Fe^{2+} importer (Wang 1969b, Hantke 1987, Kammler 1993) ubiquitous across the Bacteria and Archaea, although it may not be responsible for Fe^{2+} import in all species in which it is found (Raphael 2003).

Several families of Mg^{2+} importers have been discovered in bacterial species. CorA is the predominant Mg^{2+} importer in bacteria, which is also capable of Co^{2+} and Ni^{2+} import (Nelson 1972, Park 1976, Snavely 1989, Papp 2004). MgtA and MgtB are P-type ATPases discovered as secondary Mg^{2+} importers, also capable of importing Ni^{2+}, in *Salmonella enterica* serovar Typhimurium (Hmiel 1989, Maguire 1992). The MgtE family of Mg^{2+}/Co^{2+} transporters (Smith 1995) is present in multiple Gram-positive and Gram-negative bacterial species, but it is not as widespread as CorA (Townsend 1995). No energetic mechanism has been determined for CorA or MgtE import activity; transport activity appears to be driven by ligand-gating, in which the channel remains in the closed position when bound by cytosolic Mg^{2+} and opens due to a change in stabilization energies when the cation binding sites are unbound (Takeda 2014, Matthies 2016).

As metals are toxic at too high a concentration (see “Metal toxicity to living cells” below), many efflux protein families have evolved in bacteria to prevent intracellular metal buildup. The cation diffusion facilitator family of heavy metal transporters, found ubiquitously across all three domains of life, includes exporters of Zn^{2+}, Fe^{2+}, Cd^{2+}, Co^{2+}, Ni^{2+}, and Mn^{2+}; members of this family utilize membrane potential to drive substrate export (Nies 1995, Paulsen 1997, Montanini 2007). The P-type ATPase family includes the cadmium resistance transporter CadA (Nucifora 1989) and the cobalt exporter CoaT (Rutherford 1999). MntP and MneA are more recently discovered Mn^{2+} exporters (Waters 2011, Fisher 2016). CorA also appears to perform Mg^{2+} efflux rather than influx under certain conditions in strains that also carry *corBCD* (Gibson 1991). Mechanisms for Mn^{2+} and Mg^{2+} efflux by MntP, MneA, and CorA have yet to be determined.

1.5 Metal toxicity to living cells

While metals are required for numerous cellular processes, it is critical that intracellular concentrations of metals do not reach toxic levels. Unregulated, heavy metals will catalyze various detrimental reactions within a cell.

Cuprous copper (Cu^{+}), for example, damages iron-sulfur clusters, replacing the iron atoms and causing their release from proteins (Macomber 2009). Copper also reacts with O_2 and H_2O_2 to produce DNA-damaging radical oxygen species via Fenton reactions (where “Me” denotes a metal):

$$Me^{X} + O_2^{\bullet -} \rightarrow Me^{X-1} + O_2$$

$$2O_2^{\bullet -} + 2H^{+} \rightarrow H_2O_2 + O_2$$

$$Me^{X-1} + H_2O_2 \rightarrow Me^{X} + {}^{\bullet}OH + OH^{-}$$ (Stohs 1995).

Cadmium has a high affinity for sulfur and will bind sulfide groups, forming intracellular CdS precipitates (Helbig 2008). Cadmium is also believed to bind the thiols of iron-sulfur clusters and to cause the release of free iron, which increases cellular damage (Helbig 2008). Cobalt is thought to take the place of iron during the assembly of iron-sulfur clusters; as cobalt is more redox stable than iron, substituting iron with cobalt in these clusters results in less active enzymes (Ranquet 2007). Co^{2+} and Co^{+} have also

been postulated to generate radical oxygen species through Fenton chemistry (Leonard 1998).

Fe^{2+} is also believed to cause cellular damage via oxidative stress when cells are growing under or introduced to aerobic conditions (Stohs 1995). Hydroxyl radicals, calculated to be produced by Fe^{2+} via the Fenton reaction at a rate of around 50 per second per cell (Stohs 1995), readily acquire hydrogens from deoxyribose and introduce DNA strand breaks (Balasubramanian 1998). Fe^{2+} is also known to be toxic under anoxic conditions; however, the mechanism of anaerobic Fe^{2+} toxicity is not yet known. See Chapter 4 for further discussion of potential mechanisms of anaerobic Fe^{2+} toxicity.

1.6 Metal concentration control: storage and detoxification

Due to their potential for toxicity and misincorporation into proteins, most metals must be detoxified and/or sequestered inside cells. Even metals that are not required by cells may still enter the cytoplasm and cause toxicity, and therefore many bacteria living in metal-rich or -contaminated environments have mechanisms for detoxification or removal of these metals. The *mer* operons, for example, are clusters of genes found in diverse bacteria that encode enzymes to reduce organic mercury complexes to Hg^{2+} and subsequently to Hg^0, which passively exits the cytoplasm as a gas (reviewed in Barkay 2003).

Several storage systems for various metals exist, the most well-studied of which are metallothioneins (copper-binding proteins) and ferritins (iron-binding proteins). Bacterial metallothioneins coordinate metal ions through four Cys residues in a zinc finger-like structure (reviewed in Blindauer 2009 and Capdevila 2011). The first metallothionein discovered in bacteria, SmtA in *Synechococcus* PCC 7942, is able to bind Cd^{2+}, Zn^{2+}, and Hg^{2+} in addition to copper (Shi 1992). Indeed, the genomes of many bacteria examined appear to encode just one metallothionein, suggesting that most bacterial metallothioneins may bind multiple metal species (Blindauer 2009). There are exceptions, however, particularly in organisms that have adapted to metal-rich environments and are therefore more likely to have evolved multiple means of metal toxicity resistance. Three metallothionein-like proteins called “pseudothioneins,” for

example, were identified in a *Pseudomonas putida* strain isolated from sewer sludge, which were found to bind cadmium, zinc, and copper (Higham 1986).

Ferritins utilize a unique, roughly spherical three-dimensional structure to bind iron within the interior of the protein and sequester it from the cytoplasm (reviewed in Andrews 2010). Ferritin-like molecules discovered in bacteria include the classical ferritins (Granick 1942), Dps proteins (Almirón 1992, Evans 1995), and bacterioferritins (Stiefel 1979). As Fe^{3+} is much less soluble and less toxic than Fe^{2+} under physiological conditions, ferritins oxidize Fe^{2+} to Fe^{3+} via “ferroxidase centers” before storage (Andrews 2010).The classical ferritins and bacterioferritins are thought to function primarily as storage molecules, whereas Dps proteins may function more as Fe^{2+} detoxifiers (Andrews 2010). More recently, a novel iron- and copper-binding Dps-like protein was discovered in *Borrelia burgdorferi* (Wang 2012). It is likely that further sequestration proteins for the storage and detoxification of other metals will continue to be discovered.

1.7 AAA+ Proteases

As discussed above, metalloproteins that receive the incorrect metal may be misfolded or display the incorrect activity. Proteolysis is required for the degradation of misfolded or mutant proteins and the regulation of various enzymes under different conditions (Gottesman 1996). The first ATP-dependent protease discovered in bacteria was Lon (originally called La), which was determined to depend on a serine residue for catalytic activity (Swamy 1981, Waxman 1982). Shortly thereafter, several other ATP-dependent proteases were discovered in *E. coli*, including ClpP (originally called Ti), another serine protease (Hwang 1987, Katayama 1987). ClpP and Lon were later categorized as AAA+ proteases.

The term AAA+ was coined by Kunau et al (1993) to define ATPases associated with diverse cellular activities, a broad category of proteins that require ATP for activity. There are five AAA+ proteases encoded in the genomes of *S. oneidensis* and other gammaproteobacteria: ClpXP, ClpAP, Lon, FtsH, and HslVU. ClpXP, ClpAP, and HslVU are comprised of two subunits, an ATPase (ClpX, ClpA, and HslU) and a peptidase (ClpP and HslV) (Gottesman 1990, Chuang 1993), whereas Lon and FtsH are encoded

by discrete genes and display both ATPase and peptidase activities (Charette 1981, Herman 1993, Kihara 1995). The ATPase subunit or domain of the AAA+ proteases determines substrate specificity, using ATP to unfold target proteins and feed them into the peptidase subunit or domain for degradation into peptide fragments (Katayama 1988, Wojtkowiak 1993).

Proteolysis targets are usually recognized by proteases via amino acid sequence tags near their C- or N-terminus (Flynn 2003) or via short peptide tags that are attached to targets by delivery proteins (Keiler 1996). AAA+ proteases are involved in numerous cellular functions. Lon was originally discovered due to the inability of *lon* mutants to degrade abnormal protein fragments and missense proteins (Gottesman 1978). Since then, AAA+ proteases have been implicated in the regulation of a vast array of cellular processes as diverse as DNA damage response, cell cycle and differentiation, heat shock response, lipid synthesis, and DNA transcription and replication (reviewed in Gottesman 1996, Van Melderen 2009, Ambro 2012, Okuno 2013). Further discussion of the cellular functions regulated by ClpXP can be found in Chapter 4.

1.8 Thesis summary

This thesis describes the investigation of the ways in which *S. oneidensis* interacts with iron and the mechanisms encoded in its genome that allow it to resist Fe^{2+} toxicity. Chapter 2 discusses the Fe^{2+} exporter FeoE. FeoE is a member of the cation diffusion facilitator protein family and is taxonomically related to FieF, which is an *E. coli* protein that has been determined to be a $Zn^{2+}/Cd^{2+}/Fe^{2+}$ exporter. This chapter demonstrates that FeoE is required for optimal growth of *S. oneidensis* under iron-respiring conditions, and FeoE requirement is due to its function in exporting excess Fe^{2+} from the cytoplasm. Unlike FieF, FeoE is specific for Fe^{2+} and does not export other divalent metals; FeoE also appears to be a more efficient Fe^{2+} transporter than FieF.

Chapter 3 details the discovery that FicT, an MgtE family member encoded in the *S. oneidensis* genome, imports Fe^{2+} rather than Mg^{2+}, in addition to Co^{2+}. Two other genes encoding MgtE proteins are annotated in the *S. oneidensis* genome; neither of these appears to import Mg^{2+} either. Experiments in this chapter show that FeoB is the primary Fe^{2+} importer under low-iron conditions, while FicT imports Fe^{2+} under high-iron

conditions. The evolution of different Fe^{2+} importers in *S. oneidensis* may reflect an adaptive strategy to reduce the energy involved in iron uptake when possible, given the iron-reducing conditions under which this organism frequently lives.

Chapter 4 explores the role of the protease ClpXP in resisting Fe^{2+} toxicity in *S. oneidensis*. ClpXP is important for the growth of *S. oneidensis* under high-Fe^{2+} conditions; however, previously studied cellular processes known to be regulated by ClpXP are not involved in Fe^{2+} resistance. ClpXP appears to target metalloproteins during Fe^{2+} stress, which could indicate that high Fe^{2+} causes toxicity by overwhelming metal sequestration capacity and overriding the normally tightly regulated processes for correct metal insertion into metalloproteins.

Chapter 5 introduces some preliminary work relating to the sigma factor σ^E, which appears to be necessary for wild-type levels of Fe^{3+} respiration. The role of *rpoE* in extracellular respiration is thus far unclear, but it does not appear to involve Fe^{2+} stress response or the production of biofilms.

Chapter 2: A Ferrous Iron Exporter Mediates Iron Resistance in *Shewanella oneidensis* MR-1

This chapter is a reprint, with minor alterations, of a published manuscript.

Bennett BD, Brutinel ED, Gralnick JA. 2015. A ferrous iron exporter mediates iron resistance in *Shewanella oneidensis* MR-1. *Appl Environ Microbiol*. 81:7938–7944.

2.1 Summary

Shewanella oneidensis strain MR-1 is a dissimilatory metal-reducing bacterium frequently found in aquatic sediments. In the absence of oxygen, *S. oneidensis* can respire extracellular, insoluble oxidized metals, such as iron (hydr)oxides, making it intimately involved in environmental metal and nutrient cycling. The reduction of ferric (Fe^{3+}) iron results in the production of ferrous (Fe^{2+}) iron ions, which remain soluble under certain conditions and are toxic to cells at higher concentrations. We have identified an inner-membrane protein in *S. oneidensis*, encoded by gene SO_4475 and here called FeoE, which is important for survival during anaerobic iron respiration. FeoE, a member of the cation diffusion facilitator (CDF) protein family, functions to export excess Fe^{2+} from the MR-1 cytoplasm. Mutants lacking *feoE* exhibit an increased sensitivity to Fe^{2+}. The export function of FeoE is specific for Fe^{2+}, as a *feoE* mutant is equally sensitive to other metal ions known to be substrates of other CDF proteins (Cd^{2+}, Co^{2+}, Cu^{2+}, Mn^{2+}, Ni^{2+}, or Zn^{2+}). The substrate specificity of FeoE differs from that of FieF, the *Escherichia coli* homolog of FeoE, which has been reported to be a Cd^{2+} / Zn^{2+} or Fe^{2+} / Zn^{2+} exporter. A complemented *feoE* mutant has an increased growth rate in the presence of excess Fe^{2+} compared to Δ*feoE* complemented with *fieF*. It is possible that FeoE has evolved to become an efficient and specific Fe^{2+} exporter in response to the high levels of iron often present in the types of environmental niches in which *Shewanella* species can be found.

2.2 Introduction

Shewanella oneidensis strain MR-1 is a versatile, facultatively anaerobic bacterium that lives in aquatic environments and is capable of respiring numerous organic and inorganic compounds in the absence of oxygen. The respiratory diversity of *S. oneidensis* has widespread effects on biogeochemical cycling (Nealson 2006) and has therefore been a focus for applications in biotechnology and bioremediation (Gralnick 2007). Terminal electron acceptors that *S. oneidensis* can use aside from oxygen include dimethylsulfoxide (DMSO), trimethylamine N-oxide, fumarate, nitrate, and sulfite (Myers 1998, Myers 2001, Samuelsson 1985, Shirodkar 2011), as well as oxidized metals such as iron and manganese (hydr)oxides (Myers 1998, Kostka 1995),

which are abundant in the types of sediments (Canfield 1989) allow dissimilatory metal-reducing bacteria to survive in iron-rich conditions, however, are not fully understood.

Respiration of ferric iron (Fe^{3+}) results in the production of ferrous iron (Fe^{2+}), which can remain as aqueous Fe^{2+} ions or become incorporated into solid-phase minerals (O'Reilly 2005, Blöthe 2008), depending on the environmental conditions. As iron respiration by *S. oneidensis* continues, the local concentration of aqueous Fe^{2+} may increase, and Fe^{2+} ions can be taken up by cells through transition metal ion uptake systems, primarily the iron transport complex FeoAB (Kammler 1993). At higher concentrations, however, Fe^{2+} is toxic to cells. Aerobically, Fe^{2+} toxicity is thought to be caused by oxidative damage from hydroxyl radicals produced through the Fenton reaction (Imlay 1988), but the cause of damage under anaerobic conditions is not well understood. Several possible causes of anaerobic Fe^{2+} toxicity have been proposed, such as the production of reactive nitrogen species (Carlson 2012) or inhibition of the F_0F_1 ATPase (Dunning 1998). Regardless of the basis for toxicity, microorganisms have evolved means of minimizing cellular damage caused by high concentrations of Fe^{2+} and other metal ions.

One of the well-characterized mechanisms that microorganisms use to prevent metal toxicity is efflux via membrane transporters. Metal efflux proteins are widespread in all three domains of life and comprise multiple protein families and superfamilies. For example, the major facilitator family includes the tetracycline-metal ion transporter TetL in *Bacillus subtilis* (Jin 2002) and the iron citrate exporter IceT in *Salmonella enterica* serovar Typhimurium (Frawley 2013). P-type ATPases, which couple the uptake or efflux of cations to ATP hydrolysis, include the cadmium exporter CadA in *Staphylococcus aureus* and *B. subtilis* (Nucifora 1989, Tsai 1992) and the copper transporter CopA in *Escherichia coli* (Fan 2002). To date, however, there have been no proteins mediating Fe^{2+} resistance described in *S. oneidensis*.

A transposon screen identified mutations in gene locus SO_4475 resulting in a strong growth defect during ferric citrate respiration, but not during respiration of fumarate or DMSO (Brutinel and Gralnick, unpublished data). SO_4475 is predicted to encode a metal ion exporter in the cation diffusion facilitator (CDF) family, a group of

inner membrane proteins that utilize proton motive force (PMF) to export a range of divalent metal cations (Nies 1995, Paulsen 1997). The closest homolog of SO_4475 described in the literature, at an amino acid sequence similarity of 60.9% and identity of 47.7%, is the *E. coli* protein FieF (YiiP). FieF from *E. coli* has been reported to export Zn^{2+}/Cd^{2+} by some researchers (Chao 2004, Wei 2005) and Fe^{2+}/Zn^{2+} by others (Grass 2005); the protein encoded by SO_4475 was described as exporting Zn^{2+}/Cd^{2+} (Coudray 2013), although Fe^{2+} transport was not evaluated in that study. Here we characterize SO_4475, which we name *feoE* (for *fe*rro*u*s iron *e*xport), and show physiological evidence demonstrating that the encoded protein exports excess Fe^{2+} from *S. oneidensis* and is important for survival in iron reducing conditions.

2.3 Materials and methods

Bacterial strains and growth conditions.

S. oneidensis strain MR-1 was originally isolated from Lake Oneida in New York, USA (Myers 1988). *E. coli* strains used for cloning (UQ950) and mating (WM3064) have been previously described (Saltikov 2003). *E. coli* K-12 strain MG1655 was used for FieF analysis. Cloning strains, derivative strains of MR-1 and MG1655, and plasmids used in this study are found in Table 2.1. Liquid overnight Luria-Bertani (LB) cultures supplemented with 50 µg/mL kanamycin, when appropriate, were inoculated with isolated colonies from freshly streaked -80°C stocks. All cultures were grown at 30°C (*S. oneidensis*) or 37°C (*E. coli*); liquid cultures were shaken at 250 rpm. Unless otherwise noted, all experiments using liquid and solid media were performed with LB; where indicated, *Shewanella* basal medium (SBM) (Hau 2008) supplemented with 0.05% (w/v) casamino acids, 5 mL/L vitamin solution (Balch 1979), and 5 mL/L mineral solution (Marsili 2008) was used as a defined minimal medium. Anaerobic cultures were flushed with nitrogen gas and supplemented with 20 mM sodium lactate and an electron acceptor as indicated. Results are reported as the mean of three biological replicates ± one standard deviation. Data were statistically analyzed using ANOVA.

Plasmid and mutant construction.

Primers used to construct plasmids are listed in Table 2.2. In-frame deletion of *feoE* from the MR-1 genome and *fieF* from the MG1655 genome was performed as

previously described (Saltikov 2003). Briefly, fragments 1 kb upstream and downstream of *feoE* (SO_4475) with flanking *Sac*I and *Bam*HI sites were fused via a *Spe*I restriction site and ligated into the suicide vector pSMV3, which has kanamycin resistance and *sacB* cassettes. Fragments 1 kb upstream and downstream of *fieF* (b3915) with flanking *Spe*I and *Bam*HI restriction sites were fused via a *Sac*II site and ligated into pSMV3. To make the *feoE* complementation vector, *feoE* was cloned from the *S. oneidensis* MR-1 genome with flanking *Bam*HI and *Sac*I restriction sites and inserted into the pBBR1MCS-2 multiple cloning site (Kovach 1995). To make the *fieF* complementation vector, *fieF* (b3915) was cloned from the *E. coli* MG1655 genome with flanking *Bam*HI and *Spe*I restriction sites and inserted into the multiple cloning site of pBBR1MCS-2.

Growth curves.

Overnight cultures of each strain were pelleted, washed once, and resuspended in fresh LB or SBM. For aerobic and anaerobic Fe^{3+} cultures, SBM was supplemented with 20 mM sodium lactate and 80 mM ferric citrate. Growth of anaerobic Fe^{3+} cultures was measured by periodically plating serial 1:10 dilutions of each culture to LB plates and performing colony counts after one day of incubation. Growth of aerobic Fe^{3+} cultures was measured by taking the optical density at 600 nm (OD_{600}). For cultures with divalent metals, LB was supplemented with 0.45 mM $CdCl_2$; 0.8 mM $CoCl_2$; 2.2 mM $CuCl_2$; 20 mM sodium lactate, 40 mM sodium fumarate, and 1.0 mM, 2.5 mM, 3.5 mM, 5.0 mM, or 7.0 mM $FeCl_2$; 20 mM sodium lactate, 40 mM sodium fumarate, and 8.0 mM $MnCl_2$; 1.0 mM $NiCl_2$; or 1.0 mM $ZnCl_2$. Cultures with $FeCl_2$ and $MnCl_2$ were grown anaerobically to prevent oxidation of Fe^{2+} to Fe^{3+} or Mn^{2+} to Mn^{4+}. Growth was measured periodically as OD_{600} using a spectrophotometer.

Iron citrate reduction assay.

Fe^{3+} respiration was measured using ferrozine assays as previously described (Coursolle 2010). Briefly, overnight cultures of each strain were pelleted, washed once, and resuspended in fresh SBM and adjusted to an OD_{600} of 1.00. 30 µL of this suspension was inoculated into 270 µL SBM with 20 mM sodium lactate, 5 mM ferric citrate, 5 mL/L vitamin solution, and 5 mL/L mineral solution in anaerobic 96-well plates.

Fe^{2+} production was monitored over time using ferrozine absorbance at 542 nm (Stookey 1970).

Iron retention assay.

Overnight cultures of each strain were pelleted, washed once, and resuspended in fresh LB. Suspensions were inoculated into 5 mL anaerobic cultures of LB with 20 mM sodium lactate and 40 mM sodium fumarate to an OD_{600} of 0.05. Cultures were incubated at 30°C until growth reached an OD_{600} of approximately 0.50. $FeCl_2$ was spiked into each culture to a concentration of 2.5 mM, and the cultures were incubated at 30°C for one hour. Each culture was pelleted, washed once, and resuspended in 5 mL fresh SBM. Cell suspensions were assayed for iron concentration via inductively coupled plasma mass spectrometry (ICP-MS) analysis by the Analytical Geochemistry Lab in the Department of Earth Sciences at the University of Minnesota. Iron concentrations were normalized to the final OD_{600} before harvesting.

2.4 Results

*Δ*feoE *has decreased survival with ferric citrate as an electron acceptor.*

A transposon screen indicated that inactivation of *feoE* (SO_4475) in *S. oneidensis* caused a growth defect during anaerobic ferric citrate respiration but not during respiration of fumarate or DMSO (Brutinel and Gralnick, unpublished data). These results indicated that the protein product of *feoE* is important for growth during Fe^{3+} respiration, rather than anaerobic growth in general. To confirm the results of the transposon screen, an in-frame deletion of *feoE* was made in *S. oneidensis*. No significant differences in growth rate between Δ*feoE* and wild-type were found in anaerobic cultures supplemented with 20 mM lactate and 40 mM fumarate (doubling time of 1.94 ± 0.23 and 1.91 ± 0.22 hours, respectively) or 20 mM lactate and 40 mM DMSO (doubling time of 1.48 ± 0.16 and 1.45 ± 0.15 hours, respectively). To evaluate the importance of *feoE* during respiration of Fe^{3+}, growth was monitored in anaerobic cultures supplemented with 20 mM lactate and 80 mM ferric citrate. Deletion of *feoE* resulted in impaired growth over time during iron respiration compared to wild-type (Fig. 2.1). Complementation of Δ*feoE* and wild-type with pBBR1MCS-2::*feoE* enhanced the log phase growth rate of both strains over wild-type with empty vector (doubling time of

1.57 ± 0.48, 1.48 ± 0.66, and 4.71 ± 1.20 hours, respectively). The complemented strains also displayed steeper die-off than either MR-1 or Δ*feoE* with empty vector (Fig. 2.1). A similar growth impairment of Δ*feoE* was observed in anaerobic SBM cultures supplemented with 20 mM lactate, 40 mM fumarate, and 1 mM ferric citrate (Fig. 2.6).

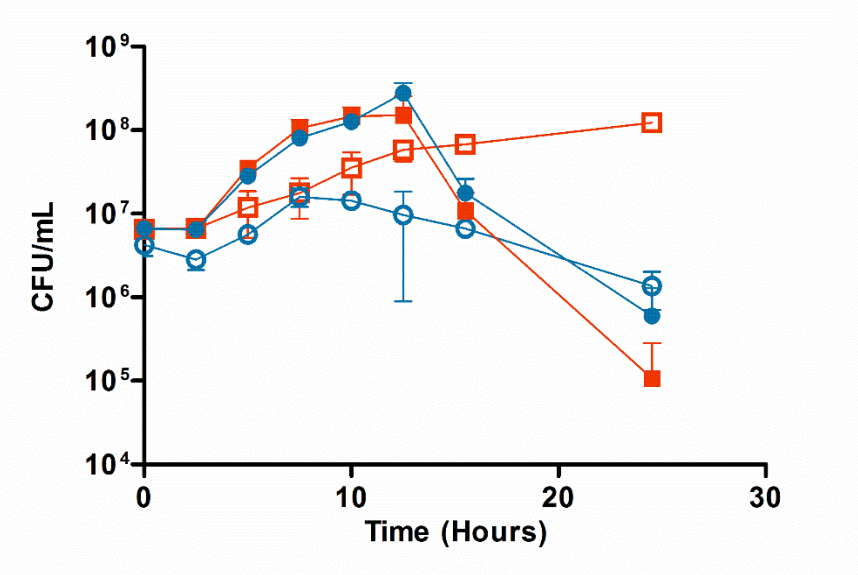

Figure 2.1 Anaerobic growth of wild-type MR-1 and Δ*feoE* strains on ferric citrate. The rate of growth in SBM with 20 mM lactate and 80 mM ferric citrate was measured for (○) Δ*feoE* with empty pBBR1MCS-2, (□) MR-1 with empty pBBR1MCS-2, (●) Δ*feoE* with pBBR1MCS-2::*feoE*, and (■) MR-1 with pBBR1MCS-2::*feoE*. Growth was determined by counting colony-forming units per mL of culture medium (CFU/mL). Results are the mean of three biological replicates ± 1 standard deviation (SD).

To rule out the possibility that the growth defect seen for Δ*feoE* during Fe^{3+} respiration was due to an increased sensitivity to citrate or soluble Fe^{3+}, aerobic growth of cultures supplemented with 20 mM lactate and 80 mM ferric citrate was evaluated. Δ*feoE* showed no difference from wild-type in growth rate during aerobic respiration in the presence of ferric citrate (doubling time of 1.16 ± 0.04 and 1.15 ± 0.04 hours, respectively, during log phase).

Deletion of feoE *does not impair ferric citrate respiration.*

To determine whether the impaired growth of Δ*feoE* during anaerobic Fe^{3+} respiration was due to a defect in the strain's ability to use Fe^{3+} as an electron acceptor, ferrozine assays were performed to measure the production of Fe^{2+} from respiration of ferric citrate. No statistically significant difference ($p > 0.05$) in the initial rate of Fe^{2+} production was observed between Δ*feoE* and MR-1, whether complemented with pBBR1MCS-2::*feoE* or with empty vector (Fig. 2.2). Complementation of Δ*feoE* and wild-type with pBBR1MCS-2::*feoE* led to slightly higher final concentrations of produced Fe^{2+} than for the empty-vector strains ($p < 0.01$; Fig. 2.2).

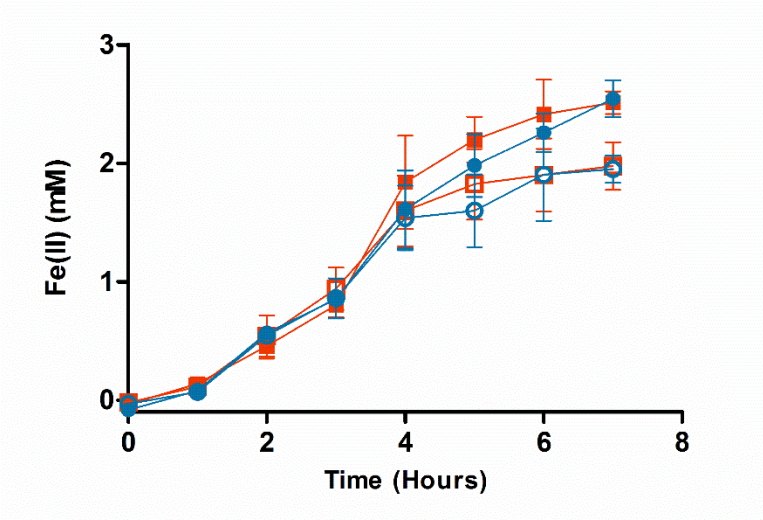

Figure 2.2 Ferric citrate reduction by wild-type MR-1 and Δ*feoE* strains.
The rate of ferric citrate reduction was measured for (○) Δ*feoE* with empty pBBR1MCS-2, (□) MR-1 with empty pBBR1MCS-2, (●) Δ*feoE* with pBBR1MCS-2::*feoE*, and (■) MR-1 with pBBR1MCS-2::*feoE*. Results are the mean of three biological replicates ± 1 SD.

feoE *mutants exhibit greater sensitivity to* Fe^{2+}.

Because Δ*feoE* was not defective in reducing Fe^{3+}, we hypothesized that the growth defect displayed by Δ*feoE* during Fe^{3+} respiration was due to increased sensitivity to Fe^{2+}, the byproduct of Fe^{3+} respiration. To determine if Δ*feoE* is more

sensitive to Fe^{2+} than wild-type, cultures of Δ*feoE* and wild-type with pBBR1MCS-2 and pBBR1MCS-2*::feoE* were grown anaerobically in LB with 20 mM lactate, 40 mM fumarate, and 1 mM $FeCl_2$. Δ*feoE* displayed a greater sensitivity to Fe^{2+} than the parent strain, as indicated by a slower growth rate (Fig. 2.3). Complementation of the mutant with pBBR1MCS-2::*feoE* restored growth in the presence of Fe^{2+} to that of wild-type (Fig. 2.3). The average doubling time during log phase was 3.69 ± 0.14 hours for Δ*feoE* with empty vector, 2.35 ± 0.16 hours for Δ*feoE* with pBBR1MCS-2::*feoE*, 2.36 ± 0.12 hours for wild-type with empty vector, and 2.41 ± 0.16 hours for wild-type with pBBR1MCS-2::*feoE*.

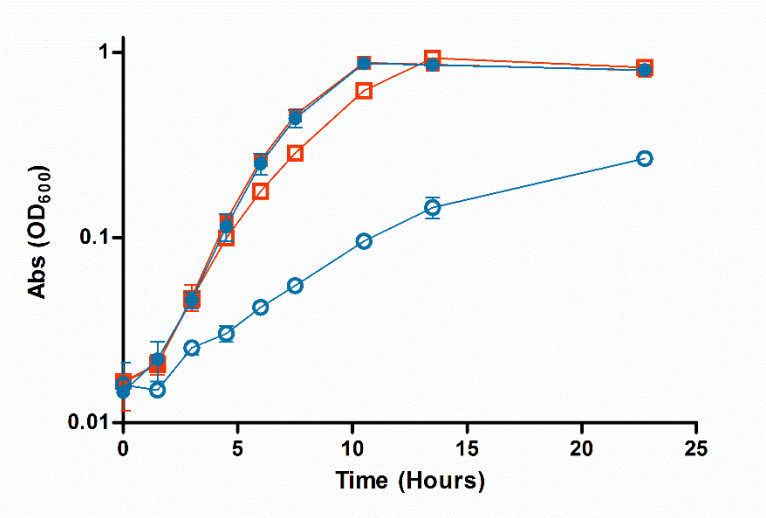

Figure 2.3 Growth of wild-type MR-1 and Δ*feoE* strains in the presence of excess Fe^{2+}.

The rate of growth in anaerobic LB with 20 mM lactate, 40 mM fumarate, and 1 mM $FeCl_2$ was measured for (○) Δ*feoE* with empty pBBR1MCS-2, (□) MR-1 with empty pBBR1MCS-2, (●) Δ*feoE* with pBBR1MCS-2::*feoE*, and (■) MR-1 with pBBR1MCS-2::*feoE*. Results are the mean of three biological replicates ± 1 SD.

Loss of feoE *increases* Fe^{2+} *retention.*

The protein product of *feoE* has been annotated as belonging to the CDF protein family, which confer increased resistance to a variety of divalent metal ions via active export of the ions from a cell's cytoplasm (Paulsen 1997). In order to determine whether the increased sensitivity to Fe^{2+} seen in Δ*feoE* was due to an impaired ability to export Fe^{2+}, iron retention assays were performed. Wild-type and Δ*feoE* with empty vector and pBBR1MCS-2::*feoE* were grown anaerobically with 20 mM lactate and 40 mM fumarate into log phase (OD_{600} approximately 0.5) and then spiked with 2.5 mM $FeCl_2$. The concentration of 2.5 mM $FeCl_2$ was chosen because growth of both the *feoE* mutant and wild-type is decreased but not arrested at this concentration. After incubation with Fe^{2+} for one hour, cells in each culture were harvested and analyzed by ICP-MS for total iron content. Δ*feoE* cells with empty pBBR1MCS-2 retained a significantly greater amount of iron ($p < 0.0001$) than did Δ*feoE* with pBBR1MCS-2::*feoE*, wild-type with empty vector, or wild-type with pBBR1MCS-2::*feoE* (218.0 ± 9.1, 148.9 ± 6.3, 141.3 ± 8.0, and 137.3 ± 7.8 $ng*mL^{-1}*OD_{600}^{-1}$ iron, respectively). Similar results were observed in experiments performed using SBM in place of LB (data not shown).

The export function of FeoE is specific for Fe^{2+}*.*

To determine the export specificity of FeoE, the sensitivity of wild-type and Δ*feoE* to various divalent metals was tested. Cultures of Δ*feoE* and wild-type were grown aerobically in LB with excess $CdCl_2$, $CoCl_2$, $CuCl_2$, $NiCl_2$, or $ZnCl_2$, and anaerobically in LB with 20 mM lactate, 40 mM fumarate, and excess $MnCl_2$. No difference in sensitivity to any of these divalent metals was observed between Δ*feoE* and wild-type (Fig. 2.4). Similarly, no difference in sensitivity to any of these metals was seen in zone of inhibition assays performed anaerobically on tryptone medium plates using noble agar as the solidifying agent (Table 2.3).

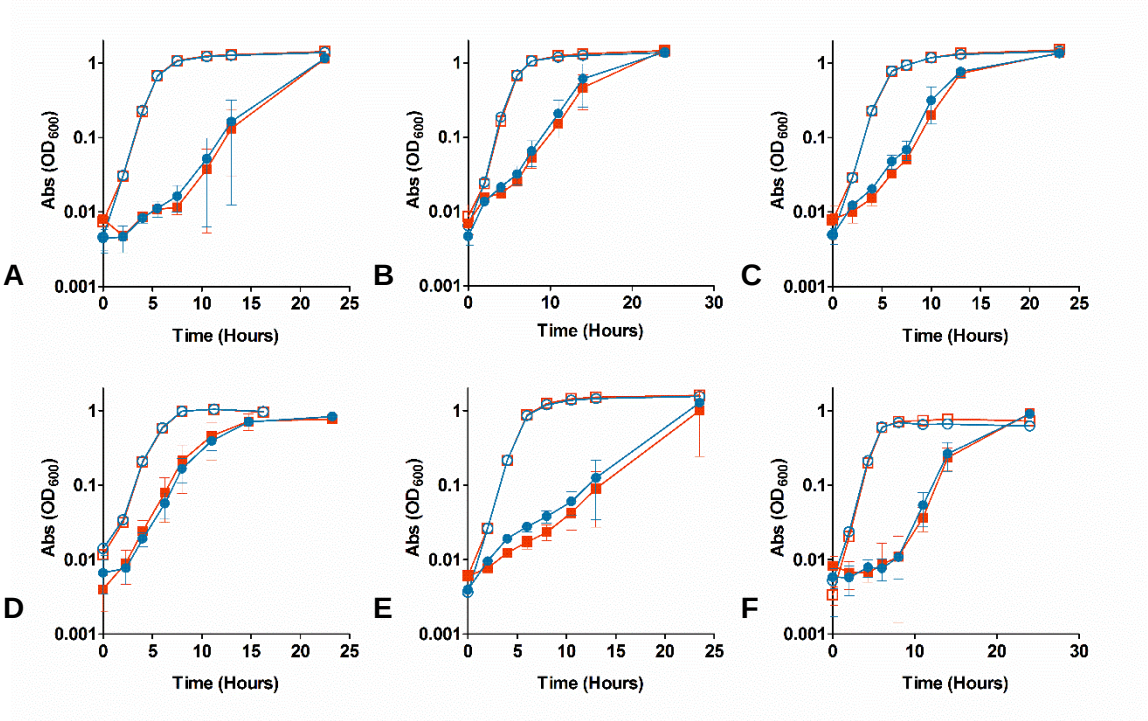

Figure 2.4 Growth of wild-type MR-1 and Δ*feoE* in the presence of divalent metals. Growth was measured over time in LB with (A) 0 mM or 0.45 mM $CdCl_2$; (B) 0 mM or 0.8 mM $CoCl_2$; (C) 0 mM or 2.2 mM $CuCl_2$; (D) 20mM sodium lactate, 40mM fumarate, and 0 mM or 8 mM $MnCl_2$; (E) 0 mM or 1.0 mM Ni Cl_2; or (F) 0 mM or 1.0 mM $ZnCl_2$. No metal added: MR-1, □; Δ*feoE*, ○. Metal added: MR-1, ■; Δ*feoE*, ●. Results are the mean of three biological replicates ± 1 SD.

FeoE confers greater resistance to Fe^{2+} *than the* E. coli *homolog FieF.*

An earlier study indicated that *E. coli* FieF, the closest characterized homolog of FeoE, may export Fe^{2+} (Coudray 2013). In order to determine how the function of FeoE compares to that of FieF, a cross-complementation study was performed in which Δ*feoE* was transformed with pBBR1MCS-2::*fieF*. Anaerobic cultures of Δ*feoE* with empty vector, pBBR1MCS-2::*feoE*, or pBBR1MCS-2::*fieF* were grown in LB with 20 mM lactate, 40 mM fumarate, and 1.0 mM, 2.5 mM, 3.5 mM, or 5.0 mM $FeCl_2$. The growth rates of Δ*feoE* complemented with pBBR1MCS-2::*fieF* were similar to those of Δ*feoE*

complemented with pBBR1MCS-2::*feoE* at 1.0 and 2.5 mM $FeCl_2$, but at higher Fe^{2+} concentrations, growth of the *fieF*-complemented mutant was considerably diminished compared to the mutant complemented with *feoE* (Fig. 2.5). Similarly, *E. coli* Δ*fieF* grown anaerobically in LB with 20 mM lactate, 40 mM fumarate, and 7 mM $FeCl_2$ showed significantly impaired growth when complemented with pBBR1MCS-2::*fieF* than with pBBR1MCS-2::*feoE* ($p < 0.001$; Fig. 2.7).

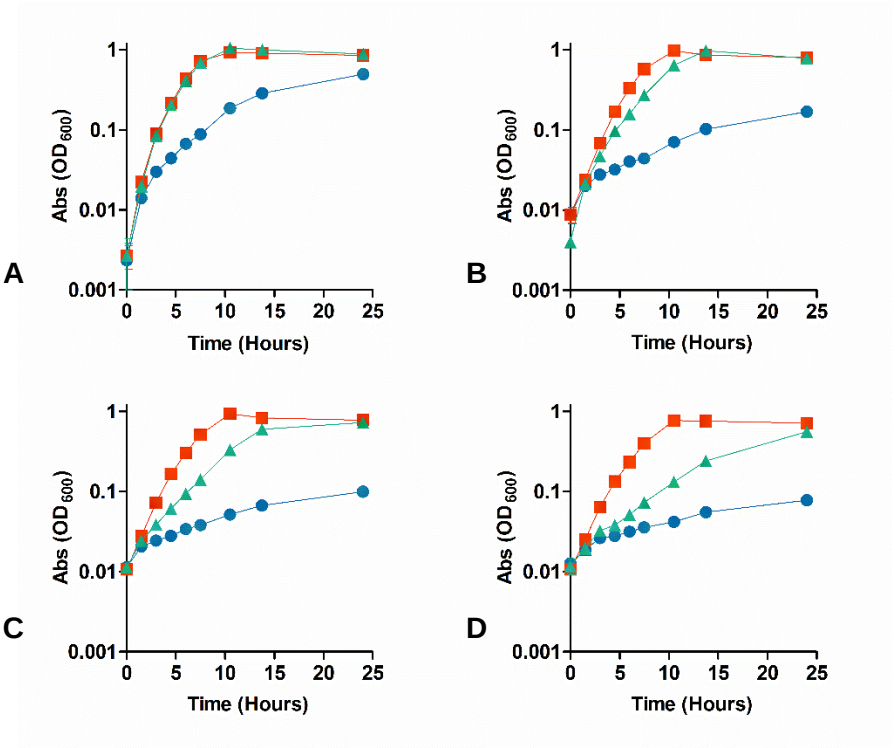

Figure 2.5 Growth of Δ*feoE* complemented with *feoE* or *fieF* in the presence of excess Fe^{2+}.

Growth in anaerobic LB with 20 mM lactate, 40 mM fumarate, and (A) 1 mM, (B) 2.5 mM, (C) 3.5 mM, or (D) 5 mM $FeCl_2$ was measured for Δ*feoE* with (●) empty pBBR1MCS-2, (■) pBBR1MCS-2::*feoE*, or (▲) pBBR1MCS-2::*fieF*. Results are the mean of three biological replicates ± 1 SD.

2.5 Discussion

Efflux proteins, responsible for the maintenance of intracellular concentrations of various small molecules, are found among all domains of life. The actions of cation

exporters allow cells to maintain sub-toxic intracellular levels of heavy metals, most frequently Cd^{2+}, Co^{2+}, Ni^{2+}, Fe^{2+}, and Zn^{2+} (Cubillas 2013). Here we have characterized FeoE, a member of the CDF family found in *S. oneidensis* MR-1, encoded by gene locus SO_4475, which specifically exports Fe^{2+} and is important for survival during Fe^{3+} respiration.

FeoE is well conserved throughout the shewanellae, with closely related homologs found in the other metal-reducing *Shewanella* spp. ANA-3, MR-4, MR-7, and *putrefaciens* CN-32 (92.0-94.3% identity), suggesting that Fe^{2+} efflux is an important strategy for iron-respiring organisms. Interestingly, distantly related FeoE homologs can also be found in the metal-reducing *Deltaproteobacteria* species *Geobacter metallireducens* and *Geobacter sulfurreducens*, but the sequence similarity between these proteins and FeoE (23.1-25.6% identity) is too low to conclude function without additional experimentation.

Initial experiments indicated that deletion of SO_4475 (*feoE*) resulted in decreased cell density over time during growth with ferric citrate as a terminal electron acceptor (Figs. 2.1 and 2.6), but not during respiration of DMSO or fumarate. Complementation of both wild-type and the *feoE* mutant with a plasmid carrying *feoE* conferred an increased rate of growth to each strain during ferric citrate respiration (Fig. 2.1), indicating that having multiple copies of the gene allows cells to minimize the inhibitory effects of increased Fe^{2+}. Unexpectedly, both *feoE*-complemented strains displayed a rapid die-off after reaching stationary phase (Fig. 2.1). One possible explanation for this phenomenon is that production of excess FeoE is energetically taxing to cells. However, we think a more likely explanation is that the initial expansion to a high cell density causes the *feoE*-complemented strains to run out of a limiting nutrient earlier than the empty-vector strains, given that the strains grow much faster with *feoE* constitutively expressed from a multi-copy vector. Alternatively, the increased amounts of FeoE in cells could result non-specific efflux of a trace metal(s) required for growth.

To confirm that the decrease in cell density seen for the *feoE* mutant during growth on ferric citrate (Fig. 2.1) was not due to a respiratory defect, production of Fe^{2+} from ferric citrate respiration by resting cells was measured. Both Δ*feoE* with empty

vector and Δ*feoE* with pBBR1MCS-2::*feoE* produced Fe^{2+} at the same rate as the corresponding wild-type strains (Fig. 2.2). Interestingly, the *feoE*-complemented wild-type and Δ*feoE* strains produced a slight but statistically significant ($p < 0.01$) increase in the amount of Fe^{2+} produced near the end of the assay (Fig. 2.2). It appears that, similar to the results seen in the ferric citrate growth curve (Fig. 2.1), producing more copies of the FeoE transporter allows *feoE*-complemented strains to minimize inhibition by Fe^{2+} and thus increase metabolic processes.

To determine whether the decline in cell density seen for Δ*feoE* during ferric citrate respiration (Fig. 2.1) was due to an increased susceptibility to Fe^{2+} toxicity, growth curves were performed with 1 mM $FeCl_2$. The *feoE* mutant with empty vector displayed a notably slower rate of growth than Δ*feoE* with pBBR1MCS-2::*feoE,* wild-type with either empty vector, or wild-type with pBBR1MCS-2::*feoE*, indicating that deletion of *feoE* caused greater sensitivity to Fe^{2+} (Fig. 2.3). Commensurate with the ferric citrate respiration assays (Figs. 2.1 and 2.2), both wild-type and Δ*feoE* complemented with *feoE* displayed a significant ($p < 0.0001$) increase in log-phase growth rate over wild-type with empty vector in the presence of excess Fe^{2+} (Fig. 2.3), again suggesting that enhanced activity of FeoE facilitates greater resistance to Fe^{2+}. Of note is that growth of Δ*feoE* was not completely abolished in excess Fe^{2+}, implying that additional mechanisms of Fe^{2+} resistance exist in *S. oneidensis*.

To verify that the increased Fe^{2+} sensitivity observed by Δ*feoE* was due to higher cellular concentrations of iron, analysis of iron concentration in wild-type and Δ*feoE* strains was performed. Δ*feoE* cells with empty vector retained considerably more iron than did Δ*feoE* with pBBR1MCS-2::*feoE*, wild-type with empty vector, or wild-type with pBBR1MCS-2::*feoE*. Greater iron retention by Δ*feoE* indicates that the increased sensitivity of Δ*feoE* to Fe^{2+} (Fig. 2.3) is due to the inability of the mutant to export excess Fe^{2+} from the cytoplasm through FeoE.

Previous studies have characterized *E. coli* FieF as being an Fe^{2+}, Cd^{2+}, and/or Zn^{2+} exporter (Wei 2005, Grass 2005). FieF and FeoE have 47.7% amino acid identity, which does not enable prediction of substrate specificity (Tian 2003, Rost 2002). In order to determine whether FeoE is responsible for export of any other divalent metals known

to be substrates of cation diffusion facilitators, growth curves in LB with or without an excess of Cd^{2+}, Co^{2+}, Cu^{2+}, Mn^{2+}, Ni^{2+}, or Zn^{2+} were performed for wild-type and Δ*feoE S. oneidensis* strains. No difference was seen between the two strains in sensitivity to any of these metals (Fig. 2.4; Table 2.3), indicating that FeoE is specific for export of Fe^{2+}.

In order to compare the functionality of *S. oneidensis* FeoE to that of *E. coli* FieF, growth rates were compared between the respective mutants and complemented strains in each species. The mutant strains complemented with pBBR1MCS-2::*feoE* and pBBR1MCS-2::*fieF* had similar growth rates at Fe^{2+} concentrations of 1.0 or 2.5 mM (Fig. 2.5), but a difference in the ability of each strain to resist Fe^{2+} toxicity emerged at higher concentrations (Figs. 2.5 and 2.7). The strains carrying *fieF* had slower growth rates in the presence of higher Fe^{2+} concentrations, suggesting that FeoE activity results in more effective Fe^{2+} export. The vector and expression strategy used for *fieF* and *feoE* complementation is identical; therefore expression levels should not influence the observed activity differences in vivo.

To determine a potential explanation for the difference in transport specificity and efficiency between FeoE and FieF, we compared the protein sequences of each. Structural studies of FieF have determined that metal binding sites A and B are responsible for Zn^{2+} transport, while binding site C is important for structural integrity of the homodimer (Coudray 2013, Lu 2009). Despite an amino acid sequence identity between FeoE and FieF of 47.7%, the key metal-coordinating residues in the three metal binding sites, as well as those responsible for salt bridge formation (Lu 2009), are conserved between all 47 *E. coli* and 29 *Shewanella* strains investigated (Table 2.4), aside from one metal-binding residue at site 285 in *E. coli* M605. However, one difference was found between FieF and FeoE in a residue at the cytoplasmic end of transmembrane helix 2 (TM2). In all *E. coli* strains investigated, this residue is a glutamine at position 65, which forms a hydrogen bond with a zinc-coordinating histidine at position 75 in binding site B (Lu 2009). All *Shewanella* spp. investigated, excepting *S. denitrificans* and *S. amazonensis*, encode a valine in place of glutamine at this position. *S. denitrificans* and *S. amazonensis* encode an alanine and a threonine at this position, respectively. The substitution of glutamine, a polar residue, with a hydrophobic one such as valine could alter the conformation of binding site B, thereby changing the metal

coordination geometry. Additionally, two residues important for dimerization in *E. coli*, an aspartic acid at site 69 and a serine at site 70, also located at the base of TM2 (Lu 2009), are poorly conserved among the shewanellae. Any of these three substitutions could also affect the position of TM2 respective to TM5 and therefore change the coordination geometry of metal binding site A. Alternatively, one or more of these substitutions could influence the hinge architecture at the base of TM2, affecting the conformational change that occurs to facilitate cation exchange (Coudray 2013). Currently there is no high-resolution structural information available for FeoE. Further investigation would be needed to determine if these residues affect transport specificity and efficiency.

The difference in Fe^{2+} transport efficacy between FieF and FeoE should not be surprising considering the environmental conditions in which their respective species are found: the primary environmental niche of *E. coli* is the mammalian and avian intestinal tract (Gordon 2003, Ishii 2007), where microorganisms frequently must scavenge for adequate iron rather than mitigate the toxic effects of high iron concentrations (Raymond 2003). Meanwhile, *Shewanella* spp. thrive in the oxic/anoxic transition zones of sediments, often rich in iron and manganese cycling between their oxidized and reduced states (Nealson 2006, DiChristina 1993), causing continual shifting in the cells between aerobic and anaerobic respiratory strategies. Retaining a low concentration of intracellular iron would become especially important upon a return to oxygen respiration, in order to minimize the production of damaging reactive oxygen species. *S. oneidensis* has therefore likely evolved greater Fe^{2+} export efficiency by FeoE, affording it better survival in iron-rich, redox-active environments.

2.6 Acknowledgments

Thanks to Rick A. Knurr in the Department of Earth Sciences at the University of Minnesota for ICP-MS analysis. This work was supported by the Office of Naval Research (N000141310552). BDB was supported by the University of Minnesota Biotechnology Training Grant Program through the National Institutes of Health.

Table 2.1 Strains and plasmids used in this work.

Strain	**Description**	**Source**
JG274	S. oneidensis MR-1, wild type	Myers 1988
JG2989	JG274 Δ*feoE*	This work
JG168	JG274 with empty pBBR1MCS-2, Km^r	Hau 2008
JG2993	JG2989 with empty pBBR1MCS-2, Km^r	This work
JG2780	JG274 with pBBR1MCS-2::*feoE*, Km^r	This work
JG2994	JG2989 with pBBR1MCS-2::*feoE*, Km^r	This work
JG2997	JG2989 with pBBR1MCS-2::*fieF*, Km^r	This work
MG1655	*E. coli* K-12, wild type	Provided by Prof. Arkady Khodursky, University of Minnesota
JG3304	MG1655 Δ*fieF*	This work
JG3306	JG3304 with empty pBBR1MCS-2, Km^r	This work
JG3307	JG3304 with pBBR1MCS-2::*fieF*, Km^r	This work
JG3308	JG3304 with pBBR1MCS-2::*feoE*, Km^r	This work
UQ950	*E. coli* DH5α λ(pir) cloning host; F- Δ(*argF-lac*)169 *Φ80dlacZ58*(ΔM15) *glnV44*(AS) *rfbD1 gyrA96*(NalR) *recA1 endA1 spoT1 thi-1 hsdR17 deoR λpir+*	Saltikov 2003
WM3064	*E. coli conjugation strain; thrB1004 pro thi rpsL hsdS lacZ*ΔM15 RP4-1360 Δ(*araBAD*)*567* Δ*dapA1341*::[*erm pir*(wt)]	Saltikov 2003
Plasmid	**Description**	**Source**
pSMV3	Deletion vector, Km^r, *sacB*	Coursolle 2010
pBBR1MCS-2	Broad-range cloning vector, Km^r	Kovach 1995
pBBR1MCS-2 ::*feoE*	SO_4475 (*feoE*), 48 bp upstream, 51 bp downstream, Km^r	This work
pBBR1MCS-2 ::*fieF*	b3915 (*fieF*), 76 bp upstream, 26 bp downstream, Km^r	This work

Table 2.2 Primers used for mutant construction and complementation in this work.

Primer	Sequence	Restriction Site
4475USF	GTACGGATCCGCAGAGCGCGTAACACTTC	*Bam*HI
4475USR	GTACACTAGTCCATTGTATATCAGCTTGGCG	*Spe*I
4475DSF	GTACACTAGTGCGACACTGAATCGATTATTCAAC	*Spe*I
4475DSR	GTACGAGCTCGCTCAGTCACAGCGGCATTAACAC	*Sac*I
4475CompF	GTACGGATCCCGCCAAGCTGATATACAATGG	*Bam*HI
4475CompR	GTACACTAGTGGCATAACCACTCCTTTGATTG	*Spe*I
ECfieFUSF	GATCACTAGTCGATACCATTTTTCTTCGGC	*Spe*I
ECfieFUSR	GATCCCGCGGCATAAATACTCCCGCTATCAAC	*Sac*II
ECfieFDSF	GATCCCGCGGCGGTCTATGCTTTCATAATCAG	*Sac*II
ECfieFDSR	GATCGGATCCCATACGGGAAGCCAGAATAC	*Bam*HI
ECfiefF	GTACGGATCCCAATTTGCCTGCTGCTTAATGC	*Bam*HI
ECfiefR	GTACACTAGTGCGGGTCTGGCTCTCTTTTATAC	*Spe*I

2.7 Supplemental material

Methods

Filter disk assays.

Filter disk assays were performed using a modified version of a previously described protocol (Rugh 1996). Overnight cultures of each strain were pelleted, washed once, resuspended in fresh tryptone medium, and adjusted to an OD_{600} of 0.05. 50 µL of this suspension was spread onto tryptone medium plates with noble agar, 20 mM lactate, and 40 mM fumarate. 20 µL of 1 M $CdCl_2$, 1 M $CoCl_2$, 1 M $CuCl_2$, 6 M $FeCl_2$, 4 M $MnCl_2$, 1 M $NiCl_2$, or 1 M $ZnCl_2$ was placed onto a 6-mm filter disk in the center of the plate. Zones of growth inhibition were measured after plates were incubated anaerobically at 37°C for two days.

Fumarate and ferric citrate growth curve.

Overnight cultures of each strain were pelleted, washed once, and resuspended in fresh SBM. Cultures of anaerobic SBM supplemented with 20 mM lactate, 40 mM fumarate, and 1 mM ferric citrate were incubated with shaking at 30°C. Growth was

measured by periodically plating serial 1:10 dilutions of each culture to LB plates and performing colony counts after one day of incubation.

Table 2.3 Inhibition of wild-type and Δ*feoE* by divalent metals in filter disk assays.

	Wild-type		**Δ*feoE***	
Metal	**Ave. zone size (mm)**	**S.D. (mm)**	**Ave. zone size (mm)**	**S.D. (mm)**
$FeCl_2$	26.3	0.6	35.0	2.0
$CdCl_2$	41.0	1.0	41.0	1.0
$CoCl_2$	36.7	2.1	36.7	1.5
$CuCl_2$	31.0	1.0	31.7	0.6
$MnCl_2$	14.3	1.5	14.3	2.1
$NiCl_2$	27.3	0.6	26.3	0.6
$ZnCl_2$	21.7	3.1	21.0	0.0

Table 2.4 *Shewanella* and *E. coli* strains used for FieF and FeoE alignment

Species name	Strain	Protein Accession No.
Escherichia coli	042	CBG37114.1
Escherichia coli	101-1	EDX38712.1
Escherichia coli	55989	CAV01107.1
Escherichia coli	ABU 83972	ADN48832.1
Escherichia coli	APEC O1	ABJ03381.1
Escherichia coli	BL21(DE3)	ACT45593.1
Escherichia coli	BW2952	ACR65792.1
Escherichia coli	CFT073	AAN83294.1
Escherichia coli	DH1(ME8569)	BAJ45640.1
Escherichia coli	ED1a	CAR10725.2
Escherichia coli	FVEC1302	EFI17836.1
Escherichia coli	H299	EGI48340.1
Escherichia coli	H591	EGI43690.1
Escherichia coli	H736	EGI08350.1
Escherichia coli	HS	ABV08323.1
Escherichia coli	IAI1	CAR00891.1
Escherichia coli	IAI39	YP_002409011.1
Escherichia coli	IHE3034	ADE89170.1
Escherichia coli	K12(DH10B)	ACB04927.1
Escherichia coli	K12(MG1655)	NP_418350.1
Escherichia coli	K12(W3110)	BAE77395.1
Escherichia coli	LF82	CAP78372.1
Escherichia coli	M605	EGI13549.1
Escherichia coli	M718	EGI18796.1
Escherichia coli	NA114	AEG38898.1
Escherichia coli	NC101	EFM53266.1
Escherichia coli	NRG 857C	YP_006122251.1
Escherichia coli	O103:H2(12009)	BAI33309.1
Escherichia coli	O111:H(11128)	BAI38485.1

Escherichia coli	O127:H6(E2348/69)	CAS11767.1
Escherichia coli	O139:H28(E24377A)	KIO42250.1
Escherichia coli	O157:H7(EDL933)	AIG71382.1
Escherichia coli	O157:H7(Sakai)	NP_312867.1
Escherichia coli	O157:H7(TW14359)	ACT74675.1
Escherichia coli	O26:H11(11368)	BAI27835.1
Escherichia coli	O55:H7(CB9615)	ADD59161.1
Escherichia coli	P12b	AFG42844.1
Escherichia coli	REL606	ACT41437.1
Escherichia coli	S88	CAR05545.1
Escherichia coli	SMS-3-5	ACB16239.1
Escherichia coli	TA143	EGI29243.1
Escherichia coli	TA206	EGI24455.1
Escherichia coli	TA271	EGI33945.1
Escherichia coli	TA280	EGI38874.1
Escherichia coli	UMN026	CAR15569.1
Escherichia coli	UM146	ADN73293.1
Escherichia coli	UTI89	ABE09910.1
Shewanella sp.	38A_GOM-205M	WP_028780032.1
Shewanella sp.	ANA-3	WP_011715494.1
Shewanella sp.	ECSMB14102	WP_039034709.1
Shewanella sp.	MR-4	WP_011621062.1
Shewanella sp.	MR-7	WP_011627504.1
Shewanella sp.	POL2	WP_037425101.1
Shewanella sp.	W3-18-1	ABM23071.1
Shewanella sp.	ZOR0012	WP_047538636.1
Shewanella amazonensis	SB2B	ABM01633.1
Shewanella baltica	OS185	ABS06427.1
Shewanella baltica	OS223	ACK44795.1
Shewanella benthica	KT99	EDP98627.1
Shewanella colwelliana	ATCC 39565	WP_028762938.1

Shewanella denitrificans	OS217	ABE56734.1
Shewanella fidelis	ATCC BAA-318	WP_028769358.1
Shewanella frigidimarina	NCIMB 400	ABI70177.1
Shewanella halifaxensis	HAW-EB4	ABZ74916.1
Shewanella loihica	PV-4	ABO25434.1
Shewanella marina	JCM 15074	WP_025821863.1
Shewanella oneidensis	MR-1	WP_011074103.1
Shewanella pealeana	ATCC 700345	ABV89241.1
Shewanella piezotolerans	WP3	ACJ27086.1
Shewanella putrefaciens	200	ADV52715.1
Shewanella putrefaciens	CN-32	ABP74101.1
Shewanella sediminis	HAW-EB3	ABV34894.1
Shewanella waksmanii	ATCC BAA-643	WP_028773609.1
Shewanella woodyi	ATCC 51908	ACA84584.1
Shewanella violacea	DSS12	BAJ00217.1
Shewanella xiamenensis	BC01	KEK26877.1

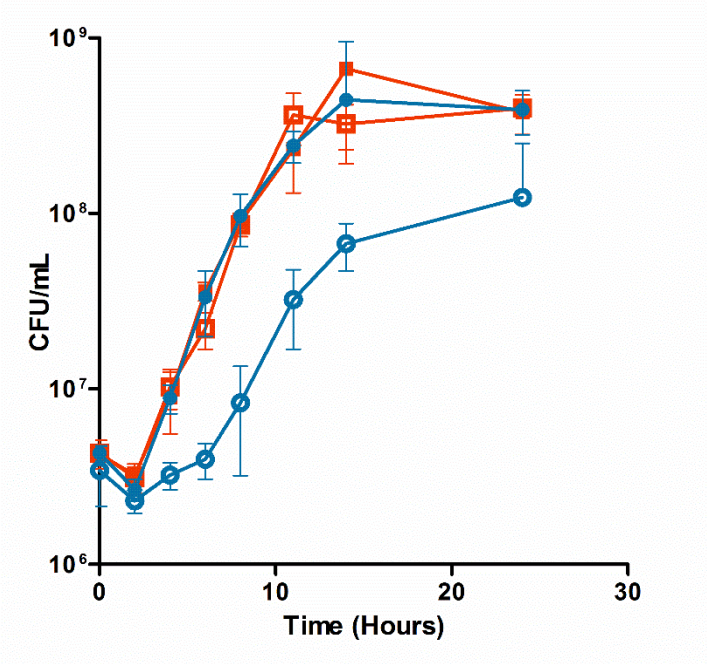

Figure 2.6 Anaerobic growth of wild-type MR-1 and Δ*feoE* strains on fumarate and ferric citrate.

The rate of growth in SBM with 20 mM lactate, 40 mM fumarate, and 1mM ferric citrate over time was measured for (○) Δ*feoE* with empty pBBR1MCS-2, (□) MR-1 with empty pBBR1MCS-2, (●) Δ*feoE* with pBBR1MCS-2::*feoE*, and (■) MR-1 with pBBR1MCS-2::*feoE*. Growth was determined by counting colony-forming units per mL of culture medium (CFU/mL).

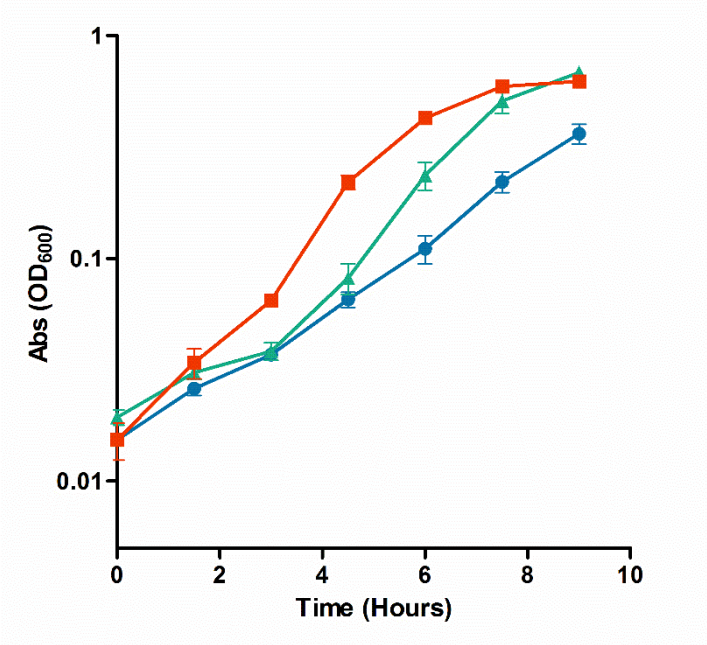

Figure 2.7 Growth of *E. coli* Δ*fieF* complemented with *fieF* or *feoE* in the presence of excess Fe^{2+}.

Growth in anaerobic LB with 20 mM lactate, 40 mM fumarate, and 7 mM $FeCl_2$ was measured for *E. coli* Δ*fieF* with (●) empty pBBR1MCS-2, (■) pBBR1MCS-2::*feoE*, or (▲) pBBR1MCS-2::*fieF*.

Chapter 3: An MgtE Homolog Acts as a Secondary Ferrous Iron Importer in *Shewanella oneidensis* MR-1

3.1 Summary

The transport of metals into and out of cells is necessary for the maintenance of appropriate intracellular concentrations. Metals are needed for incorporation into metalloproteins but become toxic at higher concentrations. Many metal transport proteins have been discovered in bacteria, including the Mg^{2+} Transporter-E (MgtE) family of passive Mg^{2+}/Co^{2+} importers. Low sequence identity exists between members of the MgtE family, indicating that substrate specificity may differ among MgtE transporters. Under anaerobic conditions, dissimilatory metal-reducing bacteria such as *Shewanella* and *Geobacter* are exposed to high levels of soluble metals including Fe^{2+} and Mn^{2+}. Here we describe the role of SO_3966, which encodes an MgtE homolog in *Shewanella oneidensis* strain MR-1 that we name FicI, in maintaining metal homeostasis. A SO_3966 deletion mutant has a growth benefit over wild-type when grown under high Fe^{2+} or Co^{2+} concentrations but exhibits wild-type Mg^{2+} transport and retention phenotypes. Conversely, deleting *feoB,* which encodes an energy-dependent Fe^{2+} importer, confers a growth defect in low Fe^{2+} concentrations but not in high Fe^{2+} conditions. FicI represents a secondary, less energy-dependent mechanism for iron uptake by *S. oneidensis* under high Fe^{2+} concentrations.

3.2 Introduction

The dissimilatory metal-reducing bacterium *Shewanella oneidensis* strain MR-1, commonly found in the oxic-anoxic transition zones of aquatic sediments (Myers 1988), can have a large impact on geochemical cycling of metals. Known for their highly versatile respiratory capacity, most *Shewanella* species are able to use numerous compounds as terminal electron acceptors, including oxygen, fumarate, nitrate, and sulfite (Myers 1988, Samuelsson 1985, Shirodkar 2011), as well as extracellular metals such as iron(III), manganese(IV), chromium(IV), arsenate(VI), uranium(IV), and cobalt(III) (Myers 1988; Myers 2000, Saltikov 2003, Truex 1997, Liu 2002). The oxidation or reduction of a metal can influence its physical properties, including solubility. Iron, for example, is commonly found in soils and sediments as an insoluble ferric (Fe^{3+}) (hydr)oxide; upon reduction to ferrous iron (Fe^{2+}), however, it may become soluble or reincorporate into mixed-valence minerals, depending on environmental conditions (O'Reilly 2005, Blöthe 2008). Therefore, as Fe^{3+} respiration by dissimilatory metal-

reducing bacteria proceeds, minerals can dissolve, releasing into the surrounding medium bioavailable metals, toxins, and nutrients that had previously been adsorbed to the minerals. When the sediment is again exposed to oxygen, the iron will become oxidized and reform into insoluble minerals. Due to the cyclic nature of the availability of electron acceptors and soluble metals in its environment, *S. oneidensis* and other bacteria living in metal-rich conditions have evolved means of rapidly adapting to changes in extracellular metal concentrations.

Microorganisms require metals to facilitate structure stability and enzymatic activity in numerous proteins, including cytochromes, peptidases, and oxidoreductases (Malmström 1964). The major mechanism by which bacteria maintain appropriate intracellular metal concentrations is through the activity of transport proteins. Numerous metal transport proteins have been described across all three domains of life, including members of the Cation Diffusion Facilitator (Nies 1995, Paulsen 1997), Metal Ion Transporter (Vidal 1993, Cellier 1995), Mg^{2+} Transporter-E (MgtE) (Smith 1995, Townsend 1995, Hattori 2007), and P-type ATPase (Pedersen 1987, Snavely 1991, Odermatt 1993) protein families. *S. oneidensis* requires a large iron supply for the production of heme groups, the redox-active cofactors in the many *c*-type cytochromes that allow *S. oneidensis* to respire numerous anaerobic electron acceptors. Bacteria have multiple mechanisms for maintenance of intracellular iron concentration: In *S. oneidensis* growing anaerobically, when Fe^{2+} levels become too high, the inner-membrane exporter FeoE removes excess Fe^{2+} from the cytoplasm (Bennett 2015). When iron levels are low, the trans-periplasmic TonB-dependent Fe^{3+} import system and the inner-membrane Fe^{2+} importer FeoB drive the uptake of iron into the cytoplasm (Wang 1969, Hantke 1987, Kammler 1993). In this work, we describe a second transport protein in *S. oneidensis* that imports Fe^{2+} under higher Fe^{2+} concentrations.

Three genes in the *S. oneidensis* genome have been annotated as encoding MgtE-family Mg^{2+}/Co^{2+} transporters: SO_1145, SO_1565, and SO_3966 (Heidelberg 2002, Daraselia 2003). Homologs of these three MgtE proteins are well conserved among many *Shewanella* species (of 36 *Shewanella* genomes, 16 encode a homolog of SO_1145, 21 encode a homolog of SO_1565, and 26 encode a homolog of SO_3966). However, the amino acid sequences encoded by each *S. oneidensis mgtE* gene share

little sequence identity with each other and with described MgtE proteins in other species (Table 3.1). While the mechanism of metal transport is likely to be similar between the *S. oneidensis* homologs and other described MgtE family members, substrate specificity is more difficult to predict (Rost 2002, Tian 2003). A Tn-Seq screen indicated that while inactivation of SO_3966 had no effect on growth rate in the presence of low Fe^{2+}, the mutation conferred a fitness benefit under high Fe^{2+} conditions; no significant fitness effect was seen for either SO_1145 or SO_1565 in either condition (Table S1). Here we characterize the function and specificity of SO_3966, which we name FicI (*f*errous *i*ron and *c*obalt *i*mporter), and describe its role in mediating cytoplasmic Fe^{2+} and Co^{2+} concentrations.

3.3 Materials and methods

Bacterial strains and growth conditions.

Bacterial strains and plasmids used in this study are summarized in Table 3.2. *S. oneidensis* MR-1 was originally isolated from Lake Oneida in New York State, USA (Myers 1988). *Escherichia coli* strains for cloning (UQ950) and transformation (WM3064) have been described previously (Saltikov 2003). Liquid Luria-Bertani (LB) cultures were supplemented with 50 µg/mL kanamycin when appropriate and grown overnight using colonies from freshly streaked -80°C stocks. *E. coli* cultures were grown at 37°C and *S. oneidensis* at 30°C; all liquid cultures were shaken at 250 rpm. Experimental cultures were grown in *Shewanella* basal medium (SBM) supplemented with 5 mL/L vitamins, 5 mL/L trace minerals, and 0.05% casamino acids (Hau 2008) or tryptone medium (15 g tryptone, 5 g NaCl, and 1 pellet NaOH per liter). Where indicated, cultures were made anaerobic by flushing with nitrogen gas and supplemented with 20 mM sodium lactate and 40 mM sodium fumarate. Co(III)ethylenediaminetetraacetic acid$^-$ ($EDTA^-$) was made as previously described (Taylor 1995). Results of all experiments are reported as the mean of three biological replicates ± one standard deviation. Statistical analysis was performed using ANOVA.

Plasmid and mutant construction.

Primers used to create deletion and expression plasmids are listed in Table 3.3. In-frame deletion of *ficI* and *feoB* from the *S. oneidensis* genome was performed as

previously described (Saltikov 2003). Briefly, 1kb fragments upstream and downstream of each gene with flanking *Sac*I and *Apa*I (*ficI*) or *Spe*I and *Bam*HI (*feoB*) restriction sites were fused via internal *Sca*I (*ficI*) or *Nhe*I (*feoB*) restriction sites and ligated into pSMV3, which has *sacB* and kanamycin-resistance cassettes. SO_1145, SO_1565, and *ficI* expression plasmids were created by cloning each gene from the *S. oneidensis* genome and inserting them into the multiple cloning site of pBBR1-MCS2 via *Kpn*I and *Sac*I (SO_1145) or *Xho*I and *Xba*I (SO_1565 and *ficI*) restriction sites.

Growth curves.

Overnight cultures of each strain were pelleted, washed once, and resuspended in 1 mL fresh tryptone or SBM. Co^{2+}, Mg^{2+}, and Fe^{2+} growth curves were performed in tryptone supplemented with 0.63, 0.65, or 0.70 mM $CoCl_2$, 230 or 300 mM $MgCl_2$, or 2.0 or 2.5 mM $FeCl_2$, respectively. Co^{3+} growth curves were performed in SBM supplemented with 20 mM sodium lactate, 40 mM sodium fumarate, and 5 mM Co(III)$EDTA^-$. Growth of tryptone cultures was measured by taking the optical density at 600nm (OD_{600}). Growth of Co(III)$EDTA^-$ cultures was measured by periodically plating serial 1:10 dilutions of culture aliquots to LB agar and counting colonies after one day of incubation. Results represent the mean of three biological replicates ± one standard deviation.

Metal retention assays.

Overnight cultures were pelleted, washed once, and resuspended in fresh tryptone. Suspensions were inoculated into aerobic tryptone (Co^{2+} and Mg^{2+} experiments) or anaerobic tryptone supplemented with 20 mM sodium lactate and 40 mM sodium fumarate (Fe^{2+} experiments) to an OD_{600} of 0.05. Cultures were incubated at 30°C until growth reached ~0.5 OD_{600}. $CoCl_2$, $MgCl_2$, or $FeCl_2$ was added to cultures at a concentration of 0.7 mM, 230 mM, or 2.5 mM, respectively, and the cultures were incubated for a further one hour. Cultures were pelleted, washed once in 0.9% NaCl, and resuspended in deionized water. Cell suspensions were analyzed for cobalt, magnesium, or iron concentration using inductively coupled plasma mass spectrometry (ICP-MS) at the Analytical Geochemistry Lab in the Department of Earth Sciences at the

University of Minnesota. Metal concentrations were normalized to the final OD_{600} before pelleting.

3.4 Results

*Δ*ficI *is less sensitive to* Fe^{2+}*.*

A Tn-Seq screen indicated that mutations in *ficI* enhanced resistance to high levels of Fe^{2+} under anaerobic conditions (Table S1). To confirm the results of the transposon screen, an in-frame deletion of *ficI* was made in *S. oneidensis*. Δ*ficI* and wild-type *S. oneidensis* containing either empty vector (pBBR1MCS-2) or a complementation vector (pBBR1MCS-2::*ficI*) were grown anaerobically in tryptone medium with and without 2 mM $FeCl_2$. Δ*ficI* displayed no difference in phenotype from wild-type while growing in tryptone without metal supplementation (doubling time of 0.90 ± 0.08 and 0.88 ± 0.08 hours, respectively). When $FeCl_2$ was added to the medium, Δ*ficI* with empty vector displayed enhanced growth compared to wild-type with empty vector (Fig 3.1). Complementation with *ficI* into either wild-type or the Δ*ficI* mutant enhanced sensitivity to Fe^{2+} in both strains (Fig 3.1); wild-type with empty vector had the same growth phenotype as the complemented Δ*ficI* strain.

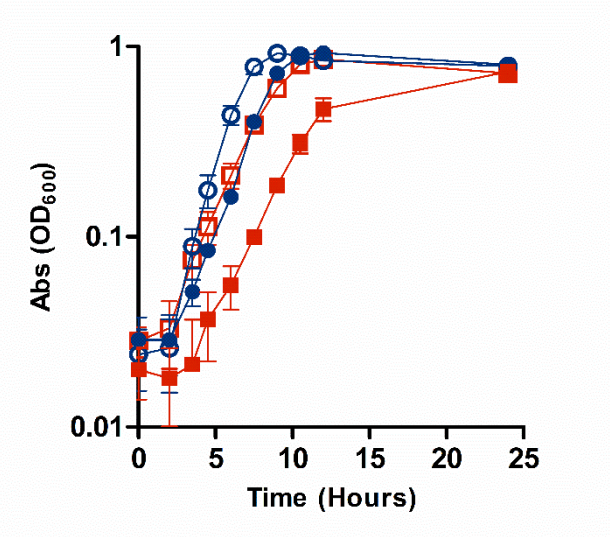

Figure 3.1 Anaerobic growth of wild-type and Δ*ficI* strains with excess $FeCl_2$. The rate of growth in anaerobic tryptone with 20 mM lactate, 40 mM fumarate, and 2 mM $FeCl_2$ was measured for (□) wild-type with empty pBBR1MCS-2, (■) wild-type with pBBR1MCS-2::*ficI*, (○) Δ*ficI* with empty pBBR1MCS-2, and (●) Δ*ficI* with pBBR1MCS-2::*ficI*.

Deletion of ficI *decreases cellular iron retention.*

To determine whether the decreased Fe^{2+} sensitivity of Δ*ficI* was due to altered Fe^{2+} uptake, iron retention assays were performed. Δ*ficI* and wild-type with empty or complementation vectors were grown anaerobically in tryptone medium with 20 mM lactate and 40 mM fumarate into log phase (~0.5 OD_{600}) and then supplemented with 2.5 mM $FeCl_2$. Cultures were harvested after one hour of further incubation and analyzed by ICP-MS for total iron content. Wild-type and Δ*ficI* carrying empty vector retained approximately half the concentration of iron ($p < 0.0001$) than did wild-type or Δ*ficI* carrying the *ficI* complementation vector (Table 3.4).

FicI imports Co^{2+} but not Mg^{2+}.

MgtE proteins have been described in other bacterial species as importers of Mg^{2+} and Co^{2+} (Smith 1995, Townsend 1995). To determine whether FicI imports either

of these metals in addition to Fe^{2+}, cultures of Δ*ficI* and wild-type *S. oneidensis* were grown in tryptone with either 0.7 mM $CoCl_2$ or 230 mM $MgCl_2$. No difference in sensitivity to Mg^{2+} was seen between wild-type and Δ*ficI*; however, Δ*ficI* displayed a faster growth rate than wild-type when grown with excess Co^{2+} (Fig. 3.2). To determine whether the increased growth rate seen for Δ*ficI* in excess Co^{2+} was due to a decrease in Co^{2+} uptake, Co^{2+} retention assays were performed on cultures grown in tryptone supplemented with 0.7 mM $CoCl_2$. Δ*ficI* retained over 50% less ($p < 0.0001$) Co^{2+} than did wild-type (Table 3.4).

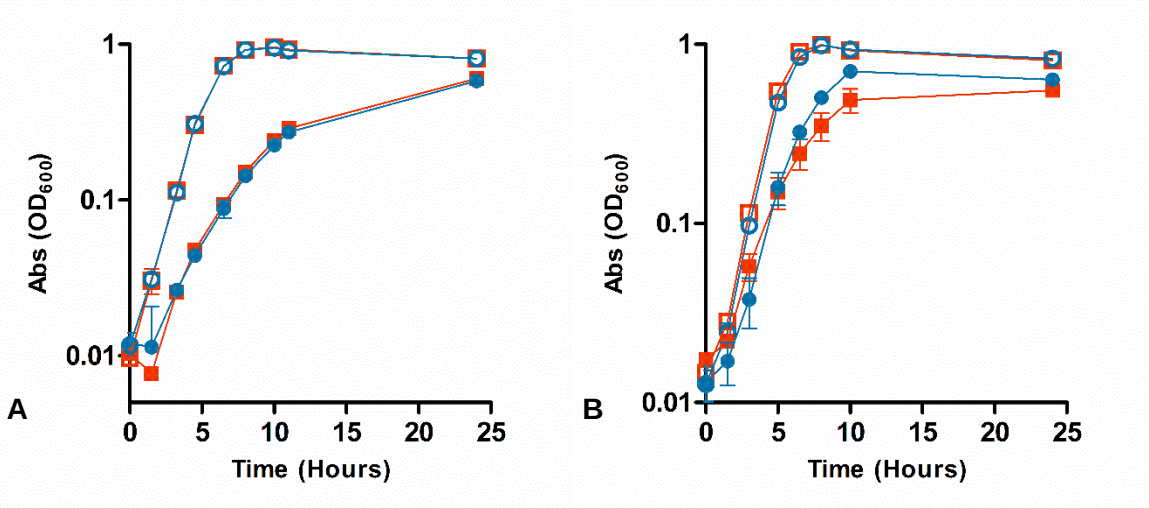

Figure 3.2 Growth of wild-type and Δ*ficI* with excess $MgCl_2$ or $CoCl_2$.
The rate of growth was measured in anaerobic tryptone with 20mM lactate, 40 mM fumarate, and (A) 0 mM or 230 mM $MgCl_2$ or (B) 0 mM or 0.7 mM $CoCl_2$. (□) wild-type with no metal added; (○) Δ*ficI* with no metal added; (■) wild-type with metal added; (●) Δ*ficI* with metal added.

*Δ*ficI *has a survival benefit during Co(III)EDTA$^-$ respiration.*

Since deletion of *ficI* conferred a faster growth rate over wild-type in the presence of a high concentration of Co^{2+}, we hypothesized that deletion of *ficI* would confer a benefit under Co^{3+} respiration conditions. Wild-type and Δ*ficI* were grown anaerobically

in SBM with 20 mM lactate, 40 mM fumarate, and 5 mM Co(III)EDTA$^-$. No difference in growth rate was seen for the two strains; however, after entry into stationary phase, wild-type displayed a significant survival defect compared to Δ*ficI* (Fig. 3.3).

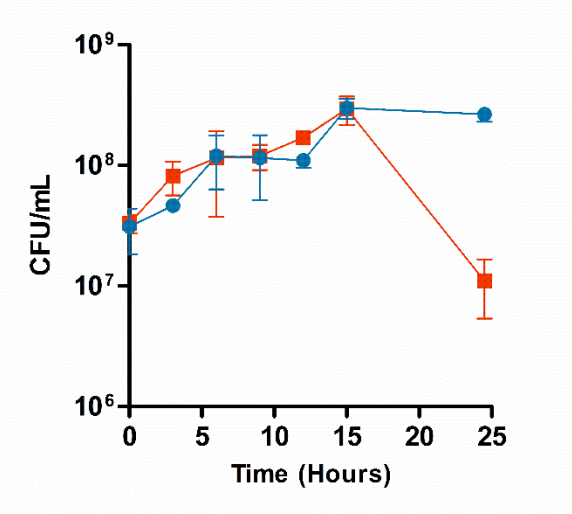

Figure 3.3 Anaerobic growth of wild-type and Δ*ficI* on Co(III)EDTA$^-$.
The rate of growth in anaerobic SBM with 20 mM lactate, 40 mM fumarate, and 5 mM Co(III)EDTA$^-$ was measured for (■) wild-type and (●) Δ*ficI*. Growth was determined by counting colony-forming units per mL of culture medium (CFU/mL).

No MgtE homologs encoded by S. oneidensis *transport Mg^{2+}.*

To determine the substrate specificity of the other two MgtE homologs encoded by the *S. oneidensis* genome, SO_1155 and SO_1565, growth curves with an excess of Co^{2+}, Mg^{2+}, or Fe^{2+} were performed. Cultures of wild-type *S. oneidensis*, ΔSO_1155, ΔSO_1565, and Δ*ficI* were grown anaerobically in tryptone with or without 2.5 mM $FeCl_2$ or 0.63 mM $CoCl_2$. Only Δ*ficI* displayed a growth benefit in the presence of either excess Fe^{2+} or Co^{2+} (Fig. 3.4). Cultures of the wild-type strain carrying empty pBBR1MCS-2, pBBR1MCS-2::SO_1145, pBBR1MCS-2::SO_1565, or pBBR1MCS-2::*ficI* were grown aerobically in tryptone with or without 0.65 mM $CoCl_2$ or 300 mM $MgCl_2$, or anaerobically in tryptone supplemented with 20 mM lactate and 40 mM fumarate with or without 2.5

mM $FeCl_2$. No difference in growth rate was observed between any of the four strains under excess Mg^{2+} conditions (Fig. 3.5A). Each strain of wild-type overexpressing an *mgtE* homolog displayed a slower growth rate under high Fe^{2+} or Co^{2+} conditions than wild-type with empty vector (Figs. 3.5B and 3.5C).

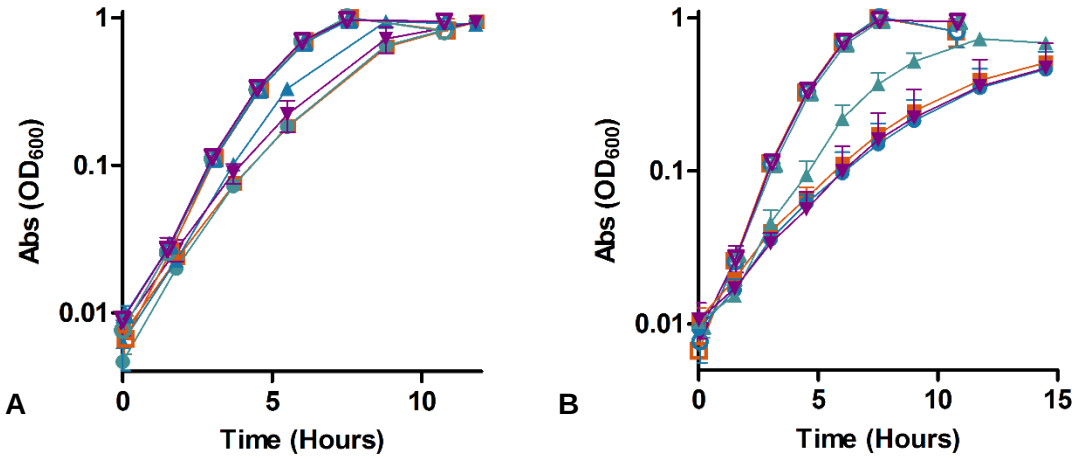

Figure 3.4 Anaerobic growth of wild-type, ΔSO_1145, ΔSO_1565, and Δ*ficI* in excess Fe^{2+} and Co^{2+}.

The rate of growth in anaerobic LB with 20 mM lactate, 40 mM fumarate, and A) 2.5 mM $FeCl_2$ or B) 0.63 mM $CoCl_2$ was measured for (□/■) wild-type *S. oneidensis*, (○/●) ΔSO_1145, (Δ/▲) ΔSO_1565, and (▽/▼) Δ*ficI*. No metal added, empty symbols; excess metal, closed symbols.

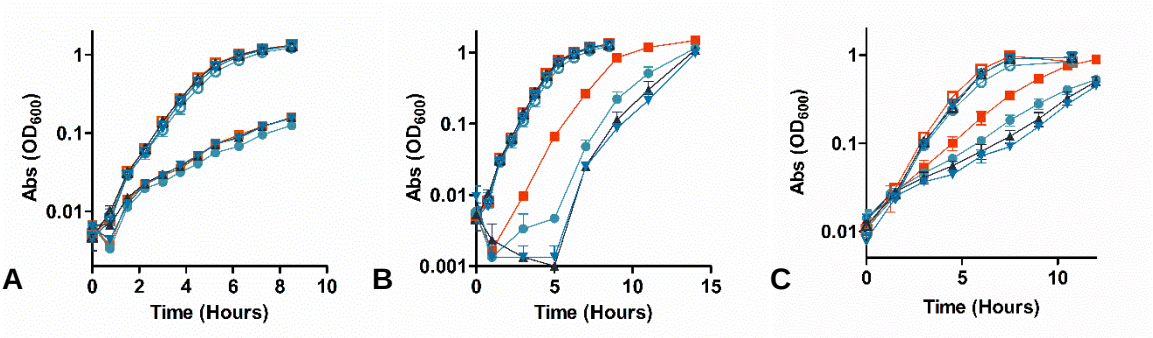

Figure 3.5 Growth of wild-type strains overexpressing *mgtE* homologs.
The rate of growth was measured in (A) aerobic tryptone with or without 300 mM $MgCl_2$, (B) aerobic tryptone with or without 0.65 mM $CoCl_2$, or (C) anaerobic tryptone with 20 mM lactate, 40 mM fumarate, and 2.5 mM $FeCl_2$. Wild-type with (□/■) empty pBBR1MCS-2, (○/●) pBBR1MCS-2::SO_1145, (Δ/▲) pBBR1MCS-2::SO_1565, (▽/▼) pBBR1MCS-2::*ficI*. No metal added, empty symbols; excess metal, closed symbols.

ficI *and* feoB *mutants vary in* Fe^{2+} *requirement and sensitivity.*

The iron retention phenotypes of strains either missing *ficI* or with enhanced expression of *ficI* are consistent with a role for this putative transporter in Fe^{2+} import. The *S. oneidensis* genome also encodes the energy-dependent FeoAB import system, which has been described as the primary Fe^{2+} importer in multiple bacterial species (Kammler 1993, Velayudhan 2000). To determine the conditions under which FeoB and FicI import Fe^{2+}, cultures of wild-type *S. oneidensis*, Δ*feoB*, and Δ*ficI* were grown anaerobically in tryptone supplemented with 20 mM lactate and 40 mM fumarate, with and without 2 mM $FeCl_2$. In conditions without added Fe^{2+}, Δ*ficI* and wild-type displayed the same growth phenotype, whereas Δ*feoB* displayed a significantly slower growth rate (Fig. 3.6A). Under high Fe^{2+} conditions, Δ*feoB* displayed the same growth rate as wild-type, while Δ*ficI* had a faster growth rate than the two other strains (Fig. 3.6B).

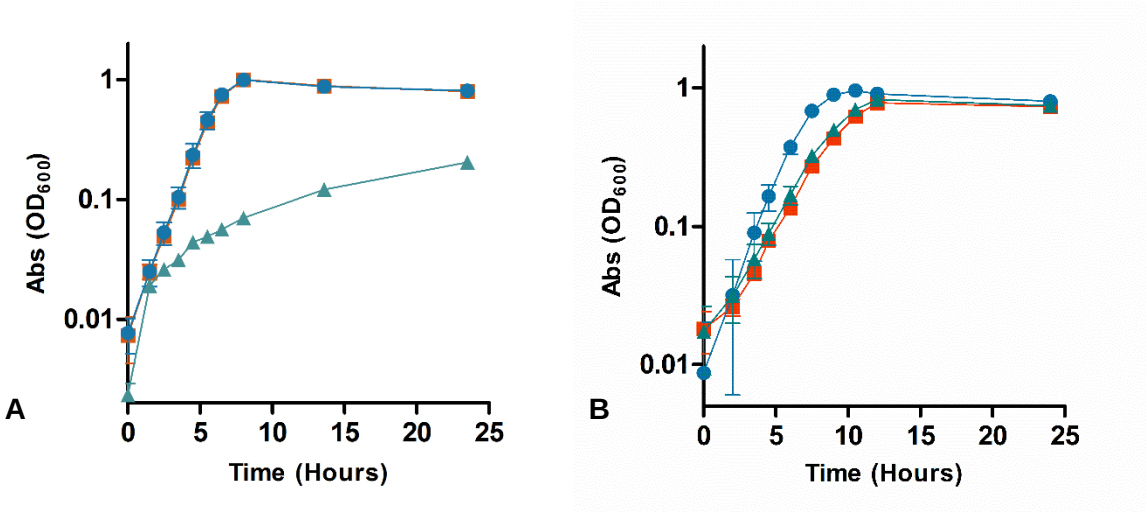

Figure 3.6 Growth of wild-type, Δ*ficI*, and Δ*feoB* strains.

The rate of growth in anaerobic tryptone with 20 mM lactate, 40 mM fumarate, and (A) without or (B) with 2 mM $FeCl_2$ was measured for (■) wild-type, (●) Δ*ficI*, and (▲) Δ*feoB*.

3.5 Discussion

The import of metals, and the maintenance of intracellular metal homeostasis, is crucial for the growth and survival of all types of living cells. As such, transport proteins for the import and export of biologically relevant metals have evolved in all three domains of life. Here we have described an Fe^{2+} and Co^{2+} importer in *S. oneidensis* that belongs to the MgtE protein family, which have until now been described as inner-membrane Mg^{2+} and Co^{2+} importers (Smith 1995, Townsend 1995).

Deletion of *ficI* increases resistance to a high Fe^{2+} concentration compared to wild-type, while overexpressing *ficI* confers increased Fe^{2+} sensitivity (Fig. 3.1). There was no difference between Δ*ficI* and wild-type during growth without added Fe^{2+} (Fig. 3.6A), indicating that Δ*ficI* does not have an inherently faster growth rate than wild-type. Strains overexpressing *ficI* retain approximately twice as much iron than those with empty vector (Table 3.4). Taking the phenotypes observed in Fe^{2+} growth curves together with the iron retention results, uptake of and sensitivity to Fe^{2+} appears to increase concomitantly with copies of *ficI*, supporting the hypothesis that *ficI* encodes a Fe^{2+} importer.

As MgtE proteins have previously been described as Mg^{2+} and/or Co^{2+} importers, we wanted to determine whether FicI imports either of these metals in addition to Fe^{2+}. Δ*ficI* had the same phenotype as wild-type when grown in excess Mg^{2+} but had a growth benefit over wild-type when grown in excess Co^{2+} (Fig. 3.2). Metal retention assays showed that while Δ*ficI* cells contained less cobalt than wild-type, there was no difference in magnesium content between the strains (Table 3.4). Together these results indicate that *ficI* encodes a transporter that imports Fe^{2+} and Co^{2+} but not Mg^{2+}. We also determined that, due to the uptake of Co^{2+} by FicI, deletion of *ficI* confers a survival benefit during respiration of Co(III)EDTA^{-} and consequent production of Co^{2+} (Fig. 3.3). The uptake of Fe^{2+} or Co^{2+} via FicI could be a double-edged sword for *S. oneidensis*: FicI presents a lower energy option for obtaining metals required for cellular functions, but excessive influx can cause toxicity, as seen when Δ*ficI* is exposed to high concentrations of either metal (Fig. 3.1, Fig. 3.2B).

Three genes in the *S. oneidensis* genome have been annotated as encoding MgtE homologs: SO_1145, SO_1565, and FicI. As FicI does not appear to transport Mg^{2+}, we wanted to determine the activity of the proteins encoded by SO_1145 and SO_1565. In a transposon screen, inactivation of SO_1145 and SO_1565 had no significant fitness effect under either normal or high Fe^{2+} concentrations (Table S1). Additionally, deletion of SO_1145 or SO_1565 conferred no change in growth rate in the presence of excess Fe^{2+} or Co^{2+} (Fig. 3.4). Surprisingly, when SO_1145, SO_1565, and *ficI* were over-expressed in wild-type, all three strains displayed increased sensitivity over wild-type with empty vector to high levels of both Fe^{2+} and Co^{2+}, but none enhanced sensitivity to Mg^{2+} (Fig. 3.5). The Mg^{2+} growth curves indicate that none of the MgtE homologs in *S. oneidensis* is an Mg^{2+} importer under the conditions we tested, underscoring the importance of determining a gene's physiological role with experimental data.

Aside from MgtE, three other families of Mg^{2+} importers have been discovered in bacteria: CorA, MgtA, and MgtB (Hmiel 1989). CorA, like MgtE, is predicted to be an ion channel that imports cations along an electrochemical gradient (Lunin 2006), while MgtA and MgtB are P-type ATPases (Snavely 1991, Tao 1995). There are no genes annotated as *mgtA* or *mgtB* homologs in the *S. oneidensis* genome, but there is a

predicted *corA* gene. CorA is more widespread in bacteria and has been shown to have a lower K_m than MgtA, MgtB, or MgtE in other Gammaproteobacteria species (Hmiel 1986, Townsend 1995), suggesting that CorA is most likely to be the primary Mg^{2+} importer even in species encoding multiple Mg^{2+} transporters. As no other Mg^{2+} import genes are annotated in the MR-1 genome, we postulate that CorA is the predominant Mg^{2+} importer in *S. oneidensis*.

Global expression profiles of *S. oneidensis* have reported no differential expression for SO_1145, SO_1565, or *ficI* under numerous conditions, including respiration of various substrates including iron and other metals (Beliaev 2002, Beliaev 2005, Bencheikh-Latmani 2005), metal stress (Brown 2006a, Brown 2006b), or deletion of the iron-response regulator Fur (Thompson 2002, Wan 2004). SO_1145 expression may increase approximately twofold upon exposure to alkaline pH (Leaphart 2006), the only condition shown to induce an expression change for any of these three genes. The discrepancy between the phenotypes observed for transposon and deletion mutants (Table S1, Fig. 3.4) and over-expression strains (Fig. 3.5), along with the results from various expression profiles, indicates that SO_1145 and SO_1565 are likely expressed at low levels in wild-type cells, at least in the conditions tested thus far. Low expression of SO_1145 and SO_1565 could indicate that the proteins encoded by SO_1145 and SO_1565 are not normally produced under the conditions tested in our experiments, explaining why knocking out each gene would not manifest in a detectable phenotype. Overexpression of each gene indicates that the function of each of the three MgtE transporters in *S. oneidensis* is the import of Fe^{2+} and Co^{2+}; however, the transport by SO_1145 and SO_1565 is likely to be low under physiologically relevant conditions. The evolutionary imperative for retaining all three *mgtE* genes in the *S. oneidensis* genome remains unclear at this time.

The deactivation of *feoB*, which encodes an Fe^{2+} importer (Wang 1969, Kammler 1993), confers a strong fitness defect in lower Fe^{2+} conditions but has little effect on growth in high Fe^{2+} (Table S1, Fig. 3.6). Conversely, a *ficI* mutant has the same growth rate as wild-type under lower Fe^{2+} conditions but is less sensitive to high Fe^{2+} (Table S1, Fig. 3.6). These results indicate that FeoB is likely the primary importer of Fe^{2+} when concentrations are low, and the transporter encoded by *ficI* is likely a secondary importer

active only when extracellular Fe^{2+} concentrations are high. That *S. oneidensis* has evolved to have two separate systems for Fe^{2+} import should not be surprising considering that it inhabits redox transition zones of metal-rich sediments (Myers 1988). The transitory respiration of solid Fe^{3+} minerals creates temporary high local concentrations of soluble Fe^{2+} available for uptake. Additionally, *S. oneidensis* respires numerous substrates anaerobically and therefore produces more cytochromes than, for example, *E. coli* or *Salmonella enterica,* and it thus has a high requirement for iron. As such, it is likely that *S. oneidensis* has adapted to have two different systems for Fe^{2+} transport under different conditions: FeoB, which uses nucleotide hydrolysis to take up Fe^{2+} (Kammler 1993, Velayudhan 2000), and FicI, a member of the MgtE family of passive metal importers (Takeda 2014). In this way, *S. oneidensis* can maximize energy conservation by using FicI to import Fe^{2+} under higher local Fe^{2+} concentrations during periods of anaerobic iron respiration and lower ATP production.

3.6 Conclusion

Metal-respiring bacteria have adapted to metal-rich environments and large fluctuations in local concentrations of soluble metals. Their mechanisms for maintenance of metal homeostasis are extremely important for survival. Here we have discovered a transport protein in *S. oneidensis* that imports Fe^{2+} and Co^{2+}, which was unexpected based on phenotypic descriptions of MgtE proteins in other bacterial species. Additionally, we have determined that none of the three MgtE homologs encoded by the *S. oneidensis* genome is an Mg^{2+} importer, but all three can import Fe^{2+} and Co^{2+}. Furthermore, we posit that while SO_1145 and SO_1565 may not import physiologically relevant concentrations of Fe^{2+}, FicI represents a secondary, less energy-dependent Fe^{2+} importer active under high Fe^{2+} concentrations.

Table 3.1 Amino acid identities between MgtE homologs.

	SO_1145	SO_1565	FicI	*Providencia stuartii*	*Thermus thermophilus* HB8	*Pseudomonas aeruginosa* PAO1
SO_1565	23%					
FicI	24%	36%				
Providencia stuartii	31%	24%	25%			
Thermus thermophilus HB8	33%	25%	29%	33%		
Pseudomonas aeruginosa PAO1	27%	35%	40%	28%	29%	
Aeromonas piscicola AH-3	29%	25%	25%	55%	35%	27%

Table 3.2 Strains and plasmids used in this work.

Strain	Description	Source
JG274	*S. oneidensis* MR-1, wild type	Myers 1988
JG3275	JG274 Δ*ficI* (SO_3966)	This work
JG168	JG274 with empty pBBR1MCS-2	Hau 2008
JG3376	JG3275 with empty pBBR1MCS-2	This work
JG379	JG3275 with pBBR1MCS-2::*ficI*	This work
JG3373	JG274 with pBBR1MCS-2:: SO_1145	This work
JG3374	JG274 with pBBR1MCS-2:: SO_1565	This work
JG3375	JG274 with pBBR1MCS-2::*ficI*	This work
JG3574	JG274 Δ*feoB* (SO_1784)	This work
UQ950	*E. coli* DH5α λ(pir) cloning host; F- Δ(*argF-lac*)169 Φ80dlacZ58(ΔM15) glnV44(AS) rfbD1 gyrA96(NalR) recA1 endA1 spoT1 thi-1 hsdR17 deoR λpir+	Saltikov 2003
WM3064	*E. coli* conjugation strain; *thrB1004 pro thi rpsL hsdS lacZΔM15 RP4-1360 Δ(araBAD)567 ΔdapA1341::[erm pir(wt)]*	Saltikov 2003

Plasmid	Description	Source
pSMV3	Deletion vector, Km^r, *sacB*	Coursolle 2010
pBBR1MCS-2	Broad-range cloning vector, Km^r	Kovach 1995
pBBR1MCS-2:: SO_1145	SO_1145, 11 bp upstream, 54 bp downstream, Km^r	This work
pBBR1MCS-2:: SO_1565	SO_1565, 18 bp upstream, 15 bp downstream, Km^r	This work
pBBR1MCS-2::*ficI*	*ficI*, 39 bp upstream, 24 bp downstream, Km^r	This work

Table 3.3 Primers used for mutant construction and complementation in this work.

Primer	Sequence	Restriction Site
FeoBUSF	GTACACTAGTGTTATGATTACCCAGCGGG	*Spe*I
FeoBUSR	GTACGCTAGCGTGACGCAATGAAACTGCTTAG	*Nhe*I
FeoBDSF	GTACGCTAGCCGGATTATTACTGAGTAAACCC	*Nhe*I
FeoBDSR	GTACGGATCCCTCATATTGACGAGTACGATTTGG	*Bam*HI
3966USF	GTACGAGCTCCCATTAAACTCGAAGGCAAGC	*Sac*I
3966USR	GTACAGTACTCATGTTTCCTCCAGGGTG	*Sca*I
3966DSF	GTACAGTACTGCGACCTTGTATTTAATGCACTAG	*Sca*I
3966DSR	GTACGGGCCCCATTGATGGCGGGTATGG	*Apa*I
1145CompF	GTACGGTACCGAGAATGAACTATGAACATGAAC	*Kpn*I
1145CompR	GTACGAGCTCGCTCGTACCTTTTACGCAGC	*Sac*I
1565CompF	GTACCTCGAGCAGCAGAAGGGCGTTTAG	*Xho*I
1565CompR	GTACTCTAGACGCTTAATATCAAACTTAAAGG	*Xba*I
3966CompF	GTACCTCGAGCAACCTATGCTCCACCGC	*Xho*I
3966CompR	GTACTCTAGAGCTTTAGCAAGGCTTGGG	*Xba*I

Table 3.4 Metal retention by wild-type and Δ*ficI* strains.

Strain	**Average Fe (ng*OD_{600}^{-1}*mL^{-1})**	**S.D.**
Wild-type + empty pBBR1MCS-2	109.1	12
Wild-type + pBBR1MCS-2::*ficI*	225.5	15.1
Δ*ficI* + empty pBBR1MCS-2	99.9	4
Δ*ficI* + pBBR1MCS-2::*ficI*	200.9	16.32

Strain	**Average Co (ng*OD_{600}^{-1}*mL^{-1})**	**S.D.**
Wild-type	55.4	2.1
Δ*ficI*	26	1.4

Strain	**Average Mg (ng*OD_{600}^{-1}*mL^{-1})**	**S.D.**
Wild-type	204.2	10.4
Δ*ficI*	204.6	13.2

Chapter 4: The Protease ClpXP is Required for Fe^{2+} Resistance by *Shewanella oneidensis* MR-1

4.1 Summary

Shewanella oneidensis MR-1 is a versatile bacterium capable of respiring extracellular, insoluble ferric oxide minerals under anaerobic conditions. The respiration of iron minerals results in the production of soluble ferrous ions, which at high concentrations are toxic to living organisms. It is not fully understood how Fe^{2+} is toxic to cells anaerobically; nor is it fully understood how *S. oneidensis* is able to resist high levels of Fe^{2+}. Here we describe the results of a transposon screen and deletion of the genes *clpX* and *clpP* in *S. oneidensis*, which indicate that the protease ClpXP is required for anaerobic Fe^{2+} resistance. Many cellular processes are regulated by ClpXP, including entry into stationary phase, envelope stress response, and the turnover of stalled ribosomes. None of these processes, however, appear to be responsible for mediating Fe^{2+} resistance in *S. oneidensis*. Protein trapping studies to identify ClpXP targets indicate that ClpXP degrades metalloproteins in *S. oneidensis* under Fe^{2+} stress. These data indicate that Fe^{2+} may be toxic under anaerobic conditions by becoming misincorporated into non-iron metalloproteins, causing misfolding. These misfolded, mismetallated proteins may then become targets for degradation by ClpXP in order to prevent the cytoplasmic buildup of nonfunctional proteins.

4.2 Introduction

The bacterium *Shewanella oneidensis* MR-1 is a member of the gammaproteobacteria that resides in the oxic-anoxic transition zones of water columns and aquatic sediments (Myers 1988, Nealson 1991, Brettar 1993). *S. oneidensis* is a facultative anaerobe able to utilize numerous compounds as terminal electron acceptors in the absence of oxygen, including nitrate, sulfite, trimethylamine N-oxide, fumarate (Samuelsson 1985, Shirodkar 2011, Myers 1988), and metals such as iron and manganese (hydr)oxide minerals (Myers 1988, Kostka 1995), which are frequently abundant in aquatic sediments (Canfield 1989). The respiration of and consequent change in oxidation state of a metal can influence that metal's solubility. For example, ferric iron (Fe^{3+}) is often found in sediments as insoluble iron oxides (Schwertmann 1991), but upon reduction, these minerals can dissolve and release soluble Fe^{2+} (Schwertmann 1991, O'Reilly 2005).

Like many transition metals, iron is required for numerous biological functions (Riordan 1977), but at higher concentrations it becomes toxic to organisms (Moore 1908, Stohs 1995, Dunning 1998). Fe^{2+} toxicity during aerobic respiration is believed to be due to oxidative stress resulting from the production of hydroxyl radicals (Sutton 1985, Touati 1995, Stohs 1995), but the mechanism for anaerobic Fe^{2+} toxicity is not known. *S. oneidensis* is capable of tolerating millimolar levels of Fe^{2+} anaerobically (Kostka 1995), higher than many other bacterial species (Berman 1993, Kersters 1996, Dunning 1998), likely due to its adaptation to metal-rich environments. *S. oneidensis* is able to limit the buildup of intracellular iron via the activities of the iron uptake regulator Fur, which suppresses the production of siderophores and iron import systems under iron-replete conditions (Hantke 1981, Wan 2004, Yang 2008). The inner-membrane efflux protein FeoE removes excess Fe^{2+} from the cytoplasm produced during Fe^{3+} respiration and lowers Fe^{2+} sensitivity (Bennett 2015). To discover other Fe^{2+} resistance mechanisms encoded in the *S. oneidensis* genome, and to look for mechanisms of anoxic Fe^{2+} toxicity, we performed a transposon screen under excess Fe^{2+} conditions. In this paper, we present two genes that, upon inactivation, conferred a defect in the presence of excess Fe^{2+}: *clpP* and *clpX*.

clpP and *clpX* encode the AAA+ (ATPases associated with diverse cellular activities) cytoplasmic protease ClpXP. The ATP-dependent unfoldase ClpX recognizes substrate proteins (Wojtkowiak 1993) and feeds them into the serine protease ClpP, which degrades the unfolded target proteins into small peptides (Hwang 1987, Katayama 1987). ClpXP is one of five AAA+ proteases encoded in the *S. oneidensis* genome, the other four being ClpAP, Lon, HslVU, and FtsH (Gottesman 1990, Chung 1981, Charette 1981, Chuang 1993, Herman 1993). Of the genes encoding these five AAA+ proteases, only deactivation of *clpX* and *clpP* conferred a significant defect in the presence of excess Fe^{2+} in the above-mentioned transposon screen. ClpXP has several roles in bacterial cells, including regulating entry to stationary phase via degradation of the stress response regulator σ^S, degradation of cell division proteins, promoting release of the envelope stress response regulator σ^E, and turning over ribosomes by degrading proteins stalled during translation (30–36). Here we investigate the role of ClpXP in

responding to Fe^{2+} stress in *S. oneidensis*, which appears to be unrelated to previously described cellular processes in which ClpXP is involved.

4.3 Materials and methods

Bacterial strains and growth conditions.

Table 4.1 lists bacterial strains and plasmids used in this work. *S. oneidensis* MR-1 was isolated from Lake Oneida, New York State (Myers 1988). *Escherichia coli* strains for cloning (UQ950) and mating (WM3064) are described in Saltikov et al (2003). Overnight liquid Luria-Bertani (LB) cultures, supplemented with 50mg/mL kanamycin when appropriate, were inoculated from freshly streaked -80°C stocks. *S. oneidensis* and *E. coli* cultures were grown at 30°C and 37°C, respectively. Cultures were grown in LB or *Shewanella* basal medium (Hau 2008) supplemented with 5 mL/L vitamins, 5 mL/L trace minerals, and 0.05% casamino acids. Anaerobic cultures were flushed with nitrogen gas and supplemented with 20 mM sodium lactate and 40 mM sodium fumarate. Liquid cultures, except for 1 L cultures prepared for protein purification, were shaken at 250 rpm.

Creation and analysis of Tn-Seq mutant libraries.

Transposon library creation and selection were performed as previously described (Brutinel 2012). Briefly, a delivery vector with MmeI restriction sites surrounding the MiniHimar transposon, which is randomly inserted into a chromosomal TA site (Bouhenni 2005), was transferred into wild-type and Δ*feoE S. oneidensis* strains via conjugation. Parent transposon libraries were outgrown for selection in anaerobic *Shewanella* basal medium with or without 0.8 mM $FeCl_2$. Cultures were harvested and DNA extracted after approximately five doublings. Parent and outgrown DNA libraries were processed and sequenced as previously described (van Opijnen 2009). Adapters and primers used to prepare the DNA for sequencing have been published previously (van Opijnen 2010). Briefly, DNA was phenol-chloroform extracted and digested with MmeI. Adapters containing library-identifying barcodes were ligated to the digested DNA, and the transposon-insertion sites were PCR-amplified using primers containing Illumina-specific sequences. Single-read, 50 base-pair sequence analysis was performed on an Illumina HiSeq250 at the University of Minnesota Genomics Center.

Downstream sequence processing was performed using the Galaxy server maintained by the Minnesota Supercomputing Institute. Between 20 million and 33 million reads were mapped to the *S. oneidensis* chromosome and megaplasmid (NC_004347.2 and NC_004349.1, respectively) for each parent and outgrown library. Reads that did not match the genome sequence 100%, did not match uniquely to a gene, or fell in the first 1% or last 10% of the coding sequence were omitted from analysis. The number of reads for each gene was normalized to the total number of reads in each library. Fitness effects of each gene under the outgrowth conditions were calculated by taking the natural log of the normalized number of reads in the outgrowth libraries divided by that in the parent library. Tn-Seq results are reported in Table S1. To exclude genes that confer a growth benefit or defect upon deactivation regardless of Fe^{2+} concentration, the net fitness effect of growing in excess Fe^{2+} for each gene was calculated by subtracting the fitness effect for the low Fe^{2+} condition from that in the high Fe^{2+} condition. A net fitness effect of ≥ ± 1.0 was considered significant.

Plasmid and mutant construction.

Table 4.2 lists primers used for construction of deletion and expression plasmids. In-frame deletion of genes was performed via homologous recombination as described in Saltikov et al (2003). Briefly, 1kb upstream and downstream fragments for each gene were fused via a restriction site and inserted into the multiple-cloning site of pSMV3, which has kanamycin-resistance and *sacB* cassettes. Complementation plasmids were created by cloning *clpPX* from the *S. oneidensis* genome and *clpPX* and *clpX* from *E. coli* MG1655 genome and inserted into the multiple cloning site of pBBR1MCS-2 via *Bam*HI and *Spe*I restriction sites. Tagged genes for protein purification were ordered as gBlocks from Integrated DNA Technologies and ligated into the expression vector pBBR1MCS-2 via *Eco*RI and *Bam*HI restriction sites. Tagged alleles of *clpP* were created without the propeptide sequence (Δ2-9), a C-terminal affinity (His_6-TEV-Myc_3) tag codon-optimized for *S. oneidensis*, and with or without a point mutation in the active site (S106A), creating $clpP^{Trap}$ and $clpP^{Tag}$, respectively. $clpP^{Tag}$ and $clpP^{Trap}$ sequences are listed in Table 4.2.

Growth curves.

Overnight liquid LB cultures were grown from freshly streaked -80°C stocks. Cells were pelleted, washed once, and resuspended in LB or tryptone. Fe^{2+} cultures were supplemented with 2 or 2.5 mM $FeCl_2$. A higher Fe^{2+} concentration was needed for growth curves than in Tn-Seq to visualize the growth defects of mutants. Growth was measured by taking the optical density at 600 nm (OD_{600}). Results are reported as the mean ± one standard deviation of three biological replicates.

ClpP trapping and protein purification.

A previously described ClpP trapping protocol (Flynn 2003) was adapted for *S. oneidensis*. Briefly, Δ*smpB*Δ*clpP*Δ*clpA*, Δ*smpB*Δ*clpPX,* and Δ*smpB*Δ*clpPX*Δ*clpA* with pBBR1MCS-2::*clpP*^{Trap} were grown anaerobically for 12 hours in 1 L anaerobic LB supplemented with 20 mM lactate and 40 mM fumarate; Δ*smpB*Δ*clpP*Δ*clpA* with pBBR1MCS-2::*clpP*^{Trap} was also grown for 12 hours in in 3 L anaerobic LB supplemented with 20 mM lactate, 40 mM fumarate, and 1.1 mM $FeCl_2$. 1.1 mM $FeCl_2$ was chosen because *clpP* mutant strains are impaired but still able to grow at this concentration (data not shown). Cell pellets were centrifuged 10 minutes at 5,000 rpm, resuspended in 40 mL TRIS-buffered saline with 1 mM ethylenediaminetetraacetic acid and 10 µM phenylmethylsulfonyl fluoride (pH 7.5), and centrifuged 10 minutes at 5,000 rpm. Cell pellets were resuspended in 40 mL TRIS-buffered saline and 10 µM phenylmethylsulfonyl fluoride (pH 8.0) and lysed by passing through a French press three times at 1200 PSI. The lysate was centrifuged 20 minutes at 10,000 rpm. The lysate supernatant was incubated with 4 mL anti-c-Myc agarose (25% slurry; Thermo Scientific) 5 hours on a rocker at 4°C. The resin was collected on a 10 mL column and washed with 10 mL TRIS-buffered saline with 0.5% Tween-20. The resin was eluted with 4 mL 50 mM NaOH, which was concentrated to 100 µL in a SpeedVac (Thermo Scientific).

Protein analysis.

20 µg of each protein elution was run into a Bio-Rad 8-16% Criterion precast polyacrylamide gel for 22 minutes at 25 mA. Bands were excised, digested in-gel with trypsin, and analyzed on Orbitrap Velos and Orbitrap Fusion mass spectrometers.

Detected peptides were mapped to *S. oneidensis* MR-1 (Ref Seq *Shewanella* 70863) and common laboratory contaminants protein databases with Scaffold (Proteome Software Inc.). The abundance of proteins trapped by $ClpP^{S106A\text{-}Trap}$ for each sample was quantified by evaluating both exclusive spectrum counts and percentage of total spectra for each protein. Proteins with fewer than two spectra in the Fe^{2+} condition were excluded from analysis. Complete Scaffold results are listed in Table S2. Protein cofactors were determined using Uniprot (The Uniprot Consortium 2014) and the Conserved Domain Database (Marchler-Bauer 2015).

4.4 Results

Tn-Seq reveals genes required for Fe^{2+} toxicity response.

To find genes involved in responding to high concentrations of Fe^{2+}, Tn-Seq was performed on wild-type and Δ*feoE S. oneidensis* libraries grown in the presence or absence of 0.8 mM $FeCl_2$. Both wild-type and Δ*feoE* strains were used in order to serve as replicates for the experiment while providing a means to discover genes that, upon deactivation, confer a stronger fitness defect in a strain with increased Fe^{2+} sensitivity. The results of the Tn-Seq screen are listed in Table S1. The fitness costs of genes encoding proteins known to interact with Fe^{2+} were evaluated as controls to confirm the validity of the Tn-Seq results. *feoB*, which encodes an Fe^{2+} importer (Kammler 1993), had a strong net Fe^{2+} fitness benefit in both wild-type and Δ*feoE* (+3.68 and +1.77, respectively; see Materials and Methods for an explanation of fitness effect calculations). *feoE*, which encodes an Fe^{2+} efflux pump (Bennett 2015), had a significant net Fe^{2+} fitness defect (-1.24) in wild-type. No reads were mapped to *feoE* in any of the Δ*feoE* libraries, indicating that no cross-library contamination had occurred.

Two genes that, upon deactivation, gave strong net fitness defects under high Fe^{2+} were *clpP* and *clpX* (-1.09 and -1.55 in the wild-type background, -2.05 and -2.73 in Δ*feoE*, respectively). Together *clpP* and *clpX* encode the protease ClpXP (Wojtkowiak 1993). To confirm the Tn-Seq results, in-frame single- and double-deletions were made of *clpP* and *clpX* from the *S. oneidensis* genome. Δ*clpP*, Δ*clpX*, and Δ*clpPX* had strong growth defects compared to wild-type when grown anaerobically in LB supplemented

with 20 mM lactate, 40 mM fumarate and 2 mM $FeCl_2$, but not when grown without added $FeCl_2$ (Fig. 4.1).

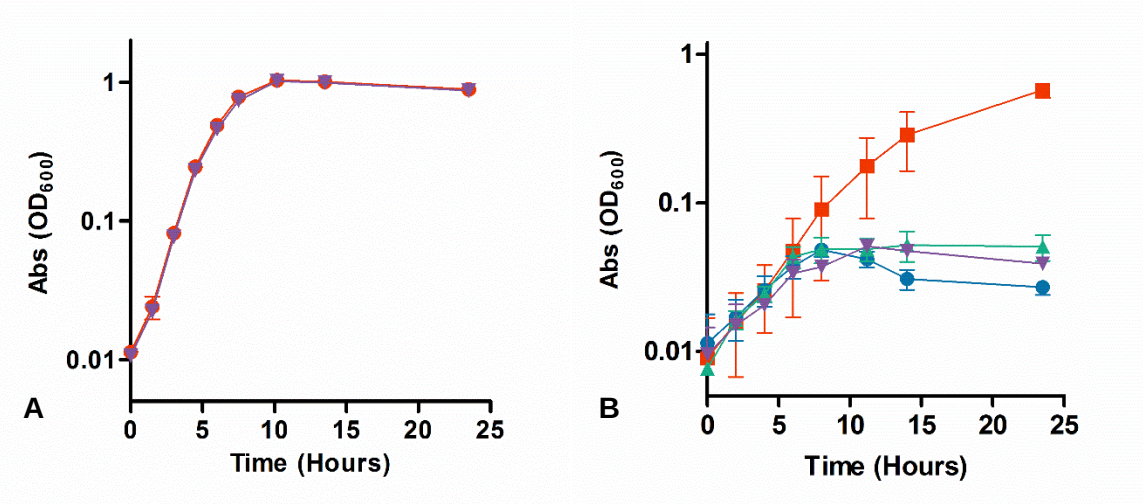

Figure 4.1 Growth of Δ*clpP*, Δ*clpX*, and Δ*clpPX* with and without high $FeCl_2$. A) The rate of growth over time in anaerobic LB supplemented with 20 mM lactate and 40 mM fumarate was measured for wild-type *S. oneidensis* (■) and Δ*clpPX* (▼). B) The rate of growth over time in anaerobic LB supplemented with 20 mM lactate, 40 mM fumarate, and 2 mM $FeCl_2$ was measured for wild-type *S. oneidensis* (■), Δ*clpPX* (▼), Δ*clpX* (▲), and Δ*clpP* (●).

ClpXP role in Fe^{2+} response is not related to known proteolytic functions.

ClpXP is a widely conserved and well-studied protease responsible for the degradation of numerous cytoplasmic proteins. Much of the research into its functions and structure has taken place in *E. coli*, although as more recent work on ClpXP in other bacterial species and mitochondria has grown, the list of roles this protease plays continues to expand. We limit our investigation of ClpXP proteolysis targets here to those encoded in the *S. oneidensis* genome. ClpXP targets the starvation and stationary-phase regulator sigma factor σ^S during exponential growth, thereby regulating growth rate (Schweder 1996). ClpXP also degrades proteins stalled in translation via recruitment by SspB and recognition of the SsrA transfer-messenger RNA tag, which is

attached to the stalled protein by SmpB (Gottesman 1998, Karzai 1999, Levchenko 2000). None of these genes had significant net Fe^{2+} fitness effects (our threshold for significance being ≥ ± 1.0) in our Tn-Seq data (*rpoS*: -0.08, *sspB*: -0.57, *ssrA*: +0.19, and *smpB*: +0.36 in the wild-type background, Table S1).

A group of *E. coli* proteins believed to be regulated by ClpXP are the cell-division proteins FtsZ, ZapC, FtsA, MinD, and SulA (Flynn 2003, Neher 2006, Buczek 2016). The *S. oneidensis* genome does not encode a ZapC homolog, but it does contain genes encoding the cell-division proteins ZapA and ZapB. Deactivation of neither *zapA*, *zapB*, *ftsA*, *minD*, nor *sulA* conferred a net Fe^{2+} fitness defect in our Tn-Seq data (-0.34, +0.33, +0.85, -0.15, and +0.29, respectively, in the wild-type background; Table S1). *ftsZ* appears to be an essential gene in *S. oneidensis* according to our Tn-Seq data, as no sequencing reads were mapped to the gene in any of the libraries (Table S1), consistent with previous observations (Brutinel 2012).

ClpXP is involved in the release of the cell envelope stress-response sigma factor σ^E by degrading the cytoplasmic domain of the anti-sigma factor RseA (Flynn 2004). The periplasmic protease DegS and intramembrane peptidase RseP are also required for degradation of RseA (Ades 1999, Saito 2011), while RseB acts as a secondary negative regulator of σ^E (De Las Peñas 1997). None of the genes encoding proteins involved in regulating σ^E had significant net Fe^{2+} fitness costs in our Tn-Seq data (+0.61, -0.42, +0.09, +0.31 in the wild-type background, respectively). However, deactivation of *rpoE*, the gene encoding σ^E, did confer a net Fe^{2+} defect near our significance threshold (-0.92 in the wild-type background, -1.06 in the Δ*feoE* background). To determine whether the stress-response σ^E is involved in Fe^{2+} toxicity resistance, an in-frame deletion of *rpoE* was made in the wild-type *S. oneidensis* genome. The growth rate of Δ*rpoE* was not significantly impaired compared to wild-type in either the presence or absence of excess Fe^{2+} (Fig. 4.2).

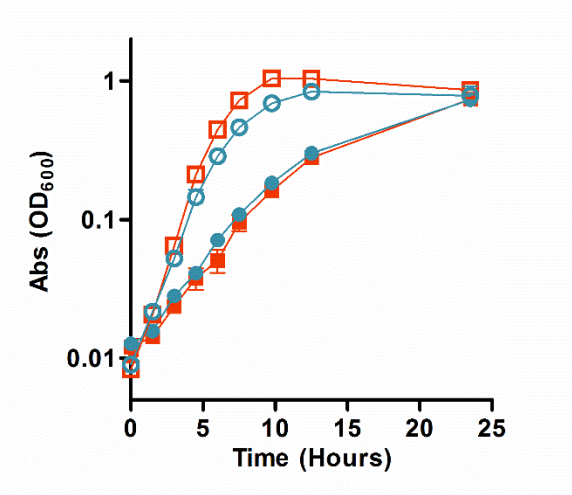

Figure 4.2 Growth of Δ*rpoE* with high $FeCl_2$.
The rate of growth over time for wild-type *S. oneidensis* and Δ*rpoE* in anaerobic LB supplemented with 20 mM lactate and 40 mM fumarate, with or without 2.5 mM $FeCl_2$. No metal added: wild-type, □; Δ*rpoE*, ○. Metal added: wild-type, ■; Δ*rpoE*, ●.

ClpXP targets metal-binding proteins for degradation in high Fe^{2+} conditions.

To determine the proteolysis targets of ClpXP under high Fe^{2+} conditions, we set up a ClpP trapping experiment modified from Flynn et al (2003). Mutation of the catalytic serine in the active site of ClpP (S106A) abrogates proteolytic activity, creating $ClpP^{Trap}$. $ClpP^{Trap}$ folds correctly and continues to bind the ATPase subunits ClpA or ClpX, which feed protease targets into $ClpP^{Trap}$. Substrate proteins are slowly released by $ClpXP^{Trap}$ or $ClpAP^{Trap}$ (Singh 2000), allowing for the use of $ClpP^{Trap}$, in conjunction with protein mass spectrometry, to detect which proteins are targeted for degradation by ClpXP or ClpAP.

A Δ*smpB*Δ*clpP* background was used for all trapping strains, in order to remove ssrA-tagged proteins from protein analysis and to prevent degradation of ClpXP targets by an active ClpP protease (Flynn 2003). *clpA* and *clpX* deletions were created in this background to isolate proteins specifically targeted for degradation by either ClpXP or ClpAP. Additionally, a Δ*clpA*Δ*clpX* mutant was used to identify proteins that non-

specifically bind to ClpP^{Trap} or the anti-Myc resin without being targeted by ClpX or ClpA. Each strain was transformed with pBBR1MCS-2::*clpP*^{Trap}.

To confirm that deletion of *smpB* and *clpA* did not affect the growth of *S. oneidensis*, wild-type, Δ*smpB*, and Δ*clpA* were grown anaerobically in LB supplemented with 20 mM lacatae, 40 mM fumarate, and 2 mM $FeCl_2$. There was no difference in growth rate between wild-type Δ*smpB*, and Δ*clpA* (Fig 3A). Δ*smpB*Δ*clpP*Δ*clpA* with pBBR1MCS-2::*clpP*^{Trap} had the same growth defect as Δ*smpB*Δ*clpP*Δ*clpA* with empty pBBR1MCS-2 when grown in anaerobic LB supplemented with 20 mM lactate, 40 mM fumarate, and 2 mM $FeCl_2$ (Fig. 4.3B), confirming that the S106A mutation inactivates ClpP. Δ*smpB*Δ*clpP*Δ*clpA* with pBBR1MCS-2::*clpP*^{Tag} had a faster growth rate than Δ*smpB*Δ*clpP*Δ*clpA* with pBBR1MCS-2::*clpP*^{Trap} (Fig. 4.3B), confirming that removal of the propeptide sequence from and addition of the purification tag to ClpP did not interfere with proper folding.

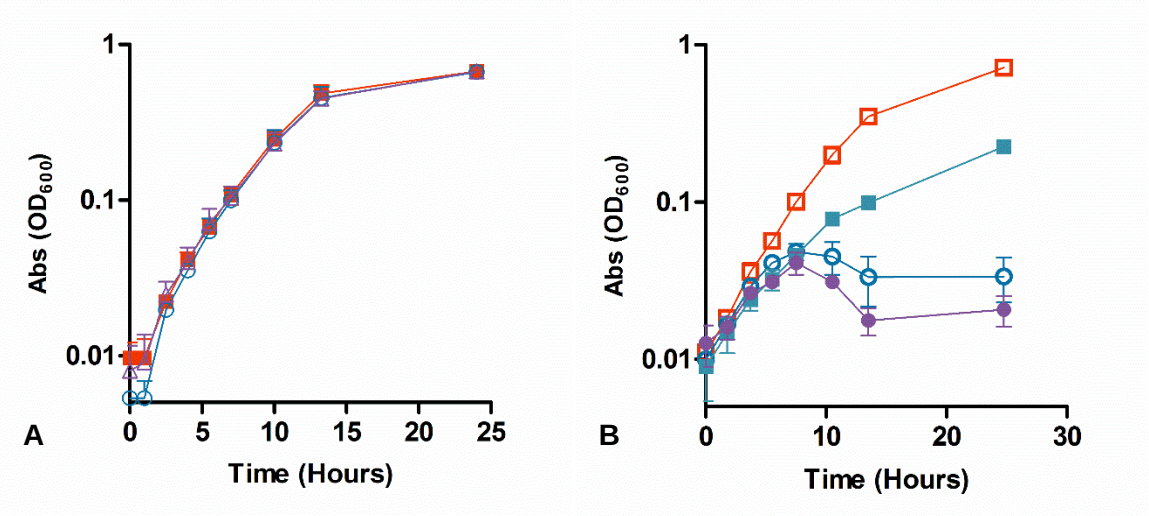

Figure 4.3 Growth of proteomics analysis strains.

A) The rate of growth over time for wild-type *S. oneidensis* (■), Δ*smpB* (○), and Δ*clpA* (Δ) was measured in anaerobic LB supplemented with 20 mM lactate, 40 mM fumarate, and 2 mM $FeCl_2$. B) The rate of growth over time for wild-type *S. oneidensis* with empty pBBR1MCS-2 (□), Δ*smpB*Δ*clpA*Δ*clpP* with empty pBBR1MCS-2 (○), Δ*smpB*Δ*clpA*Δ*clpP* with pBBR1MCS-2::*clpP*^{Tag} (■), and Δ*smpB*Δ*clpA*Δ*clpP* with pBBR1MCS-2::*clpP*^{Trap} (●)

was measured in anaerobic LB supplemented with 20 mM lactate, 40 mM fumarate, and 2 mM $FeCl_2$.

The three ClpP trapping strains were grown anaerobically in LB supplemented with 20 mM lactate and fumarate; the ClpX-only strain was also grown in anaerobic LB supplemented with 20 mM lactate, 40 mM fumarate, and 1.1 mM $FeCl_2$. ClpP-trapped proteins were identified using mass spectrometry. Proteins listed in Table 4.3 were detected at least twice as frequently in the Fe^{2+} culture as in any of the others in at least two of three mass spectrometry runs. Proteins trapped by ClpXP that were enriched under high Fe^{2+} conditions have disparate functions but frequently (10 of 11 proteins trapped) contain metal binding sites (Table 4.3, Table S2), a higher proportion than the proteins trapped with ClpXP in lower Fe^{2+} conditions (7 of 15), ClpAP (11 of 33), or ClpP with no ATPase adapter (17 of 37).

E. coli clpPX *complements* S. oneidensis *Δ*clpPX.

The % amino acid identities for ClpP and ClpX between *E. coli* and *S. oneidensis* are high (78% and 81%, respectively). To determine whether the proteolytic activity of ClpXP is required for Fe^{2+} resistance in *E. coli* as well as in *S. oneidensis*, Δ*clpPX* was complemented with pBBR1MCS-2::$clpPX_{E.\ coli}$, and Δ*clpX* was complemented with pBBR1MCS-2::$clpX_{E.\ coli}$ There was no difference in growth rate between wild-type with empty vector, Δ*clpPX* with pBBR1MCS-2::$clpPX_{E.\ coli}$, Δ*clpPX* with pBBR1MCS-2::$clpPX_{MR-1}$, and Δ*clpX* with pBBR1MCS-2::$clpX_{E.\ coli}$ when grown anaerobically in LB supplemented with 20 mM lactate, 40 mM fumarate, and 2.5 mM $FeCl_2$ (Fig. 4.4).

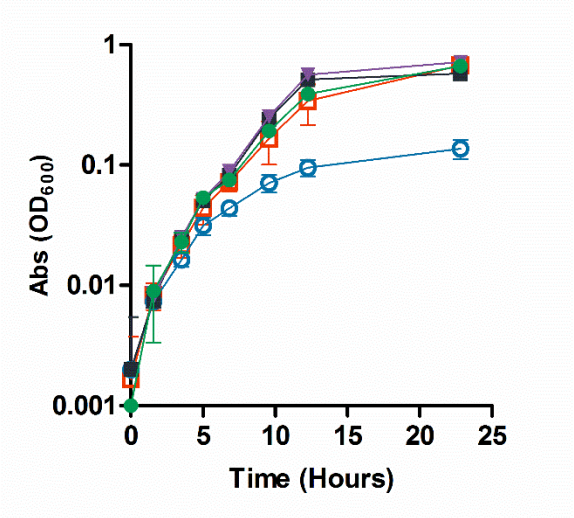

Figure 4.4 Growth of Δ*clpPX* and Δ*clpX* complemented with *cpPX* and *clpX* from *E. coli* in excess Fe^{2+}.

The rate of growth over time in anaerobic tryptone supplemented with 20 mM lactate, 40 mM fumarate, and 2.5 mM $FeCl_2$ was measured for wild-type *S. oneidensis* with empty pBBR1MCS-2 (□), Δ*clpPX* with empty pBBR1MCS-2 (○), Δ*clpPX* with pBBR1MCS-2::$clpPX_{MR\text{-}1}$ (■), Δ*clpPX* with pBBR1MCS-2::$clpPX_{E.\ coli}$ (▼), and Δ*clpX* with pBBR1MCS-2::$clpX_{E.\ coli}$ (●).

4.5 Discussion

AAA+ proteases have been implicated in numerous cellular processes in various bacterial species. Here we have provided evidence for a new function of the AAA+ protease ClpXP: resistance to Fe^{2+} toxicity via the degradation of metalloproteins.

The loss of either *clpP* or *clpX* was shown to be detrimental to *S. oneidensis* growing under high Fe^{2+} conditions but not in lower Fe^{2+} concentrations (Table S1, Fig. 4.1). The loss of *clpA*, which encodes another ATP-dependent chaperone that complexes with ClpP (Mauizi 1991), or *clpS*, which encodes an adaptor to the ClpAP complex (Erbse 2006), had no effect on the sensitivity of *S. oneidensis* to high Fe^{2+} concentrations (Table S1, Fig. 4.3A), indicating that the proteins specifically targeted by ClpX but not ClpA for degradation by ClpP are involved in Fe^{2+} sensitivity.

ClpXP regulates a number of cytoplasmic proteins, including cell-division proteins (Flynn 2003, Neher 2006, Buczek 2016) and the stress-response sigma factors σ^S and σ^E (Schweder 1996, Flynn 2004), and it facilitates the turnover of ribosomes by degrading stalled nascent proteins (Gottesman 1998). None of these processes, however, appear to be involved in the resistance of *S. oneidensis* to high Fe^{2+} concentrations (Table S1, Figs. 4.2 and 4.3).

Previous studies of σ^E in *E. coli* have indicated that σ^E is essential and *rpoE* mutants can be made only in conjunction with suppressor mutations (De las Peñas 1997b). Suppressor mutations could explain why we did not see an increase in Fe^{2+} sensitivity for our Δ*rpoE* strain; however, we believe that σ^E is neither essential in *S. oneidensis* nor critical for Fe^{2+} stress response. We had no trouble making *rpoE* transposon or deletion mutants, none of which displayed a significant increase in Fe^{2+} sensitivity (Table S1, Fig. 4.2). Additionally, we tested multiple Δ*rpoE* strains, all of which displayed identical phenotypes regarding resistance to Fe^{2+} and increased sensitivity over wild-type to Cu^{2+} and ethanol (data not shown). Therefore, we hold that the role ClpXP plays in Fe^{2+} resistance is not the promotion of σ^E release.

As we could not identify the function of ClpXP in response to Fe^{2+} toxicity through Tn-Seq data or phenotypic tests with deletion mutants, we adapted a ClpP-trapping method (Flynn 2003) to identify ClpXP proteolysis targets in *S. oneidensis*. While one-fourth to one-third of cellular proteins are believed to require a metal cofactor (Waldron 2009), nearly all proteins that were enriched for ClpXP trapping under Fe^{2+} conditions are predicted to contain metal-binding domains (Table 4.3), many more than for the proteins trapped by ClpAP or ClpXP in lower Fe^{2+} (Table S2). The mass-spectrometry data provided here can be only suggestive of relative quantitation; however, the protein-trapping results were largely repeatable. We therefore believe that, given the controls and conditions used here, the proteomics results are highly suggestive of a pattern of ClpXP targeting metalloproteins in *S. oneidensis* under Fe^{2+} stress.

It is notable that many proteins targeted by $ClpP^{Trap}$ in the high Fe^{2+} condition bind Mg^{2+} (Table 4.3, Table S2). The Irving-Williams series places the order of metal affinity to proteins as $Ca^{2+} < Mg^{2+} < Mn^{2+} < Fe^{2+} < Co^{2+} < Ni^{2+} < Cu^{2+} > Zn^{2+}$ (Irving 1953),

making Fe^{2+} likelier to bind proteins than Mg^{2+}, Ca^{2+}, Mn^{2+}, and, under certain conditions, Zn^{2+}. Cells have delivery systems to direct the insertion of most metals into their proper protein binding sites: the molybdenum cofactor Moco (Leimkühler 2011), copper chaperones such as CopZ and CusF (Argüello 2013), iron chelatases (reviewed in Ferreira 1995), nickel chaperones such as UreE and HypA (Brayman 1996, Song 2011, Xia 2009), and cobalt chelatases such as CbiK and CbiX (Raux 1997, Raux 1998). Proper insertion of metals at the lower end of the Irving-Williams series, such as Mn^{2+} and Mg^{2+}, on the other hand, frequently simply depends upon high relative intracellular concentrations of those metals (Tottey 2008, Hung 2011).

The intracellular concentration of Mg^{2+} is commonly kept around 1 mM, the highest concentration of all metals evaluated (Foster 2014). Not coincidentally, the intracellular concentrations of each metal in the Irving-Williams series is inversely correlated with its affinity for proteins (Foster 2014), indicating that cells compensate for low binding affinity with high relative concentration. It is therefore not surprising that Mg^{2+}-binding proteins were most frequently targeted by ClpXP under high Fe^{2+} in our study: as the concentration of Fe^{2+} rose, it likely overwhelmed the cells' iron-storage capacity and began outcompeting Mg^{2+} and other metals less dependent on specific delivery systems for insertion into the correct protein binding sites.

Corroborating the hypothesis that high Fe^{2+} concentrations interfere with Mg^{2+} insertion into metalloproteins, inactivation of the *corA* gene in our Tn-Seq screen caused a strong net fitness defect in both wild-type and Δ*feoE* under high Fe^{2+} (-1.23 and -1.70, respectively; Table S1). CorA is a high-affinity Mg^{2+} importer (Hmiel 1989, Snavely 1989), which appears to be the primary Mg^{2+} importer in bacteria (Niegowski 2007). Further lowering the ratio of Mg^{2+} to Fe^{2+} by knocking out *corA* increases sensitivity to high Fe^{2+}, which we believe occurs due to mismetallation of Mg^{2+}-requiring proteins.

While Fe^{2+} is believed to be toxic under aerobic conditions due to Fenton chemistry and the production of radical oxygen species (Sutton 1985, Touati 1995, Stohs 1995), the mechanism by which Fe^{2+} is toxic under anoxic conditions has not been well understood. Previously published hypotheses about Fe^{2+} anoxic toxicity have included formation of organic radicals, inhibition of the F-ATPase (Dunning 1998), or

reduction of Cu^{2+} to the more toxic Cu^{+} (Bird 2013). However, based on our findings in this study, we propose that a major mechanism by which Fe^{2+} is toxic under anoxia is through overwhelming the normal mechanisms of proper metal insertion into metalloproteins, with Fe^{2+} replacing the required metal. These “mismetallation” events interfere with proper enzyme activity, causing a buildup of inactive cytoplasmic proteins.

Previous works have indicated the ability of other metals to interfere with proper metal insertion into proteins. Zn^{2+} is believed to cause toxicity in *Streptococcus pneumoniae* by outcompeting Mn^{2+} for binding to the Mn^{2+} permease PsaA (McDevitt 2011). Mn^{2+} is believed to replace Mg^{2+} and thus deactivate the Mg^{2+}-dependent enzymes isocitrate lyase, isocitrate dehydrogenase, and 5-aminolevulinic acid dehydratase in *Bradyrhizobium japonicum* (Hohle 2015). UO_2^{2+} was shown to replace Ca^{2+} in the binding site of *Pseudomonas aeruginosa* pyrroloquinoline quinone PQQ (VanEngelen 2011), and Cu^{+} causes the release of Fe^{2+} from the iron-sulfur cluster in fumarase A in *E. coli* (Macomber 2009). However, this work appears to be the first to implicate toxic levels of a metal as causing general metalloprotein inactivation.

How mismetallated proteins may become targets of ClpXP is not fully clear from the results presented here. We speculate that mismetallation causes protein misfolding, which could expose a ClpX recognition site that would remain sequestered inside the properly folded protein. Complementing Δ*clpPX* with the *clpPX* genes from *E. coli* restores wild-type growth of *S. oneidensis* (Fig. 4.4), indicating that both proteases target the same substrates during Fe^{2+} toxicity. Five different ClpX recognition sequence motifs in *E. coli* were described by Flynn et al (2003), three N-terminal signal patterns and two C-terminal tags similar to the SsrA and MuA recognition sequences. Of the 11 proteins we identified as ClpXP targets during Fe^{2+} stress in our trapping experiment, eight have tags similar to those identified previously. RecA and the DEAD box helicase encoded by SO_1383, for example, have N-terminal residues identical to the start of Motif 2 (NH_2-Met-basic-hydrophobic) as described by Flynn et al (2003). The N-terminal residues of GapA encode Motif 2 (NH_2-Met-basic-hydrophobic-hydrophobic-hydrophobic-X-X-X-hydrophobic) (Flynn 2003), although offset by two residues from the N-terminal Met. The C-terminal residues of CydA, LepB, the CzcA family permease encoded by SO_0520, and the metal transporter encoded by SO_1145 match the ssrA-like motif (Flynn 2003).

Additionally, the C-terminal end of the RNA helicase DeaD shares three basic residues with the MuA sequence in crucial locations (Flynn 2003). The C- and N-terminal residues in these eight proteins in could be ClpXP recognition sequences. Of 61 proteins listed as ClpXP targets by Flynn et al (2003), eight (13%) did not have N- or C-terminal tags matching the five motifs they described. It is therefore probable that there are other ClpX recognition sequences that have not yet been determined, which could explain the lack of similarity between some ClpXP targets in our study and previously described ClpX recognition tags.

To conclude, *S. oneidensis* requires several mechanisms to resist high Fe^{2+} concentrations, which occur transiently and locally during the respiration of solid Fe^{3+} minerals. Here we have determined that the AAA+ protease ClpXP is an important factor in Fe^{2+} resistance by *S. oneidensis*, and that no previously described functions of ClpXP are involved in resistance to Fe^{2+}. Proteomic evidence indicates that ClpXP targets metalloproteins for degradation under Fe^{2+} stress. This may be due to an imbalance in the intracellular concentrations of divalent metal cations, causing the mismetallation of metalloproteins with Fe^{2+}. These mismetallated proteins must be degraded by ClpXP in order to prevent cytoplasmic buildup of misfolded, inactive proteins, and therefore for *S. oneidensis* to continue to thrive in an iron-rich environment.

4.6 Acknowledgements

Many thanks to LeeAnn Higgins and Todd Markowski in the Center for Mass Spectrometry and Proteomics at the University of Minnesota for proteomics guidance and mass spectrometry analysis. This work was supported by the Office of Naval Research (N000141310552). BDB was supported in part by the University of Minnesota Biotechnology Training Grant Program through the National Institutes of Health.

Table 4.1 Bacterial strains and plasmids used in this study.

Strain	Description	Source
JG274	*S. oneidensis* MR-1, wild type	Myers 1988
JG2989	JG274 Δ*feoE*	Bennett 2015
JG3354	JG274 Δ*rpoE*	This work
JG3355	JG274 Δ*clpPX*	This work
JG3486	JG274 Δ*clpP*	This work
JG3492	JG274 Δ*clpX*	This work
JG3552	JG274 Δ*smpB*	This work
JG3556	JG274 Δ*clpA*	This work
JG3560	JG274 Δ*smpB*Δ*clpP*Δ*clpA*	This work
JG3565	JG274 Δ*smpB*Δ*clpPX*	This work
JG3632	JG274 Δ*smpB*Δ*clpPX*Δ*clpA*	This work
JG168	JG274 with empty pBBR1MCS-2, Km^r	Hau 2008
JG3488	JG3355 with empty pBBR1MCS-2, Km^r	This work
JG3549	JG3486 with empty pBBR1MCS-2, Km^r	This work
JG3495	JG3355 with pBBR1MCS-2::$clpPX_{MR-1}$	This work
JG3667	JG3355 with pBBR1MCS-2::$clpPX_{E. coli}$	This work
JG3668	JG3492 with pBBR1MCS-2::$clpX_{E. coli}$	This work
JG3570	JG3560 with pBBR1MCS-2::$clpP^{Tag}$	This work
JG3599	JG3560 with pBBR1MCS-2::$clpP^{Trap}$	This work
JG3600	JG3565 with pBBR1MCS-2::$clpP^{Trap}$	This work
JG3635	JG3632 with pBBR1MCS-2::$clpP^{Trap}$	This work
UQ950	*E. coli* DH5α λ(pir) cloning host; F-Δ(*argF-lac*)169 Φ80dlacZ58(ΔM15) glnV44(AS) rfbD1 gyrA96(NalR) recA1 endA1 spoT1 thi-1 hsdR17 deoR λpir+	Saltikov 2003

WM3064	*E. coli* conjugation strain; *thrB1004 pro thi rpsL hsdS lacZΔM15 RP4-1360 Δ(araBAD)567 ΔdapA1341::[erm pir(wt)]*	Saltikov 2003

Plasmid	**Description**	**Source**
pSMV3	Deletion vector, Km^r, *sacB*	Coursolle 2010
pBBR1MCS-2	Broad-range cloning vector, Km^r	Kovach 1995
pBBR1MCS-2::*clpPX*$_{MR-1}$	SO_1794–5 (*clpPX*), 26 bp upstream, 8 bp downstream	This work
pBBR1MCS-2::*clpPX*$_{E. coli}$	b0437–8 (*clpPX*), 22 bp upstream, 28 bp downstream	This work
pBBR1MCS-2::*clpX*$_{E. coli}$	b0438 (*clpX*), 30 bp upstream, 28bp downstream	This work
pBBR1MCS-2::*clpP*^{Tag}	SO_1794 (*clpP*) Δ2-9, downstream, HIS6-TEV-MYC3, Km^r	This work
pBBR1MCS-2::*clpP*^{Trap}	SO_1794 (*clpP*) Δ2-9, S106A, downstream HIS6-TEV-MYC3, Kmr	This work

Table 4.2 Primers and allele sequences used for mutation and complementation in this work.

Primer	Sequence	Restriction Site
1342USF	GTACGGATCCCAATGCTTCGGTCAGCAG	*Bam*HI
1342USR	GTACACTAGTCTCATCCGAGCCGACTTC	*Spe*I
1342DSF	GTACACTAGTGCCTTTGCTGGAAGAGTAAATTC	*Spe*I
1342DSR	GTACGAGCTCCACCCTGAATATGATTAGAGAGG	*Sac*I
1794USF	GTACGGATCCGATGTGGACAGCATGATTG	*Bam*HI
1794USR	GTACACTAGTGGCGAACTGCTAATCAAGTC	*Spe*I
1794DSF	GTACACTAGTGATTTTTACTTTCGACTGGGC	*Spe*I
1794DSR	GTACGAGCTCCTCAACTTGAGACAGGGTTTC	*Sac*I
1795USF	GTACGGATCCCTCTATGGCTTCTGCTTACG	*Bam*HI
1795USR	GTACACTAGTGCCCATTAATTACCTCATTTGC	*Spe*I
1795DSF	GTACACTAGTGGCGAGCAATAATTGTACAG	*Spe*I
1795DSR	GTACGAGCTCCAGACATCGGTGACATCATG	*Sac*I
2626USF	GTACGAGCTCCGCTAAACAAGCTATTGATTG	*Sac*I
2626USR	GTACGAATTCCAGATCTTTGTTCAGCATAAGC	*Eco*RI
2626DSF	GTACGAATTCGCTTAACGCCAAGCTAATTTAC	*Eco*RI
2626DSR	GCATACTAGTCTATTAGCCATAGGCTTTCG	*Spe*I
1473USF	GTACGAGCTCCTTCATCCTTGGCTTTATCAG	*Sac*I
1473USR	GTACGAATTCGTTTTTCTTTACCATAGTGGC	*Eco*RI
1473DSF	GTACGAATTCGGATAATGAACAAACGATTGAAC	*Eco*RI
1473DSR	GTACACTAGTGCAATCTGTGCTTCTCTATG	*Bam*HI
1794F	GTACGGATCCGCCATTTTTATTTAGGGAAATG	*Spe*I
1795R	GTACACTAGTCTGTACAATTATTGCTCGCC	*Spe*I
ECb0437F	GTACGGATCCCAATTTTATCCAGGAGACGG	*Sac*I
ECb0438F	GTACGGATCCGCACAAAGAACAAAGAAGAGG	*Bam*HI
ECb0438R	GTACACTAGTGGTTAACTAATTGTATGGGAATGG	*Spe*I

***clpP*^{Tag} (*EcoRI*-start-clpP(Δ2–9)-HIS$_6$-TEV-MYC$_3$ tag-stop-*BamHI*)**

GGCCCGC*GAATTC*ATGGCTTTAGTGCCTATGGTGATCGAACAGACTGCTAAAGGTG
AACGCTCATTTGATATTTATTCTCGTTTGTTAAAAGAGCGGATTATCTTTTTAGTGGG
CCAAGTAGAAGAGCATATGGCGAATCTGATTGTGGCGCAGTTACTATTCCTTGAGT
CAGAAAGCCCTGACAAGGATATTTTCTTATATATCAACTCACCTGGTGGCTCTGTTA
CCGCGGGTATGGCAATTTACGACACCATGCAGTTTATTAAGCCTAATGTGAGCACT
GTGTGTATTGGCCAAGCGGCTAGCATGGGTGCATTTTTATTAGCGGGTGGTGAAAA
GGGCAAGCGTTTCTGCTTACCTAATTCGCGCGTTATGATCCATCAACCTTTGGGTG
GTTTCCAAGGTCAGGCTTCTGATATCGCGATTCATGCTCAAGAGATTTTGGGCATTA
AGAATAAACTGAACCAGATGTTAGCTGATCATACTGGACAACCCCTCGAAGTAATTG
AGCGTGATACCGATCGTGACAACTTCATGAGTGCTACTCAAGCTGTAGAATATGGT
TTAGTTGACGCAGTGATGACTAAACGCGGCGATTCTATCTTAACTCACCGTAACCGT
TCTCACCATCACCATCACCATGGTGGTGAAAACTTATACTTCCAAGGTGCATACACC
TCTGGCGAGCAAAAGTTAATCTCTGAAGAAGATTTAAATGGAGAACAAAAATTAATC
TCTGAAGAAGATTTAAACGGTGAACAAAAATTAATCTCTGAGGAAGATCTGAACTGA
*GGATCC*GGCTC

***clpP*^{Trap} (*EcoRI*-start-clpP(Δ2–9,S106A)-HIS$_6$-TEV-MYC$_3$ tag-stop-*BamHI*)**

GGCCCGC*GAATTC*ATGGCTTTAGTGCCTATGGTGATCGAACAGACTGCTAAAGGTG
AACGCTCATTTGATATTTATTCTCGTTTGTTAAAAGAGCGGATTATCTTTTTAGTGGG
CCAAGTAGAAGAGCATATGGCGAATCTGATTGTGGCGCAGTTACTATTCCTTGAGT
CAGAAAGCCCTGACAAGGATATTTTCTTATATATCAACTCACCTGGTGGCTCTGTTA
CCGCGGGTATGGCAATTTACGACACCATGCAGTTTATTAAGCCTAATGTGAGCACT
GTGTGTATTGGCCAAGCGGCTGCCATGGGTGCATTTTTATTAGCGGGTGGTGAAAA
GGGCAAGCGTTTCTGCTTACCTAATTCGCGCGTTATGATCCATCAACCTTTGGGTG
GTTTCCAAGGTCAGGCTTCTGATATCGCGATTCATGCTCAAGAGATTTTGGGCATTA
AGAATAAACTGAACCAGATGTTAGCTGATCATACTGGACAACCCCTCGAAGTAATTG
AGCGTGATACCGATCGTGACAACTTCATGAGTGCTACTCAAGCTGTAGAATATGGT
TTAGTTGACGCAGTGATGACTAAACGCGGCGATTCTATCTTAACTCACCGTAACCGT
TCTCACCATCACCATCACCATGGTGGTGAAAACTTATACTTCCAAGGTGCATACACC
TCTGGCGAGCAAAAGTTAATCTCTGAAGAAGATTTAAATGGAGAACAAAAATTAATC
TCTGAAGAAGATTTAAACGGTGAACAAAAATTAATCTCTGAGGAAGATCTGAACTGA
*GGATCC*GGCTC

Table 4.3 Proteins trapped by ClpXP in high Fe^{2+}

Protein	Function	Metal Cofactor
RecA	Recombinase A	Mg^{2+}
DeaD	ATP-dependent RNA helicase	Mg^{2+}
NrdA	Aerobic ribonucleoside-diphosphate reductase alpha subunit	Fe^{3+}
NrdD	Anaerobic ribonucleoside-triphosphate reductase	Zn^{2+}
GapA	Glyceraldehyde-3-phosphate dehydrogenase	None
TnpB_MuSo2	Mu phage transposase OrfB	Mg^{2+}
CydA	Cytochrome *d* ubiquinol oxidase subunit I	Fe^{3+}
SO_1145	Magnesium transporter MgtE	Mg^{2+}, Ca^{2+}
SO_0520	Heavy metal efflux component permease CzcA	Cu^{2+}
SO_1383	ATP-dependent RNA helicase DEAD box family	Mg^{2+}
LepB	Signal peptidase I	Mg^{2+}, K^{+}

Chapter 5: The Stress Response Sigma Factor σ^E May be Involved in Extracellular Respiration but Does Not Respond to Fe^{2+} Stress

5.1 Introduction

Sigma factors are proteins that associate with the RNA polymerase complex and specify the genes to be transcribed (reviewed in Reznikoff 1985). Multiple sigma factors are encoded by microorganisms in order to tune the cellular response to various conditions. σ^E is a stress response sigma factor that becomes active when bacterial cells experience various stresses that lead to misfolded periplasmic and outer-membrane proteins (reviewed in Raivio 2001). Stresses shown to require σ^E response in various Gammaproteobacteria species include ethanol, elevated Cu^{2+}, and high temperature (Haines-Menges 2014, Egler 2005, Hiratsu 1995). The gene encoding σ^E, *rpoE,* is thought to be essential in *E. coli*, and it is believed that *rpoE* mutants of *E. coli* can only be made along with suppressor mutations (De las Peñas 1997).

In *S. oneidensis*, σ^E is predicted to regulate several outer membrane protein assembly genes (Dai 2015). Expression of *rpoE* is upregulated during oxygen limitation (Barchinger 2016), and inactivation of *rpoE* caused a decline in viability under Fe^{3+}-respiring conditions (Evan Brutinel, unpublished data). Taken together, this evidence indicates that σ^E may play a role in extracellular respiration by *S. oneidensis*. That hypothesis is explored further in this work.

5.2 Materials and methods

Bacterial strains and growth conditions

S. oneidensis MR-1 was isolated from Lake Oneida, New York State (Myers 1988). Deletion of *rpoE* from the *S. oneidensis* genome is described in Chapter 4. Overnight cultures were grown in LB from freshly streaked -80°C stocks. *Shewanella* strains were grown at 30°C and *E. coli* at 37°C; liquid cultures were shaken at 250 rpm. Anaerobic media were flushed with nitrogen to remove oxygen.

Growth curves

Overnight LB cultures were pelleted, washed once in LB, and resuspended in LB. Experimental cultures were grown aerobically in LB with or without 2.0mM $CuCl_2$ or 4% ethanol, or anaerobically in LB with 20mM sodium lactate and 40mM sodium fumarate with or without 2.5mM $FeCl_2$. Growth was measured by periodically taking the optical

density at 600 nm (OD_{600}). Results represent the average of three biological replicates ± 1 standard deviation (SD).

Iron respiration assays

Fe^{3+} respiration was measured using ferrozine assays as previously described (Coursolle 2010). Briefly, overnight LB cultures were pelleted, washed once in *Shewanella* basal medium (SBM) (Hau 2008), and resuspended in SBM. Cultures were inoculated to an OD_{600} of 0.1 into SBM with 20 mM lactate, 5 mM Fe^{3+} oxide (FeOOH) or 5 mM Fe^{3+} citrate, 5 mL/L vitamin mix, (Balch 1979), 5 mL/L mineral mix (Marsili 2008) in anaerobic 96-well plates. Plates were incubated at room temperature in the dark. Fe^{2+} production was measured over time using absorbance of ferrozine at 542 nm (Stookey 1970). Results are reported as the average of three biological replicates ± 1 SD.

Electrochemistry

Electrode respiration was measured using graphite electrodes. 100 µL of overnight cultures was inoculated into 5 mL anaerobic LB with 20 mM lactate and 40 mM fumarate and incubating at 30°C with shaking until the OD_{600} reached approximately 0.5. 1 mL of this culture was added to 14 mL anaerobic *Shewanella* basal medium (Hau 2008) with 60 mM lactate, 40 mM fumarate, and 0.05% casamino acids in three-electrode bioreactors containing graphite electrodes. Electrodes were constructed as previously described (Baron 2009, Kane 2013). Briefly, polished 3 cm^2 graphite flags were connected to a platinum working electrode and placed in glass cone bioreactors along with platinum counter and vycor Ag/AgCl reference electrodes. Bioreactors were capped with tops fitted with rubber gaskets and continually degassed with N_2 to prevent oxygenation. Graphite electrodes were poised at 240 mV (vs. standard hydrogen electrode). Current production was measured with a 16-channel potentiostat.

Biofilm assay

Biofilm production was measured as previously described (O'Toole 2011). Briefly, overnight LB cultures were pelleted, washed once in SBM, and resuspended in SBM. Cells were diluted to an OD_{600} of 0.05 in 100 µL SBM with 20 mM lactate, 40 mM fumarate, 5 mL/L vitamins, 5 mL/L minerals, and 0.05% casamino acids in 96-well

plates. Cultures were grown 24 hours without shaking. Wells were aspirated and washed twice with 300 µL deionized H_2O. 125 µL 0.1% crystal violet was added to wells for 15 min. Wells were aspirated and washed four times with 125 µL deionized H_2O; the plate was then dried for 3 hours. 125 µL 30% glacial acetic acid was added to each well for 15 min and then transferred to new wells. Crystal violet absorbance was measured at 550 nm. Results are the average of four biological replicates ± 1 SD.

5.3 Results and discussion

σ^E is needed for optimal extracellular respiration

To determine whether σ^E is involved in promotion of extracellular electron transfer, Fe^{3+} and electrode respiration assays were performed. Δ*rpoE* had a mild but repeatable defect in respiration of both soluble Fe^{3+} citrate and insoluble Fe^{3+} oxide (Figure A.1) and a strong defect in respiration of graphite electrodes (Figure A.2), indicating that σ^E is needed for wild-type levels of extracellular respiration. It must be noted that the electrochemistry was performed only once; however, the results are consistent with those of the Fe^{3+} respiration assays.

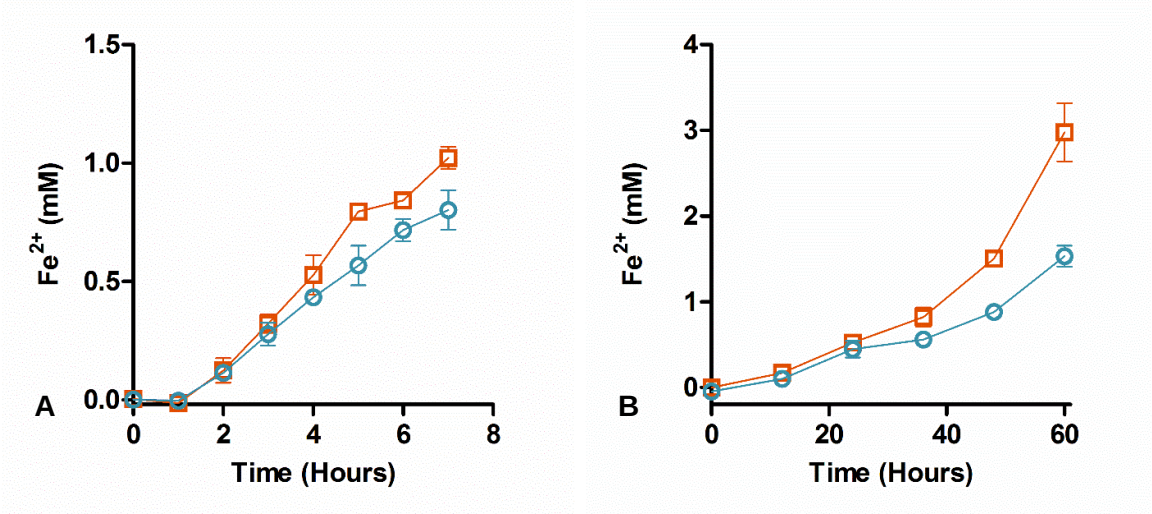

Figure 5.1 Respiration of Fe^{3+} by Δ*rpoE* and wild-type *S. oneidensis*

The rates of Fe^{2+} production from anaerobic respiration of A) soluble Fe^{3+} citrate and B) insoluble Fe^{3+} oxide were measured for Δ*rpoE* (○) and wild-type *S. oneidensis* (□).

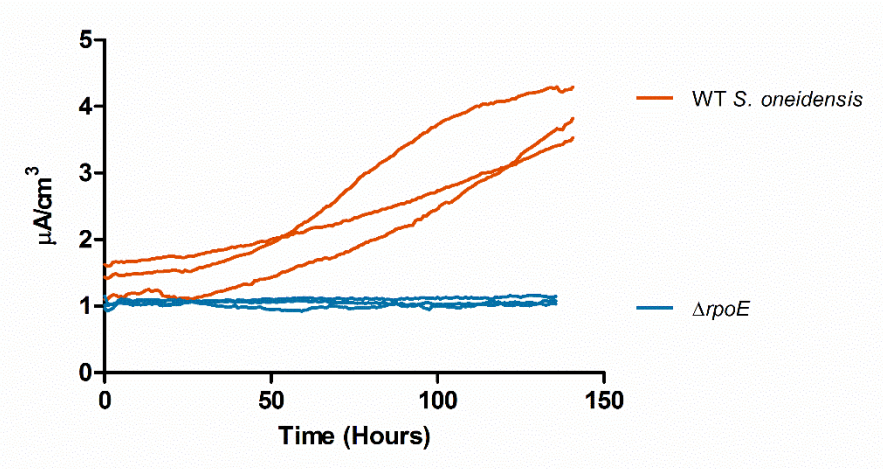

Figure 5.2 Respiration of electrodes by Δ*rpoE* and wild-type *S. oneidensis*
The rate of current produced by anaerobic respiration of graphite electrodes was measured for Δ*rpoE* (—) and wild-type *S. oneidensis* (—).

σ^E is not required for Fe^{2+} response

It is possible that the defect in Fe^{3+} respiration by Δ*rpoE* was due to an increased sensitivity to the Fe^{2+} produced by Fe^{3+} respiration. However, there was no significant difference in growth rate between Δ*rpoE* and wild-type growing anaerobically in LB with 20 mM lactate and 40 mM fumarate with or without 2.5 mM $FeCl_2$ (Fig 4.2). The lack of increased Fe^{2+} sensitivity indicates σ^E is not required for Fe^{2+} stress response, and the Fe^{3+} respiration defect observed for Δ*rpoE* is not due to increased sensitivity to Fe^{2+}.

σ^E is not essential but is required for Cu^{2+} and ethanol stress response in S. oneidensis

Transposon data indicated that *rpoE* is not essential in *S. oneidensis*, as several thousand *rpoE* transposon mutants were detected in our library (Table S1). Additionally, *rpoE* was easily deleted from the *S. oneidensis* genome. To determine whether the Δ*rpoE* mutant contained suppressor mutations that allowed for *rpoE* deletion, growth curves in ethanol and copper were performed to determine the response of Δ*rpoE* to stresses. Δ*rpoE* had a growth defect compared to wild-type when grown in LB with 4% ethanol or 2 mM Cu^{2+} (Figure A.3), indicating that the *rpoE* mutant does not have suppressor mutations that make it less sensitive to stresses other than Fe^{2+}. *rpoE* does

not appear to be essential in *S. oneidensis*, and the lack of increased Fe^{2+} sensitivity by Δ*rpoE* is likely not due to suppressor mutations.

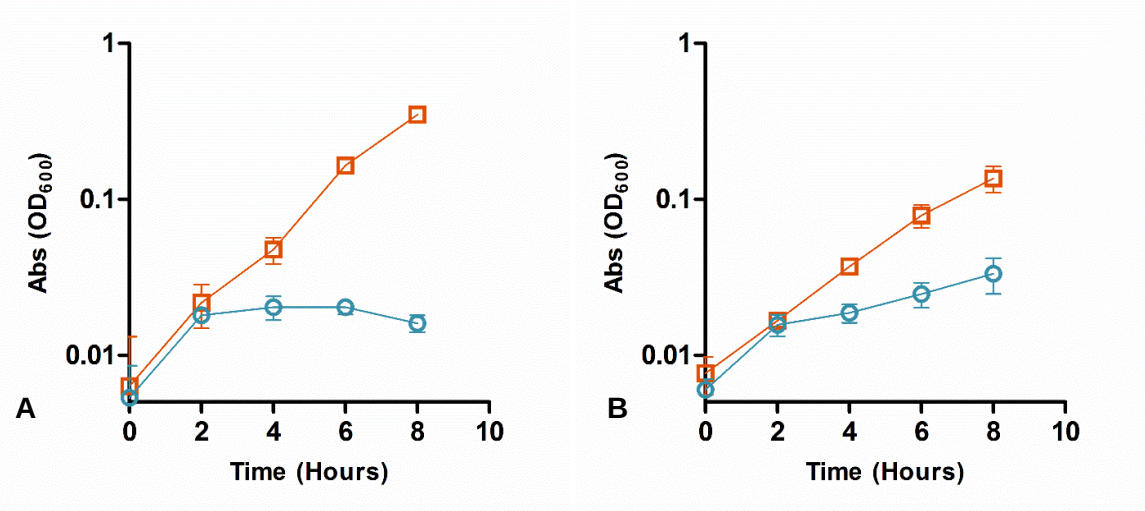

Figure 5.3 Growth of Δ*rpoE* and wild-type *S. oneidensis* in the presence of Cu^{2+} and ethanol.

The rates of growth in aerobic LB with A) 2.0 mM $CuCl_2$ or B) 4% ethanol were measured for wild-type *S. oneidensis* (□) and Δ*rpoE* (○).

*Δ*rpoE *is able to form biofilms*

Direct interaction with Fe^{3+} oxides and biofilm formation on electrodes has been shown to be involved in respiration of insoluble substrates (Das 2000, Lower 2001, Marsili 2008). To determine whether the Fe^{3+} oxide and electrode respiration defect observed for Δ*rpoE* is due to an inability by the mutant to attach to a surface, biofilm assays were performed. Δ*rpoE* was able to form biofilms as well as wild-type (crystal violet absorbance 0.040 ± 0.017 and 0.025 ± 0.010, respectively). Wild-type level production of biofilms by Δ*rpoE* indicates that σ^E is not necessary for biofilm production, and the lower rate of Fe^{3+} oxide and electrode respiration by Δ*rpoE* is not due to an inability to attach to insoluble iron.

Concluding remarks

It seems probable that, given the moderate effect of an *rpoE* mutation on Fe^{3+} respiration by *S. oneidensis* (Fig. A.1), traditional transposon screens were not sufficient to pick up *rpoE* mutants with Fe^{3+} respiration defects. Additionally, to our knowledge no transposon screens under electrode respiration have been performed for *S. oneidensis*, which is likely why the importance of *rpoE* to extracellular respiration (Fig. A.2) has not been discovered before now.

σ^E has previously been shown to respond to stress stemming from misfolded outer-membrane and periplasmic proteins (Raivio 2001). Additionally, σ^E in *S. oneidensis* is predicted to regulate genes encoding outer-membrane protein chaperones and the protease DegQ (Dai 2015), which degrades misfolded periplasmic proteins (Waller 1996). Further work must be done to elucidate the role that σ^E plays in extracellular respiration, but the work presented here indicates that σ^E is involved in extracellular electron transfer in *S. oneidensis*, perhaps through promoting the proper folding of outer-membrane and periplasmic cytochromes involved in extracellular respiration, as part of a response to the stress of decreased electron acceptor availability.

Chapter 6: Conclusions and Future Directions

In the redox transition zones of aquatic sediments, where the bacterium *Shewanella oneidensis* MR-1 can be found, the O_2 tension periodically rises and falls. This changeable environment favors organisms like *S. oneidensis* that have evolved to respond rapidly to fluctuating conditions. That *S. oneidensis* is able to respire insoluble, extracellular Fe^{3+} complexes in O_2-limited conditions has been known for several decades; however, until now it has not been well-understood how this organism is able to resist the high local concentrations of soluble Fe^{2+} produced as a byproduct of this respiration. The ways in which *S. oneidensis* interacts with Fe^{2+} are important for understanding how this organism has evolved to thrive in a metal-rich environment, particularly one in which the availability of O_2 continually waxes and wanes. The work presented in this thesis demonstrates newly discovered mechanisms by which the bacterium *S. oneidensis* transports Fe^{2+} into and out of the cytoplasm and resists Fe^{2+} toxicity.

In Chapter 2, *S. oneidensis* was determined to produce an Fe^{2+}-specific member of the Cation Diffusion Facilitator protein superfamily. This inner-membrane Fe^{2+} exporter, which was named FeoE (*fe*rr*o*us iron *e*xport), is required for optimal growth of *S. oneidensis* under anaerobic, Fe^{3+}-respiring conditions. It was shown that FeoE is not directly involved in the respiration of Fe^{3+}, but that FeoE expels from the cytoplasm excess Fe^{2+} produced by Fe^{3+} respiration, preventing the intracellular buildup of Fe^{2+} to toxic concentrations. FeoE may also represent a means by which *S. oneidensis* prevents aerobic Fe^{2+} toxicity: the expulsion of excess Fe^{2+} from the cytoplasm during anoxia would also lessen the amount of oxidative damage caused by Fe^{2+}-generated reactive oxygen species upon a return to high O_2 conditions.

Chapter 3 described a member of the Magnesium Transporter-E (MgtE) family encoded in the *S. oneidensis* genome that imports Fe^{2+} and Co^{2+}, which was named FicI (*f*errous *i*ron and *c*obalt *i*mporter). The substrate specificity of FicI contrasts with all other members of the MgtE family described in the current literature, which are importers of Mg^{2+} and Co^{2+}. FicI and FeoB, the primary Fe^{2+} importer produced by *S. oneidensis*, appear to be active under different conditions: FeoB seems to import Fe^{2+} under lower Fe^{2+} concentrations, while FicI seems to do so under high Fe^{2+} concentrations. As FeoB requires energy for Fe^{2+} uptake and FicI is likely to be a passive importer, this may

represent an adaptation by *S. oneidensis* to its lifestyle of periodic Fe^{3+} respiration. *S. oneidensis* appears to have evolved a passive Mg^{2+} transporter to import Fe^{2+} instead, allowing it to take advantage of temporarily high local Fe^{2+} concentrations produced during Fe^{3+} respiration for less energy-dependent Fe^{2+} uptake.

Taking the findings in Chapters 2 and 3 together, *S. oneidensis* appears to have adapted to an environment with continually changing O_2 and Fe^{2+} concentrations by evolving three different Fe^{2+} transporters to work in concert. FeoB, FicI, and FeoE likely work together to fine-tune the intracellular Fe^{2+} concentration to stay within viable limits: high enough for the production of cytochromes and other iron-containing proteins, but not so high that the concentration becomes toxic (Fig. 5.1). Additionally, minimizing the amount of energy required to take up Fe^{2+} at higher concentrations via FicI would be especially important during anaerobic respiration, which provides less energy than aerobic respiration.

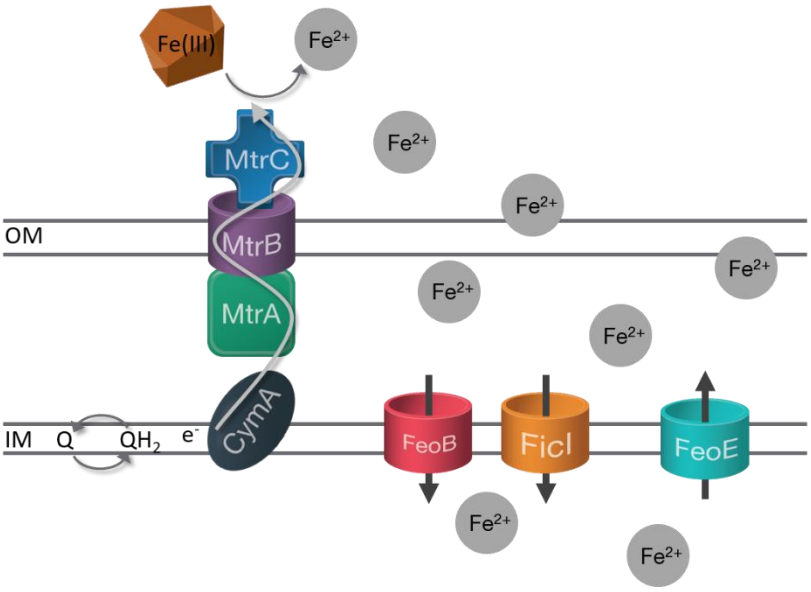

Figure 6.1 Fe^{2+} transport in *S. oneidensis*. OM, outer membrane; IM, inner membrane; Q, oxidized quinone; QH_2, reduced quinone, CymA and MtrCAB, cytochromes; FeoB, FicI, Fe^{2+} importers; FeoE, Fe^{2+} exporter.

In Chapter 4, the protease ClpXP was discovered to be required for Fe^{2+} resistance by *S. oneidensis*. ClpXP is a highly conserved, well-described cytoplasmic protease with multiple cellular functions; however, none of the previously described processes regulated by ClpXP appear to be involved in Fe^{2+} resistance. A ClpXP protein-trapping assay determined that proteins with metal binding sites were disproportionally targeted by ClpXP under Fe^{2+} stress. This indicates that Fe^{2+} may cause toxicity at high concentrations by interfering with the insertion of correct metal cofactors into metalloproteins, likely causing protein misfolding. These mismetallated, misfolded proteins would then become targets for degradation by ClpXP. As an *E. coli* Δ*clpXP* mutant has increased sensitivity to Fe^{2+}, and as the ClpXP protease from *E. coli* can complement the Δ*clpXP* Fe^{2+} sensitivity phenotype in *S. oneidensis*, it appears likely that the involvement of ClpXP in resisting Fe^{2+} stress is not limited to *S. oneidensis* but likely applies to *E. coli* and other organisms as well. It also appears likely that ClpXP homologs from both *S. oneidensis* and *E. coli* target the same subset of protein targets, at least under Fe^{2+} stress. It is likely that other metals, particularly those higher in the Irving-Williams series of metal affinities for protein, would also cause toxicity at high concentrations by the same mechanism as Fe^{2+}.

Future studies of the role ClpXP plays in Fe^{2+} resistance should be performed to confirm the quantification of proteins targeted by ClpXP during Fe^{2+} stress. Targeted experiments with synthetic peptides from proteins of interest could confirm the relative quantification of ClpXP-trapped proteins under normal and high Fe^{2+} concentrations that are suggested by the data presented in this thesis. To confirm that the proteins targeted by ClpXP under Fe^{2+} stress are mismetallated, ICP-MS analysis should be performed on purified ClpXP-targeted metalloproteins during Fe^{2+} stress to determine their metal cofactors. This would allow for confirmation that ClpXP targets proteins that have misincorporated iron as a cofactor, and it would support the hypothesis that protein misfolding due to mismetallation is a mechanism of anoxic Fe^{2+} stress.

Chapter 5 describes the finding that the stress-response regulator σ^E is involved in extracellular respiration by *S. oneidensis*. Previous work by many groups has shown that conditions causing cell envelope stress and misfolding of membrane proteins activate σ^E, which then upregulates numerous stress-response genes. σ^E is required for

wild-type rates of respiration of both Fe^{3+} and electrodes, indicating that σ^E is likely to be somehow involved in regulating the cytochromes that make up the extracellular respiration pathway. It may be that extracellular respiration, which occurs under electron-acceptor limitation, can be considered a stress condition, and that σ^E promotes proper folding of extracellular respiration proteins under electron acceptor-limitation stress. Further work to elucidate the role of σ^E in extracellular respiration should include determining which genes regulated by σ^E are required for metal respiration. For example, σ^E upregulates several outer-membrane protein assembly genes, which could be involved in promoting proper assembly and/or folding of the Mtr pathway proteins. Overexpression of these assembly genes in a σ^E mutant would show whether proper folding of outer-membrane proteins is a major factor in the importance of σ^E for extracellular respiration.

To conclude, the work in this thesis illuminates a multi-level system that maintains the intracellular concentration of Fe^{2+} in *S. oneidensis*, demonstrates several means by which *S. oneidensis* counteracts Fe^{2+} toxicity, and presents a potential mechanism for Fe^{2+} damage under anaerobic conditions. As *S. oneidensis* lives in redox-active sediments where it periodically respires Fe^{3+}, the ways in which *S. oneidensis* interacts with the Fe^{2+} produced from Fe^{3+} respiration are essential for a full understanding of how this bacterium thrives in its metal-rich niche. More broadly, a deeper understanding of the ways in which metals cause toxicity and in which bacteria interact with metals and resist metal toxicity will be important for optimal engineering of *S. oneidensis* and other microorganisms for potential uses in bioremediation.

References

Ades SE, Connolly LE, Alba BM, Gross CA. 1999. The *Escherichia coli* σ^E-dependent extracytoplasmic stress response is controlled by the regulated proteolysis of an anti-σ factor. *Genes Dev*. 13:2449–2461.

Almirón M, Link AJ, Furlong D, Kolter R. 1992. A novel DNA-binding protein with regulatory and protective roles in starved *Escherichia coli*. *Genes Dev*. 2646–2654.

Ambro L, Pevala V, Bauer J, Kutejová E. 2012. The influence of ATP-dependent proteases on a variety of nucleoid-associated processes. *J Struct Biol*. 179:181–192.

Andreini C, Bertini I, Cavallaro G, Holliday GL, Thornton JM. 2008. Metal ions in biological catalysis: from enzyme databases to general principles. *J Biol Inorg Chem.* 13:1205–1218.

Andrews SC. 2010. The ferritin-like superfamily: evolution of the biological iron storeman from a rubrerythrin-like ancestor. *Biochim Biophys Acta*. 1800:691–705.

Argüello JM, Raimunda D, Padilla-Benavides T. 2013. Mechanisms of copper homeostasis in bacteria. *Front Cell Infect Microbiol*. 3:73.

Baba T, Ara T, Hasegawa M, Takai Y, Okumura Y, Baba M, Datsenko KA, Tomita M, Wanner BL, Mori H. 2006. Construction of *Escherichia coli* K-12 in-frame, single-gene knockout mutants: the Keio collection. *Mol Sys Biol*. 2:2006.0008.

Balasubramanian B, Pogozelski WK, Tullius TD. 1998. DNA strand breaking by the hydroxyl radical is governed by the accessible surface areas of the hydrogen atoms of the DNA backbone. *Proc Natl Acad Sci U S A*. 95:9738–9743.

Balch WE, Fox GE, Magrum LJ, Woese CR, Wolfe RS. 1979. Methanogens: reevaluation of a unique biological group. *Microbiol Rev*. 43:260–296.

Barchinger SE, Pirbadian S, Sambles C, Baker CS, Leung KM, Burroughs NJ, El-Naggar MY, Golbeck JH. 2016. Regulation of gene expression in *Shewanella oneidensis* MR-1 during electron acceptor limitation and bacterial nanowire formation. *Appl Environ Microbiol*. 82:5428–5443.

Barkay T, Miller SM, Summers AO. 2003. Bacterial mercury resistance from atoms to ecosystems. *FEMS Microbiol* Rev. 27:355–384.

Baron D, LaBelle E, Coursolle D, Gralnick JA, Bond DR. 2009. Electrochemical measurement of electron transfer kinetics by *Shewanella oneidensis* MR-1. *J Biol Chem*. 284:28865–28873.

Beliaev AS, Klingeman DM, Klappenbach JA, Wu L, Romine MF, Tiedje JM, Nealson KH, Fredrickson JK, Zhou J. 2005. Global transcriptome analysis of *Shewanella oneidensis* MR-1 exposed to different terminal electron acceptors. *J Bacteriol.* 187:7138–7145.

Bencheikh-Latmani R, Williams SM, Haucke L, Criddle CS, Wu L, Zhou J, Tebo BM. 2005. Global transcriptional profiling of *Shewanella oneidensis* MR-1 during Cr(VI) and U(VI) reduction. *Appl Environ Microbiol*. 71:7453–7460.

Bird LJ, Coleman ML, Newman DK. 2013. Iron and copper act synergistically to delay anaerobic growth of bacteria. *Appl Environ Microbiol*. 79:3619–3627.

Blindauer CA. 2009. Bacterial Metallothioneins. In: *Metal ions and life sciences Volume 5: Metallothioneins and related chelators*. Royal Society of Chemistry. 51–81.

Blöthe M, Roden EE. 2008. Microbial iron redox cycling in a circumneutral-pH groundwater seep. *Appl Environ Microbiol*. 75:468–473.

Brayman TG, Hausinger RP. 1996. Purification, characterization, and functional analysis of a truncated *Klebsiella aerogenes* UreE urease accessory protein lacking the histidine-rich carboxyl terminus. *J Bacteriol.* 178:5410–5416.

Broderick JB, Duderstadt RE, Fernandez DC, Wojtuszewski K, Henshaw TF, Johnson M.K.J. 1997. Pyruvate formate-lyase activating enzyme is an iron−sulfur protein. *Am Chem Soc*. 119:7396–7397.

Brown SD, Martin M, Deshpande S, Seal S, Huang K, Alm E, Yang Y, Wu L, Yan T, Liu X, Arkin A, Chourey K, Zhou J, Thompson DK. 2006a. Cellular response of *Shewanella oneidensis* to strontium stress. *Appl Environ Microbiol*. 72:890–900.

Brown SD, Thompson MR, Verberkmoes NC, Chourey K, Shah M, Zhou J, Hettich RL, Thompson DK. 2006b. Molecular dynamics of the *Shewanella oneidensis* response to chromate stress. *Mol Cell Proteomics.* 5:1054–1071.

Canfield DE. 1989. Reactive iron in marine sediments. *Geochim Cosmochim Acta.* 53:619–632.

Capdevila M, Atrian S. 2011. Metallothionein protein evolution: a miniassay. *J Biol Inorg Chem*. 16:977–989.

Carlson HK, Clark IC, Melnyk RA, Coates JD. 2012. Toward a mechanistic understanding of anaerobic nitrate-dependent iron oxidation: balancing electron uptake and detoxification. *Front Microbiol*. 3:57.

Castresana J, Saraste M. 1995. Evolution of energetic metabolism: the respiration-early hypothesis. *Trends Biochem Sci*. 20:443–448.

Cellier M, Privé G, Belouchi A, Kwan T, Rodrigues V, Chia W, Gros P. 1995. Nramp defines a family of membrane proteins. *Proc Natl Acad Sci U S A*. 92:10089-10093.

Chao Y, Fu D. 2004. Thermodynamic studies of the mechanism of metal binding to the *Escherichia coli* zinc transporter YiiP. *J Biol Chem*. 279:17173–17180.

Charette MF, Henderson GW, Markovitz A. 1981. ATP hydrolysis-dependent protease activity of the *lon* (*capR*) protein of *Escherichia coli* K-12. *Proc Natl Acad Sci U S A.* 78:4728–4732.

Chaudhuri SK, Lack JG, Coates JD. 2001. Biogeneic magnetite formation through anaerobic biooxidation of Fe(II). *Appl Environ Microbiol*. 67:2844–2848.

Chuang SE, Burland V, Plunkett G 3rd, Daniels DL, Blattner FR. 1993. Sequence analysis of four new heat-shock genes constituting the *hslTS*/*ibpAB* and *hslVU* operons in *Escherichia coli*. *Gene*. 134:1–6.

Coudray N, Valvo S, Hu M, Lasala R, Kim C, Vink M, Zhou M, Provasi D, Filizola M, Tao J, Fang J, Penczek PA, Ubarretxena-Belandia I, Stokes DL. 2013. Inward-facing conformation of the zinc transporter YiiP revealed by cryoelectron microscopy. *Proc Natl Acad Sci U S A*. 110:2140–2145.

Coursolle D, Gralnick JA. 2010. Modularity of the Mtr respiratory pathway of *Shewanella oneidensis* strain MR-1. *Mol Microbiol*. 77:995–1008.

Cubillas C, Vinuesa P, Tabche ML, Garcia-de los Santos A. 2013. Phylogenomic analysis of cation diffusion facilitator proteins uncovers Ni^{2+}/Co^{2+} transporters. *Metallomics*. 5:1634–1643.

Dai J, Wei H, Tian C, Damron FH, Zhou J, Qiu D. 2015. An extracytoplasmic function sigma factor-dependent periplasmic glutathione peroxidase is involved in oxidative stress response of *Shewanella oneidensis*. *BMC Microbiol*. 15:34.

Daraselia N, Dernovoy D, Tian Y, Borodovsky M, Tatusov R, Tatusova T. 2003. Reannotation of *Shewanella oneidensis* genome. *OMICS*. 7:171–175.

Das A, Caccavo F Jr. 2000. Dissimilatory Fe(III) oxide reduction by *Shewanella alga* BrY requires adhesion. *Curr Microbiol*. 40:344–347.

Davison W. 1993. Iron and manganese in lakes. *Earth-Sci Rev*. 34:119–163.

De Las Peñas A, Connolly L, Gross CA. 1997a. The σ^E-mediated response to extracytoplasmic stress in *Escherichia coli* is transduced by RseA and RseB, two negative regulators of σ^E. *Mol Microbiol.* 24:373–385.

De las Penas A, Connolly L, Gross CA. 1997b. σE is an essential sigma factor in *Escherichia coli*. *J. Bacteriol*. 179:6862–6864.

DiChristina TJ, DeLong EF. 1993. Design and application of rRNA-targeted oligonucleotide probes for the dissimilatory iron- and manganese-reducing bacterium *Shewanella putrefaciens*. *Appl Environ Microbiol*. 59:4152–4160.

Diethmaier C, Newman JA, Kovács AT, Kaever V, Herzberg C, Rodrigues C, Boonstra M, Kuipers OP, Lewis RJ, Stülke J. 2014. The YmdB phosphodiesterase is a global regulator of late adaptive responses in *Bacillus subtilis*. *J Bacteriol*. 196:265–275.

Dunning JC, Ma Y, Marquis RE. 1998. Anaerobic killing of oral streptococci by reduced, transition metal cations. *Appl Environ Microbiol*.64:27-33.

Egler M, Grosse C, Grass G, Nies DH. 2005. Role of the extracytoplasmic function protein family sigma factor RpoE in metal resistance of *Escherichia coli*. *J Bacteriol.* 187:2297–2307.

Erbse A, Schmidt R, Bornemann T, Schneider-Mergener J, Mogk A, Zahn R, Dougan DA, Bukau B. 2006. ClpS is an essential component of the N-end rule pathway in *Escherichia coli*. *Nature*. 439:753–756.

Essington ME. 2015. Soil Minerals. In: *Soil and water chemistry: an integrative approach* 2nd ed. CRC Press. 55–128.

Evans DJ Jr, Evans DG, Lampert HC, Nakano H. 1995. Identification of four new prokaryotic bacterioferritins, from *Helicobacter pylori*, *Anabaena variabilis*, *Bacillus subtilis* and *Treponema pallidum*, by analysis of gene sequences. *Gene*. 153:123–127.

Fan B, Rosen BP. 2002. Biochemical characterization of CopA, the *Escherichia coli* Cu(I)-translocating P-type ATPase. *J Biol Chem*. 277: 46987–46992.

Ferreira GC, Franco R, Lloyd SG, Moura I, Moura JJG, Huynh BH. 1995. Structure and function of ferrochelatase. *J Bioenerg Biomembr*. 27:221–229.

Finn RD, Bateman A, Clements J, Coggill P, Eberhardt RY, Eddy SR, Heger A, Hetherington K, Holm L, Mistry J, Sonnhammer ELL, Tate J, Punta M. 2014. The Pfam protein families database. *Nucl Acids Res*. 42:D222–D230.

Fischer WR. 1987. Standard potentials (E_0) of iron(III) oxides under reducing conditions. *J Plant Nutr Soil Sci*. 150:286–289.

Fisher CR, Wyckoff EE, Peng ED, Payne SM. 2016. Identification and characterization of a putative manganese export protein in *Vibrio cholerae*. *J Bacteriol*. 198:2810–2817.

Flint DH, Tuminello JF, Miller TJ. 1996. Studies on the synthesis of the Fe-S cluster of dihydroxy-acid dehydratase in *Escherichia coli* crude extract. *J Biol Chem*. 271:16053–16067.

Flynn JM, Neher SB, Kim YI, Sauer RT, Baker TA. 2003. Proteomic discovery of cellular substrates of the ClpXP protease reveals five classes of ClpX-recognition signals. *Mol Cell*. 11:671–683.

Foster AW, Osman D, Robinson NJ. 2014. Metal preferences and metallation. *J Biol Chem*. 289: 28095–28103.

Frawley ER, Crouch M-LV, Bingham-Ramos LK, Robbins HF, Wang W, Wright GD, Fang FC. 2013. Iron and citrate export by a major facilitator superfamily pump regulates metabolism and stress resistance in *Salmonella* Typhimurium. *Proc Natl Acad Sci U S A.* 110:12054–12059.

Gibson MM, Bagga DA, Miller CG, Maguire ME. 1991. Magnesium transport in *Salmonella typhimurium*: the influence of new mutations conferring Co^{2+} resistance on the CorA Mg^{2+} transport system. *Mol Microbiol*. 5:2753–2762.

Gordon DM, Cowling A. 2003. The distribution and genetic structure of *Escherichia coli* in Australian vertebrates: host and geographic effects. *Microbiology*. 149:3575–3586.

Gottesman S, Zipser D. 1978. Deg phenotype of *Escherichia coli lon* mutants. *J Bacteriol*. 133:844–851.

Gottesman S, Clark WP, Maurizi MR. 1990. The ATP-dependent Clp protease of *Escherichia coli*. Sequence of *clpA* and identification of a Clp-specific substrate. *J Biol Chem*. 265:7886–7893.

Gottesman S. 1996. Proteases and their targets in *Escherichia coli*. *Annu Rev Genet*. 30:465–506.

Gottesman S, Roche E, Zhou Y, Sauer RT. 1998. The ClpXP and ClpAP proteases degrade proteins with carboxy-terminal peptide tails added by the SsrA-tagging system. *Genes Dev*. 12:1338–1347.

Gralnick JA, Hau HH. 2007. Ecology and biotechnology of the genus *Shewanella*. *Annu Rev Microbiol*. 61:237–258.

Granick S, Michaelis L. 1942. Ferritin and apoferritin. *Science*. 95:439–440.

Grass G, Otto M, Fricke B, Haney CJ, Rensing C, Nies DH, Munkelt D. 2005. FieF (YiiP) from *Escherichia coli* mediates decreased cellular accumulation of iron and relieves iron stress. *Arch Microbiol*. 183:9–18.

Gunshin H, Mackenzie B, Berger UV, Gunshin Y, Romero MF, Boron WF, Nussberger S, Gollan JL, Hediger MA. 1997. Cloning and characterization of a mammalian proton-coupled metal-ion transporter. *Nature*. 388:482–488.

Haines-Menges B, Whitaker WB, Boyd EF. 2014. Alternative sigma factor RpoE is important for *Vibrio parahaemolyticus* cell envelope stress response and intestinal colonization. *Infect Immun*. 82:3667–3677.

Hamamoto K, Miyahara M, Kouzuma A, Matsumoto A, Yoda M, Ishiguro T, Watanabe K. 2016. Evaluation of microbial fuel cells for electricity generation from oil-contaminated wastewater. *J Biosci Bioeng.* 122:589–593.

Hantke K. 1987. Ferrous iron transport mutants in *Escherichia coli* K12. *FEMS Microbiol Lett*. 44:53–57.

Hattori M, Tanaka Y, Fukai S, Ishitani R, Nureki O. 2007. Crystal structure of the MgtE Mg2+ transporter. *Nature*. 448:1072–1075.

Hau HH, Gilbert A, Coursolle D, Gralnick JA. 2008. Mechanism and consequences of anaerobic respiration of cobalt by *Shewanella oneidensis* strain MR-1. *Appl Environ Microbiol*. 74:6880–6886.

He Q, Sanford RA. 2003. Characterization of Fe(III) reduction by chlororespiring *Anaeromyxobacter dehalogenans*. *Appl Environ Microbiol.* 69:2712–2718.

Heidelberg JF, Paulsen IT, Nelson KE, Gaidos EJ, Nelson WC, Read TD, Eisen JA, Seshadri R, Ward N, Methe B, Clayton RA, Meyer T, Tsapin A, Scott J, Beanan M, Brinkac L, Daugherty S, DeBoy RT, Dodson RJ, Durkin AS, Haft DH, Kolonay JF, Madupu R, Peterson JD, Umayam LA, White O, Wolf AM, Vamathevan J, Weidman J, Impraim M, Lee K, Berry K, Lee C, Mueller J, Khouri H, Gill J, Utterback TR, McDonald LA, Feldblyum TV, Smith HO, Venter JC, Nealson KH, Fraser CM. 2002. Genome sequence of the dissimilatory metal ion-reducing bacterium *Shewanella oneidensis*. *Nat Biotechnol*. 20:1118–1123.

Helbig K, Grosse C, Nies DH. 2008. Cadmium toxicity in glutathione mutants of *Escherichia coli*. *J Bacteriol*. 190:5439–5454.

Herman C, Ogura T, Tomoyasu T, Hiraga S, Akiyama Y, Ito K, Thomas R, D'Ari R, Bouloc P. 1993. Cell growth and a phage development controlled by the same essential *Escherichia coli* gene, *ftsH*/*hflB*. *Proc Natl Acad Sci U S A*. 90:10861–10865.

Hidalgo E, Demple B. 1994. An iron-sulfur center essential for transcriptional activation by the redox-sensing SoxR protein. *EMBO J.* 13:138–146.

Higham DP, Sadler PJ, Scawen MD. 1986. Cadmium-binding proteins in *Pseudomonas putida*: pseudothioneins. *Environ Health Perspect*. 65:5–11.

Hiratsu K, Amemura M, Nashimoto H, Shinagawa H, Makino K. 1995. The *rpoE* gene of *Escherichia coli*, which encodes σ^E, is essential for bacterial growth at high temperature. *J Bacteriol*. 177:2918–2922.

Hmiel SP, Snavely MD, Miller CG, Maguire ME. 1986. Magnesium transport in *Salmonella typhimurium*: characterization of magnesium influx and cloning of a transport gene. *J Bacteriol*. 168:1444–1450.

Hmiel SP, Snavely MD, Florer JB, Maguire ME, Miller CG. 1989. Magnesium transport in *Salmonella typhimurium*: genetic characterization and cloning of three magnesium transport loci. *J Bacteriol*. 171:4742–4751.

Hohle TH, O'Brian MR. 2015. Magnesium-dependent processes are targets of bacterial manganese toxicity. *Mol Microbiol*. 93:736–747.

Hughes MN, Poole RK. 1991. Metal speciation and microbial growth—the hard (and soft) facts. *J Gen Microbiol*. 137:725–734.

Hung H-C, Chang G-G. Differentiation of the slow-binding mechanism for magnesium ion activation and zinc ion inhibition of human placental alkaline phosphatase. *Protein Sci*. 10:34–45.

Hwang BJ, Park WJ, Chung CH, Goldberg AL. 1987. *Escherichia coli* contains a soluble ATP-dependent protease (Ti) distinct from protease La. *Proc Natl Acad Sci U S A.* 84:5550–5554.

Imlay JA, Chin SM, Linn S. 1988. Toxic DNA damage by hydrogen peroxide through the Fenton reaction in vivo and in vitro. *Science*. 240:640–642.

Irving H, Williams RJP. 1953. The stability of transition-metal complexes. *J Chem Soc.* 3192–3210.

Ishii S, Hansen DL, Hicks RE, Sadowsky, MJ. 2007. Beach sand and sediments are temporal sinks and sources of *Escherichia coli* in Lake Superior. *Environ Sci Technol.* 41:2203–2209.

Jin J, Guffanti AA, Bechhofer DH, Krulwich TA. 2002. Tet(L) and tet(K) tetracycline-divalent metal/H+ antiporters: characterization of multiple catalytic modes and a mutagenesis approach to differences in their efflux substrate and coupling ion preferences. *J Bacteriol*. 184:4722–4732.

Jonasson L, Hansen JLS, Wan Z, She J. 2012. The impacts of physical processes on oxygen variations in the North Sea-Baltic Sea transition zone. *Ocean Sci*. 8:37–48.

Jones JG, Gardener S, Simon BM. 1983. Bacterial reduction of ferric iron in a stratified eutrophic lake. *J Gen Microbiol*. 129:131–139.

Kammler M, Schön C, Hantke K. 1993. Characterization of the ferrous iron uptake system of *Escherichia coli*. *J Bacteriol*. 175:6212–6219.

Kane AL, Bond DR, Gralnick JA. 2013. Electrochemical analysis of *Shewanella oneidensis* engineered to bind gold electrodes. *ACS Synth Biol*. 2:93−101.

Katayama Y, Gottesman S, Pumphrey J, Rudikoff S, Clark WP, Maurizi MR. 1988. The two-component, ATP-dependent Clp protease of *Escherichia coli*. Purification, cloning, and mutational analysis of the ATP-binding component. *J Biol Chem*. 1988 263:15226–15236.

Katayama-Fujimura Y, Gottesman S, Maurizi MR. 1987. A multiple-component, ATP-dependent protease from *Escherichia coli*. *J Biol Chem*. 262:4477–4485.

Kehres DG, Zaharik ML, Finlay BB, Maguire ME. 2000. The NRAMP proteins of *Salmonella typhimurium* and *Escherichia coli* are selective manganese transporters involved in the response to reactive oxygen. *Mol Microbiol*. 36:1085–1100

Keiler KC, Waller PR, Sauer RT. 1996. Role of a peptide tagging system in degradation of proteins synthesized from damaged messenger RNA. *Science*. 271:990–993.

Keppetipola N, Shuman S. 2008. A phosphate-binding histidine of binuclear metallophosphodiesterase enzymes is a determinant of 2',3'-cyclic nucleotide phosphodiesterase activity. *J Biol Chem*. 283:30942–30949

Kihara A, Akiyama Y, Ito K. 1995. FtsH is required for proteolytic elimination of uncomplexed forms of SecY, an essential protein translocase subunit. *Proc Natl Acad Sci U S A*. 92:4532–4536.

Kim B, Kim HJ, Hyun MS, Park DH. 1999. Direct electrode reaction of Fe(III)-reducing bacterium, *Shewanella putrefaciens*. *J Microbiol Biotechnol*. 9:127–131.

Kimura S, Suzuki T. 2015. Iron-sulfur proteins responsible for RNA modifications. *Biochim Biophys Acta*. 1853:1272–1283.

Kostka JE, Nealson KH. 1995. Dissolution and reduction of magnetite by bacteria. *Environ Sci Technol*. 29:2535–2540.

Kovach ME, Elzer PH, Hill DS, Robertson GT, Farris MA, Roop RM, Peterson KM. 1995. Four new derivatives of the broad-host-range cloning vector pBBR1MCS, carrying different antibiotic-resistance cassettes. *Gene*. 166:175–176.

Kunau WH, Beyer A, Franken T, Götte K, Marzioch M, Saidowsky J, Skaletz-Rorowski A, Wiebel FF. 1993. Two complementary approaches to study peroxisome biogenesis in *Saccharomyces cerevisiae*: forward and reversed genetics. *Biochimie*. 75:209–224.

Leaphart AB, Thompson DK, Huang K, Alm E, Wan XF, Arkin A, Brown SD, Wu L, Yan T, Liu X, Wickham GS, Zhou J. 2006. Transcriptome profiling of *Shewanella oneidensis* gene expression following exposure to acidic and alkaline pH. *J Bacteriol*. 188:1633–1642.

Leimkühler S, Wuebbens MM, Rajagopalan KV. 2011. The history of the discovery of the molybdenum cofactor and novel aspects of its biosynthesis in bacteria. *Coord Chem Rev*. 255:1129–1144.

Leonard S, Gannett PM, Rojanasakul Y, Schwegler-Berry D, Castranova V, Vallyathan V, Shi X. 1998. Cobalt-mediated generation of reactive oxygen species and its possible mechanism. *J Inorg Biochem*. 70:239–244.

Liu C, Gorby YA, Zachara JM, Fredrickson JK, Brown CF. 2002. Reduction kinetics of Fe(III), Co(III), U(VI), Cr(VI), and Tc(VII) in cultures of dissimilatory metal-reducing bacteria. *Biotechnol Bioeng*. 80:637–649.

Liu J, Chakraborty S, Hosseinzadeh P, Yu Y, Tian S, Petrik I, Bhagi A, Lu Y. 2014. Metalloproteins containing cytochrome, iron-sulfur, or copper redox centers. *Chem Rev.* 114:4366–4469.

Lovley DR, Phillips EJ. 1988. Novel mode of microbial energy metabolism: organic carbon oxidation coupled to dissimilatory reduction of iron or manganese. *Appl Environ Microbiol.* 54:1472–1480.

Lovley DR, Phillips EJP, Gorby YA, Landa ER. 1991. Microbial reduction of uranium. *Nature*. 350:413–416.

Lovley DR. 2003. Cleaning up with genomics: applying molecular biology to bioremediation. *Nat Rev Microbiol*. 1:35–44

Lower SK, Hochella MF Jr, Beveridge TJ. 2001. Bacterial recognition of mineral surfaces: nanoscale interactions between *Shewanella* and α-FeOOH. *Science*. 292:1360–1363.

Lu M, Chai J, Fu D. 2009. Structural basis for auto-regulation of the zinc transporter YiiP. *Nat Struct Mol Biol.* 16:1063–1067.

Lunin VV, Dobrovetsky E, Khutoreskaya G, Zhang R, Joachimiak A, Doyle DA, Bochkarev A, Maguire ME, Edwards AM, Koth CM. 2006. Crystal structure of the CorA Mg2+ transporter. *Nature*. 440:833–837.

Macomber L, Imlay JA. 2009. The iron-sulfur clusters of dehydratases are primary intracellular targets of copper toxicity. *Proc Natl Acad Sci U S A*. 106:8344–8349.

Maguire ME. 1992. MgtA and MgtB: prokaryotic P-type ATPases that mediate Mg^{2+} influx. *J Bioenerg Biomembr*. 24:319–328.

Malmström BG, Neilands JB. 1964. Metalloproteins. *Annu Rev Biochem*. 33:331–354.

Maloney PC, Kashket ER, Wilson TH. 1974. A protonmotive force drives ATP synthesis in bacteria. *Proc Natl Acad Sci U S A.* 71:3896–3900.

Marshall KC. 1979. Biogeochemistry of manganese minerals. In: *Biogeochemical cycling of mineral-forming elements*. Elsevier. 253–292.

Marsili E, Baron DB, Shikhare ID, Coursolle D, Gralnick JA, Bond DR. 2008. *Shewanella* secretes flavins that mediate extracellular electron transfer. *Proc Natl Acad Sci USA.* 105:3968–3973.

Matisoff G, Neeson TM. 2005. Oxygen concentration and demand in Lake Erie sediments. *J Great Lakes Res*. 31:284–295.

Matthies D, Dalmas O, Borgnia MJ, Dominik PK, Merk A, Rao P, Reddy BG, Islam S, Bartesaghi A, Perozo E, Subramaniam S. 2016. Cryo-EM structures of the magnesium channel CorA reveal symmetry break upon gating. *Cell*. 164:747–756.

Maurizi MR. 1991. ATP-promoted interaction between Clp A and Clp P in activation of Clp protease from *Escherichia coli*. *Biochem Soc Trans.* 19:719–723.

McDevitt CA, Ogunniyi AD, Valkov E, Lawrence MC, Kobe B, McEwan AG, Paton JC. 2011. A molecular mechanism for bacterial susceptibility to zinc. *PLOS Pathog*. 7: e1002357.

McDonough WF. 2000. The composition of the Earth. In: *Earthquake thermodynamics and phase transformations in the earth's interior* 1st ed. Academic Press. 5–24.

Méjean V, Iobbi-Nivol C, Lepelletier M, Giordano G, Chippaux M, Pascal MC. 1994. TMAO anaerobic respiration in *Escherichia coli*: involvement of the *tor* operon. *Mol Microbiol*. 11:1169–1179.

Mitchell P. 1961. Coupling of phosphorylation to electron and hydrogen transfer by a chemi-osmotic type of mechanism. *Nature*. 191:144–148.

Moncrief MB, Maguire ME. 1999. Magnesium transport in prokaryotes. *J Biol Inorg Chem*. 4:523–527.

Montanini B, Blaudez D, Jeandroz S, Sanders D, Chalot M. 2007. Phylogenetic and functional analysis of the Cation Diffusion Facilitator (CDF) family: improved signature and prediction of substrate specificity. *BMC Genomics*. 8:107.

Myers CR, Nealson KH. 1988. Bacterial manganese reduction and growth with manganese oxide as the sole electron acceptor. *Science*. 240:1319–1321.

Myers CR, Myers JM. 1997. Cloning and sequence of *cymA*, a gene encoding a tetraheme cytochrome *c* required for reduction of iron(III), fumarate, and nitrate by *Shewanella putrefaciens* MR-1. *J Bacteriol*. 179:1143–1152.

Myers CR, Carstens BP, Antholine WE, Myers JM. 2000. Chromium(VI) reductase activity is associated with the cytoplasmic membrane of anaerobically grown *Shewanella putrefaciens* MR-1. *J Appl Microbiol*. 88:98–106.

Myers JM, Myers CR. 2001. Role for outer membrane cytochromes OmcA and OmcB of *Shewanella putrefaciens* MR-1 in reduction of manganese dioxide. *Appl Environ Microbiol.* 67:260–269.

Nealson KH, Scott J. 2006. Ecophysiology of the genus *Shewanella*. In: *Prokaryotes* 6th ed. New York: Springer Science. 1133–1151.

Nelson DL, Kennedy EP. 1972. Transport of magnesium by a repressible and nonrepressible system in *Escherichia coli*. *Proc Natl Acad Sci U S A.* 69:1091–1093.

Nesbitt HW, Markovics G. 1997. Weathering of granodioritic crust, long-term storage of elements in weathering profiles, and petrogenesis of siliciclastic sediments. *Geochim Cosmochim Acta*. 61:1653–1670.

Niegowski D, Eshaghi S. 2007. The CorA family: structure and function revisited. *Cell Mol Life Sci*. 64:2564–2574.

Nies DH, Silver S. 1995. Ion efflux systems involved in bacterial metal resistances. *J Ind Microbiol*. 14:186–199.

Nucifora G, Chu L, Misra TK, Silver S. 1989. Cadmium resistance from *Staphylococcus aureus* plasmid, p1258 *cadA* results from a cadmium-efflux ATPase. *Proc Natl Acad Sci USA*. 86:3544–3548.

O'Reilly SE, Watkins J, Furukawa Y. 2005. Secondary mineral formation associated with respiration of nontronite, NAu-1 by iron reducing bacteria. *Geochem Trans*. 6:67–76.

O'Toole GA. 2011. Microtiter Dish Biofilm Formation Assay. *J Vis Exp*. 2437.

Odermatt A, Suter H, Krapf R, Solioz M. 1993. Primary structure of two P-type ATPases involved in copper homeostasis in *Enterococcus hirae*. *J Biol Chem*. 268:12775–12779.

Okuno T, Ogura T. 2013. FtsH protease-mediated regulation of various cellular functions. *Subcell Biochem*. 66:53–69.

Ottow JGC, Glathe H. 1971. Isolation and identification of iron-reducing bacteria from gley soils. *Soil Biol Biochem.* 3:43–55.

Papp KM, Maguire ME. 2004. The CorA Mg^{2+} transporter does not transport Fe^{2+}. *J Bacteriol*. 186:7653–7658.

Park MH, Wong BB, Lusk JE. 1976. Mutants in three genes affecting transport of magnesium in *Escherichia coli*: genetics and physiology. *J Bacteriol*. 126:1096–1103.

Paulsen IT, Saier MH Jr. 1997. A novel family of ubiquitous heavy metal ion transport proteins. *J Membr Biol.* 156:99–103.

Pedersen PL, Carafoli E. 1987. Ion Motive ATPases. I. Ubiquity, properties, and significance to cell function. *Trends Biochem Sci*. 12:146–150.

Raivio TL, Silhavy TJ. 2001. Periplasmic stress and ECF sigma factors. *Annu Rev Microbiol*. 55:591–624.

Ranquet C, Ollagnier-de-Choudens S, Loiseau L, Barras F, Fontecave M. 2007. Cobalt stress in *Escherichia coli*. The effect on the iron-sulfur proteins. *J Biol Chem.* 282:30442–30451.

Raphael BH, Joens LA. 2003. FeoB is not required for ferrous iron uptake in *Campylobacter jejuni*. *Can J Microbiol*. 49:727–731.

Raux E, Thermes C, Heathcote P, Rambach A, Warren MJ. 1997. A role for *Salmonella typhimurium cbiK* in cobalamin (vitamin B12) and siroheme biosynthesis. *J Bacteriol.* 179:3202–3212.

Raux E, Lanois A, Rambach A, Warren MJ, Thermes C. 1998. Cobalamin (vitamin B12) biosynthesis: functional characterization of the *Bacillus megaterium cbi* genes required to convert uroporphyrinogen III into cobyrinic acid a,c-diamide. *Biochem J*. 335:167–173.

Raymond KN, Dertz EA, Kim SS. 2003. Enterobactin: an archetype for microbial iron transport. *Proc Natl Acad Sci USA*. 100: 3584–3588.

Reznikoff WS, Siegele DA, Cowing DW, Gross CA. 1985. The regulation of transcription initiation in bacteria. *Ann Rev Genet.* 19:355–387.

Roden EE, Lovley DR. 1993. Dissimilatory Fe(III) reduction by the marine microorganism *Desulfuromonas acetoxidans*. *Appl Environ Microbiol.* 59:734–742.

Rosenberg H, Young IG. 1974. Iron transport in the enteric bacteria. In: *Microbial iron metabolism: a comprehensive treatise*. Academic Free Press. 67–82.

Rosselló-Mora RA, Ludwig W, Kämpfer P, Amann R, Schleifer KH. 1995. *Ferrimonas balearica* gen. nov., spec. nov., a new marine facultative Fe(III)-reducing bacterium. *Syst Appl Microbiol.* 18:196–202.

Rost B. 2002. Enzyme function less conserved than anticipated. *J Mol Biol*. 318:595–608.

Rudolf J, Makrantoni V, Ingledew WJ, Stark MJ, White MF. 2006. The DNA repair helicases XPD and FancJ have essential iron-sulfur domains. *Mol Cell*. 23:801–808.

Rugh CL, Wilde HD, Stack NM, Thompson DM, Summers AO, Meagher RB. 1996. Mercuric ion reduction and resistance in transgenic *Arabidopsis thaliana* plants expressing a modified bacterial *merA* gene. *Proc Natl Acad Sci USA*. 93:3182–3187.

Rui Z, Li X, Zhu X, Liu J, Domigan B, Barr I, Cate JH, Zhang W. 2014. Microbial biosynthesis of medium-chain 1-alkenes by a nonheme iron oxidase. *Proc Natl Acad Sci U S A*. 111:18237–18242.

Rutherford JC, Cavet JS, Robinson NJ. Cobalt-dependent transcriptional switching by a dual-effector MerR-like protein regulates a cobalt-exporting variant CPx-type ATPase. *J Biol Chem*. 274:25827–25832.

Saier MH Jr, Tran CV, Barabote RD. 2006. TCDB: the Transporter Classification Database for membrane transport protein analyses and information. *Nucl Acids Res.* 34:D181–186.

Saito A, Hizukuri Y, Matsuo E, Chiba S, Mori H, Nishimura O, Ito K, Akiyama Y. 2011. Post-liberation cleavage of signal peptides is catalyzed by the site-2 protease (S2P) in bacteria. *Proc Natl Acad Sci USA.* 108:13740-13745.

Saltikov CW, Newman DK. 2003. Genetic identification of a respiratory arsenate reductase. *Proc Natl Acad Sci USA.* 100:10983–10988.

Samuelsson MO. 1985. Dissimilatory nitrate reduction to nitrate, nitrous oxide, and ammonium by *Pseudomonas putrefaciens. Appl Environ Microbiol*. 50:812–815.

Schauer K, Rodionov DA, de Reuse H. 2008. New substrates for TonB-dependent transport: Do we only see the ‘tip of the iceberg’? *Trends Biochem Sci*. 33:330–338

Shi J, Lindsay WP, Huckle JW, Morby AP, Robinson NJ. 1992. Cyanobacterial metallothionein gene expressed in *Escherichia coli*: metal-binding properties of the expressed protein. *FEBS Lett.* 303:159–163.

Shirodkar S, Reed S, Romine M, Saffarini D. 2011. The octahaem SirA catalyses dissimilatory sulfite reduction in *Shewanella oneidensis* MR-1. *Environ Microbiol*. 13: 108–115.

Singh SK, Grimaud R, Hoskins JR, Wickner S, Maurizi MR. 2000. Unfolding and internalization of proteins by the ATP-dependent proteases ClpXP and ClpAP. *Proc Natl Acad Sci USA.* 97:8898–8903.

Smith RL, Thompson LJ, Maguire ME. 1995. Cloning and characterization of MgtE, a putative new class of Mg^{2+} transporter from *Bacillus firmus* OF4. *J Bacteriol*. 177:1233–1238.

Snavely MD, Florer JB, Miller CG, Maguire ME. 1989. Magnesium transport in *Salmonella typhimurium*: $^{28}Mg^{2+}$ transport by the CorA, MgtA, and MgtB systems. *J Bacteriol*. 171:4761–4766.

Snavely MD, Miller CG, Maguire ME. 1991. The *mgtB* Mg2+ transport locus of *Salmonella typhimurium* encodes a P-type ATPase. *J Biol Chem*. 266:815–823.

Song HK, Mulrooney SB, Huber R, Hausinger RP. 2001. Crystal structure of *Klebsiella aerogenes* UreE, a nickel-binding metallochaperone for urease activation. *J Biol Chem*. 276:49359–49364.

Stiefel EI, Watt GD. *Azotobacter* cytochrome b557.5 is a bacterioferritin. *Nature*. 279:81–83.

Stohs SJ, Bagchi D. 1995. Oxidative mechanisms in the toxicity of metal ions. *Free Radic Biol Med*. 18:321–336.

Stookey LL. 1970. Ferrozine – a new spectrophotometric reagent for iron. *Anal Chem.* 42:779–781.

Swamy KHS, Goldberg AL. 1981. *E. coli* contains eight soluble proteolytic activities, one being ATP dependent. *Nature.* 292:652−654.

Takeda H, Hattori M, Nishizawa T, Yamashita K, Shah ST, Caffrey M, Maturana AD, Ishitani R, Nureki O. 2014. Structural basis for ion selectivity revealed by high-resolution crystal structure of Mg^{2+} channel MgtE. *Nat Commun*. 5:5374.

Tao T, Snavely MD, Farr SG, Maguire ME. 1995. Magnesium transport in *Salmonella typhimurium*: *mgtA* encodes a P-type ATPase and is regulated by Mg2+ in a manner similar to that of the *mgtB* P-type ATPase. *J Bacteriol*. 177:2654–2662.

Taylor DL, Jardine PM. 1995. Analysis of cobalt(II)EDTA and cobalt(III)EDTA in pore water by ion chromatography. *J Environ Qual*. 24:789–792.

Teintze M, Slaughter M, Weiss H, Neupert W. 1982. Biogenesis of mitochondrial ubiquinol:cytochrome c reductase (cytochrome bc1 complex). Precursor proteins and their transfer into mitochondria. *J Biol Chem*. 257:10364–10371.

Thamdrup B, Fossing H, Jørgensen BB. 1994. Manganese, iron, and sulfur cycling in a coastal marine sediment, Aarhus Bay, Denmark. *Geochim Cosmochim Acta*. 58:5115–5129.

Thompson DK, Beliaev AS, Giometti CS, Tollaksen SL, Khare T, Lies DP, Nealson KH, Lim H, Yates J 3rd, Brandt CC, Tiedje JM, Zhou J. 2002. Transcriptional and proteomic analysis of a ferric uptake regulator (Fur) mutant of *Shewanella oneidensis*: possible

involvement of fur in energy metabolism, transcriptional regulation, and oxidative stress. *Appl Environ Microbiol*. 68:881–892.

Tian W, Skolnick J. 2003. How well is enzyme function conserved as a function of pairwise sequence identity? *J Mol Biol*. 333:863–882.

Tottey S, Waldron KJ, Firbank SJ, Reale B, Bessant C, Sato K, Cheek TR, Gray J, Banfield MJ, Dennison C, Robinson NJ. 2008. Protein-folding location can regulate manganese-binding versus copper- or zinc-binding. *Nature*. 455:1138–1142.

Townsend DE, Esenwine AJ, George J 3rd, Bross D, Maguire ME, Smith RL. 1995. Cloning of the *mgtE* Mg^{2+} transporter from *Providencia stuartii* and the distribution of *mgtE* in gram-negative and gram-positive bacteria. *J Bacteriol.* 177:5350–5354.

Truex MJ, Peyton BM, Valentine NB, Gorby YA. 1997. Kinetics of U(VI) reduction by a dissimilatory Fe(III)-reducing bacterium under non-growth conditions. *Biotechnol Bioeng*. 55:490–496.

Tsai KJ, Yoon KP, Lynn AR. 1992. ATP-dependent cadmium transport by the cadA cadmium resistance determinant in everted membrane vesicles of *Bacillus subtilis*. *J Bacteriol*. 174:116–121.

Tucker NP, D'Autréaux B, Yousafzai FK, Fairhurst SA, Spiro S, Dixon R. 2007. Analysis of the nitric oxide-sensing non-heme iron center in the NorR regulatory protein. *J Biol Chem.* 283:908–918.

Van Melderen L, Aertsen A. 2009. Regulation and quality control by Lon-dependent proteolysis. *Res Microbiol*. 160:645–651.

VanEngelen MR, Szilagyi RK, Gerlach R, Lee BD, Apel WA, Peyton BM. 2011. Uranium exerts acute toxicity by binding to pyrroloquinoline quinone cofactor. *Environ Sci Technol*. 45:937–942.

Vassiliev IR, Antonkine ML, JH. 2001. Iron–sulfur clusters in type I reaction centers. *Biochim Biophys Acta Bioenerg*. 1507:139–160.

Velayudhan J, Hughes NJ, McColm AA, Bagshaw J, Clayton CL, Andrews SC, Kelly DJ. 2000. Iron acquisition and virulence in *Helicobacter pylori*: a major role for FeoB, a high-affinity ferrous iron transporter. *Mol Microbiol*. 37:274–286.

Vidal SM, Malo D, Vogan K, Skamene E, Gros P. 1993. Natural resistance to infection with intracellular parasites: isolation of a candidate for Bcg. *Cell*. 73:469–485.

Waldron KJ, Robinson NJ. 2009. How do bacterial cells ensure that metalloproteins get the correct metal? *Nat Rev Microbiol.* 7:25–35.

Waller PR, Sauer RT. 1996. Characterization of degQ and degS, *Escherichia coli* genes encoding homologs of the DegP protease. *J Bacteriol.* 178:1146–1153.

Wan XF, Verberkmoes NC, McCue LA, Stanek D, Connelly H, Hauser LJ, Wu L, Liu X, Yan T, Leaphart A, Hettich RL, Zhou J, Thompson DK. 2004. Transcriptomic and proteomic characterization of the Fur modulon in the metal-reducing bacterium *Shewanella oneidensis*. *J Bacteriol*. 186:8385–8400.

Wang CC, Newton A. 1969a. Iron transport in *Escherichia coli*: relationship between chromium sensitivity and high iron requirement in mutants of *Escherichia coli*. *J Bacteriol*. 98:1135–1141.

Wang CC, Newton A. 1969b. Iron transport in *Escherichia coli*: roles of energy-dependent uptake and 2,3-dihydroxybenzoylserine. *J Bacteriol*. 98:1142–1150.

Wang P, Lutton A, Olesik J, Vali H, Li X. 2012. A novel iron- and copper-binding protein in the Lyme disease spirochaete. *Mol Microbiol.* 86:1441–1451.

Wang Z, Giammar DE. 2015. Metal contaminant oxidation mediated by manganese redox cycling in subsurface environment. In: *Advances in the environmental biogeochemistry of manganese oxides*. American Chemical Society. 29–50.

Waters LS, Sandoval M, Storz G. The *Escherichia coli* MntR miniregulon includes genes encoding a small protein and an efflux pump required for manganese homeostasis. *J Bacteriol*. 193:5887–5897.

Waxman L, Goldberg AL. 1982. Protease La from *Escherichia coli* hydrolyzes ATP and proteins in a linked fashion. *Proc Natl Acad Sci U S A*. 79:4883–4887.

Webster DP, TerAvest MA, Doud DF, Chakravorty A, Holmes EC, Radens CM, Sureka S, Gralnick JA, Angenent LT. 2014. An arsenic-specific biosensor with genetically engineered *Shewanella oneidensis* in a bioelectrochemical system. *Biosens Bioelectron.* 62:320–324.

Wei Y, Fu D. 2005. Selective metal binding to a membrane-embedded aspartate in the *Escherichia coli* metal transporter YiiP (FieF). *J Biol Chem*. 280:33716–33724.

White, D, Drummond J, Fuqua C. 2012. Electron transport. In: *The physiology and biochemistry of prokaryotes* 4th ed. Oxford University Press. 146–174.

Wojtkowiak D, Georgopoulos C, Zylicz M. 1993. Isolation and characterization of ClpX, a new ATP-dependent specificity component of the Clp protease of *Escherichia coli*. *J Biol Chem*. 268:22609–22617.

Wrighton KC, Thrash JC, Melnyk RA, Bigi JP, Byrne-Bailey KG, Remis JP, Schichnes D, Auer M, Chang CJ, Coates JD. 2011. Evidence for direct electron transfer by a gram-positive bacterium isolated from a microbial fuel cell. *Appl Environ Microbiol.* 77:7633–7639.

Xia W, Li H, Sze KH, Sun H. 2009. Structure of a nickel chaperone, HypA, from *Helicobacter pylori* reveals two distinct metal binding sites. *J Am Chem Soc*. 131:10031–10040.